STUDIES ON THE ROLE OF CONNEXIN43 PHOSPHORYLATION IN THE INJURY-RESISTANT HEART

By

WATTAMON SRISAKULDEE

A Thesis submitted to the Faculty of Graduate Studies of

The University of Manitoba

in partial fulfillment of the requirements of the degree of

DOCTOR OF PHILOSOPHY

Department of Physiology and Pathophysiology

University of Manitoba

Winnipeg, Manitoba

Canada

TABLE OF CONTENTS

Page

Page

Chapter 3. Results

Page

Chapter 4. Discussion

ABSTRACT

Ischemic heart disease and ischemia/reperfusion-associated pathologies can lead to heart failure, a major cause of death worldwide. Identification of endogenous molecular mechanisms that mediate cardiac resistance to ischemic injury ('cardioprotection'), and understanding their regulation, can contribute to new approaches for the management and amelioration of cardiac injury. The overall goal of my studies was to investigate the role of the cardiac membrane channel and hemi-channel forming protein connexin43 (Cx43) in cardioprotection. Cx43 is a potential downstream effector of PKCε-mediated cardioprotection. There is evidence from studies with isolated cardiomyocytes that the FGF-2/ PKCε –induced cytoprotection is mediated, at least in part, by the phosphorylation of Cx43 at PKCε-target sites such as serine (S) 262.

In a first series of studies, I examined **the hypothesis (1)** that several PKCε-mediated cardioprotective manipulations would be associated with acute increases in cardiac Cx43 phosphorylation at PKCε-target sites (S262, S368), and prevention of ischemia and/or reperfusion-induced Cx43 remodeling. Isolated perfused rat hearts were subjected to various pre-conditioning-like protective treatments (ischemic preconditioning, FGF-2 perfusion, diazoxide administration), followed by 30 min global ischemia and 60 min of reperfusion. A post-conditioning treatment (FGF-2 perfusion after 30 min ischemia, during reperfusion) was also used. Western blot of heart lysates was used to analyze Cx43 levels and phosphorylation status at the end of treatment. My findings showed that all treatments elicited a "P*Cx43" state, defined as above-physiological levels of phospho-S262-Cx43 and phospho-S368-Cx43. P*Cx43 was sustained during global ischemia, and reperfusion, and was accompanied by attenuation of ischemia-induced Cx43 dephosphorylation, and prevention of Cx43 lateralization away from intercalated disks. It was concluded that increased P*Cx43 signposts a cardioprotected state.

In addition to localization at the intercalated disks and gap junctions, Cx43 is present at the cardiac subsarcolemmal (SSM) but not interfibrillar (IFM) mitochondrial populations. Ischemic preconditioning promotes translocation of Cx43

to mitochondria, where it is considered important for developing increased resistance to injury. In a second series of studies, I addressed the **hypothesis (2)** that FGF-2 administration to the isolated heart exerts protective effects on cardiac SSM and IFM mitochondrial populations, and that the protective effects on SSM are associated with development of mitochondrial P*Cx43 state, and mediated by mitochondrial Cx43 function. Mitochondria (SSM and IFM) isolated from control and FGF-2-perfused hearts were examined for their calcium tolerance (calcium overload induced permeability transition, mPTP) assessed spectrophotometrically as cyclosporine A-inhibitable swelling. FGF-2 perfusion increased resistance to calcium-induced mPTP in SSM and IFM suspensions by 2.9- and 1.7-fold, respectively, compared to their counterparts from vehicle-perfused hearts. The salutary effect of FGF-2 was lost in SSM but not IFM in the presence of Gap27, a Cx43 channel and hemi-channel blocker. FGF-2 perfusion increased relative levels of PKCε, phospho(p)PKCε and Tom-20 translocase in SSM and IFM, and of Cx43 in SSM. Phospho-S262, and -S368- Cx43 showed a 30-fold and 8-fold increase, respectively, in SSM from FGF-2-treated, compared to untreated, hearts. Stimulation of control SSM with phorbol 12-myristate 13-acetate (PMA), a potent PKC activator, increased both calcium tolerance and mitochondrial Cx43 phosphorylation at S262 and S368 (mito-P*Cx43). The PMA-induced phosphorylation of mitochondrial Cx43 was prevented by εV_{1-2}, a PKCε-inhibiting peptide. It was concluded that SSM are more responsive than IFM to FGF-2-triggered protection from calcium-induced mPTP, by a mitochondrial Cx43-channel-mediated pathway, associated with mitochondrial Cx43 phosphorylation at PKCε-target sites (mito-P*Cx43).

FGF-2 is present in nuclear and cytoplasmic subcellular sites where it is believed to activate intracrine signaling pathways. There is no information if FGF-2 can exert direct effects on cardiac mitochondria. In a third series of studies I examined the **hypothesis (3)** that FGF-2 can exert direct protective effects on isolated cardiac mitochondria (SSM), by activating a mitochondria-based pathway leading to mitochondrial P*Cx43 and increased resistance to calcium-induced mPTP. Direct FGF-2 stimulation of mitochondrial suspensions from control hearts was

indeed found to upregulate mitochondrial phospho-S262- and -S368 (P* Cx43), and to stimulate resistance to calcium-induced mPTP. Both end-points were abolished in the presence of peptide $\varepsilon V_{1\text{-}2}$, demonstrating a requirement for mitochondrial PKCε activity. The direct protective effects of FGF-2 on mitochondria were inhibited in the presence of SU5402, an FGFR inhibitor, or anti-FGFR neutralizing antibodies. In addition, Western blotting of mitochondrial suspensions revealed presence of anti-FGFR1 reactive bands. It is concluded that an FGFR1-like protein is present at cardiac mitochondria and mediates direct protective effects of FGF-2. This newly identified intracellular mechanism of cytoprotection implies that endogenous intracellular levels of FGF-2 protein expression may determine constitutive levels of cardiac mitochondrial resistance to mPTP.

ACKNOWLEDGEMENTS

First and foremost, I would like to express my deepest gratitude and thanks to my mentor and supervisor, Dr. Elissavet Kardami, for giving me the opportunity to study under her guidance and always keeping her door open for me. Thank you very much for your constant encouragement, understanding, guidance, patience, mentorship, and all your help at both the scientific and personal level. Thank you is not enough for the support you have given me all these years. Thank you Vetta for everything!

I would like to thank my advisory committee: Dr. Grant Hatch, Dr. Thomas Netticadan, and Dr. Peter Zahradka for their constant support, advice, and encouragement throughout my studies. I would like to further thank to Dr. Balwant S. Tuana for being the external examiner and his helpful and constructive comments. Thank you very much!

I would like thank to the Kardami lab. My special thanks to Dr. Barbara Nickel for being an awesome second supervisor and troubleshooter for the experiments. Thank you very much for all your help and advice over the years. Thank you Barb!!! Great thanks to Janna Makazan for all the help in mitochondrial techniques. Big thanks to Robert Fandrich for all the help with experimental techniques (and new interesting English vocabulary). Thank you to past and present students in the Kardami lab, Sarah Jimenez, Maya Jeyaraman, (Oba)Ma Xin, Jon-Jon Santiago, and Navid Koleini for their friendship, encouragement, support, interesting conversations (and silly stories too!!), laughs, and learning together. Thanks to all of you for making the lab enjoyable, fun, and great place to do research.

I would like to extend my thanks to the Department of Physiology and Pathophysiology, especially Dr. Peter Cattini, Dr. Janice Dodd, Ms. Gail McIndless, and Ms. Judy Olfert for all your support and helping me from the beginning and throughout my studies.

I would like to further thank to the Manitoba Health Research Council (MHRC) and Institute of Cardiovascular Sciences for financial support for my Ph.D studies.

I would like to thanks my sister (Ms. Kanjasorn), brother (Mr. Pitchapat), and the Reimers for their love, understanding, support and encouragement. Lastly, I would like to thank my dear parents (Mr. Sombat and Mrs. Pitchanun Srisakuldee) for your continuous love, constant encouragement, support, guidance and for being there for me always. Thank you for everything!!!

LIST OF FIGURES

Page

LIST OF TABLES

LIST OF ABBREVIATIONS

AcCN	Acetylcarnitine
ADP	Adenosine diphosphate
AIF	Apoptosis-inducing factor
AMO	Amobarbital
AMPK	AMP-activated protein kinases
ANT	Adenine nucleotide translocase
ATP	Adenosine triphosphate
AV node	Atrioventricular node
Bid	BH3-interacting domain death agonist
BSA	Bovine serum albumin
BZ	Border zone
Ca^{2+}	Calcium
$[Ca^{2+}]_i$	Intracellular calcium
CaMKs	Calmodulin-dependent protein kinases
cAMP	Cyclic adenosine monophosphate
cGMP	Cyclic guanosine monophosphate
Cox II	Cytochrome C oxidase subunit II
CPT-I	Carnitine palmityl transferase
CRC	Calcium retention capacity
Cx43	Connexin43
CsA	Cyclosporine A
Cyp-D	Cyclophilin -D
DCM	Dilated cardiomyopathy
DMEM	Dulbecco's modified Eagle's medium
DMSO	Dimethyl sulfoxide
D-Cx43	Dephosphorylated connexin 43

Dzx	Diazoxide
EGFR	Epidermal growth factor receptor
Endo G	Endonuclease G
eNOS	Endothelial nitric oxide
ER	Endoplasmic reticulum
ERKs	Extracellular signal-regulated kinases
ETC	Electron transport chain
FADD	FAS-associated death domain protein
$FADH_2$	Flavin adenine dinucleotide
FGF-2	Fibroblast growth factor-2
FGFR	Fibroblast growth factor receptor
GAPDH	Glyceraldehyde 3-phosphate dehydrogenase
GE	Glycyrrhetinic acid
GJIC	GJ-mediated intercellular communication
GJs	Gap junctions
GPCRs	Gi-protein-coupled receptors
GSH	Glutathione
GSK-3β	Glycogen synthase kinase-3β
HCM	Hypertrophic cardiomypathy
HK II	Hexokinase II
H_2O	Water
H_2O_2	Hydrogen peroxide
HTRA2	High temperature requirement protein A2
IAP	Inhibitor of apoptosis protein
ICD	Intercalated disk
IFM	Interfibrillar mitochondria
IP3	Inositol triphosphate

IPC	Ischemic preconditioning
I-R	Ischemia-reperfusion
JNKs	c-Jun N-terminal kinases
kDa	Kilodalton
K-H	Kreb-Henseleit perfusion solution
LDH	Lactate dehydrogenase
LV	Left ventricle
LVDP	Left ventricular developed pressure
$\Delta\Psi m$	Mitochondrial membrane potential
MAOs	Monoamine oxidases
MAPK	Mitogen-activated protein kinase
Mc	Mitochondrial cristae
MF	Myofibril
MI	Myocardrial infarction
MIS	Mitochondrial intermembrane space
MitoCx43	Mitochondrial connexin 43
MitoK_{ATP} channel	Mitochondrial ATP-sensitive potassium channel
MitoPKCε	Mitochondrial protein kinase Cε
MnSOD	Manganese superoxide dismustase
MOMP	Mitochondrial outer membrane permeability
mPTP	Mitochondrial permeability transition pore
mTOR	Mammalian target of rapamycin
MVO_2	Myocardial oxygen consumption
$[Na^+]_i$	Intracellular sodium
NADH	Nicotinamide adenine dinucleotide
NHE	Sodium hydrogen exchanger
NCX	Sodium calcium exchanger

O_2	Oxygen
O_2^-	Superoxide
O.D.	Optical density
ODDD	Oculodentodigital dysplasia
OMM	Outer mitochondrial membrane
Ox-Phos	Oxidative Phosphorylation
Δ pH	pH gradient
Δp	Proton-motive force
P.AB	Rabbit polyclonal anti-Cx43 antibody
P-Cx43	Phosphorylated connexin 43
P*Cx43	Above normal phosphorylation of Cx43 at PKCε sites, serine 262 and 368
PCD	Programmed cell death
pH_i	Intracellular pH
Pi	inorganic phosphate
PiC	Phosphate carrier
PIC	Protease inhibitor cocktail
PI3K	Phosphotidylinositol 3-kinase
PKA	Protein kinase A
PKB	Protein kinase B (or AKT)
PKCε	Protein kinase Cε
PKG	Protein kinase G
PMA	Phorbol 12-myristate 13-acetate
PPIC	Phosphatase inhibitor cocktail
PRX	Peroxiredoxins
PVDF	Polyvinylidene difluoride
RIPs	Receptor-interacting proteins

ROS	Reactive oxygen species
S262/S368	Serine 262/ serine 368
SA node	Sinoatrial node
SDS	Sodium dodecyl sulfate
SSM	Subsarcolemmal mitochondria
TAK-1	Transforming growth factor-β activated kinase-1
tBID	Truncated BID
TBST	Tris- buffered saline with TWEEN-20
TCA cycle	Tricarboxylic acid cycle (or citric cycle)
TrkB	Neurotrophin receptor (TrkB)
VDAC	Voltage-dependent anion channel
Wt	wild-type

LIST OF COPYRIGHT MATERIAL FOR WHICH PERMISSION WAS OBTAINED

Some of the works presented in this thesis has been previously published and is reproduced here by permission. Publications include:

1. Phosphorylation of connexin-43 at serine 262 promotes a cardiac injury-resistant state.

Srisakuldee W, Jeyaraman MM, Nickel BE, Tanguy S, Jiang ZS, Kardami E. Cardiovascular Research. 2009 September 1; 83(4):672-81.

Contributions: I did all the *ex vivo* experiments, analyzed the data, drafted the manuscript, and revised as required. This work is presented in the section 1 of the thesis.

2. The FGF-2-triggered protection of cardiac subsarcolemmal mitochondria from calcium overload is mitochondria connexin 43-dependent.

Srisakuldee W, Makazan Z, Nickel BE, Zhang F, Thliveris JA, Pasumarthi KB, Kardami E. Cardiovascular Research. 2014 July 1; 103 (1):72-80.

Contributions: I did all the experiments, analyzed the data, drafted the manuscript, and revised as required. This works is presented in the section 2 of the thesis.

Copies of the permission letters are attached at the end of this thesis as an appendix.

CHAPTER 1. LITERATURE REVIEW

I. CONNEXIN 43 AND CARDIOPROTECTION

I-1. Gap junction channels, hemi-channels, and connexin 43

Gap junctions (GJ) are low-resistance, non-selective trans-membrane channels which connect the cytoplasm of neighboring cells to permit the passage of ions, amino acids, nucleotides, glucose, and small metabolites with a molecular weight up to 1.0 kDa (Goodenough et al., 1996). Intercellular communication via GJ channel is essential for electrical and metabolic coupling of cells (Bedner et al., 2003; Beyer et al., 1990; Laird, 2006). GJ exist in all cell types with the exception of mature skeletal muscle, spermatocytes, and blood cells (Simburger et al., 1997; Simon and Goodenough, 1998). GJ channels play significant roles in embryonic development, electrical coupling, metabolic transport, cell differentiation, homeostasis, apoptosis, and carcinogenesis (Dobrowolski and Willecke, 2009; Laird, 2010; Naus and Laird, 2010).

GJ channels are made up of proteins encoded by the connexin gene family, which is comprised of at least 20 different connexins in rodents and 21 connexins in humans and all are named according to their molecular weights (Willecke et al., 2002). All connexins have a similar structure, consisting of four highly conserved α-helical transmembrane domains, two extracellular loops, one intracellular loop and the amino (N) and carboxyl (C) terminal domains. The N- and C-terminals are located intracellularly. The intracellular domains are important for cellular

regulation. The third intracellular domain is involved in pore formation (Hoh et al., 1991)

A connexon or hemi-channel is composed of six connexin subunits arranged hexagonally around an aqueous pore. Most cells can express different types of connexins, which may oligomerize into homomeric (formed by an identical type of connexin) or heteromeric (formed by combination of different types of connexins) hemi-channels. Each GJ channel is formed by docking of two opposing hemi-channels (or connexons), interacting via intra-molecular disulfide bonds. Each extracellular loop has three highly conserved cysteine residues, which are responsible for the formation of the disulfide bonds (Hoh et al., 1991; Severs, 1994).

Pore dimension of GJs range from approximately 6.5-15 Å, which is wide enough to allow the passage of all cations and anions as Ca^{2+}, Na^{+}, K^{+}, Cl^{-}, second messengers as IP3, cAMP, cGMP, and water, and molecules of up to 1 kDa, depending on the connexin type, or charge of the permeating molecule (Goodenough et al., 1996).

GJ channels are gated ion channels with regulation of gating different for each type of connexin. Conductance of GJ is controlled by several factors, such as transjunctional voltage, pH (Ek-Vitorin et al., 1996), intracellular calcium ($[Ca^{2+}]_i$), connexin phosphorylation (Lampe and Lau, 2000) and composition of extracellular fatty acid. In cardiomyocytes, the conductance of single channels ranges from ≈20 pS for Cx45 channels to ≈75 pS for Cx43 channels and ≈200 pS for Cx40 channels (Jansen et al., 2010)

In the heart, GJ channels provide rapid propagation of electrical impulse along the conductive system to coordinate rhythmic cardiac muscle contraction. GJ are primarily located at the intercalated disk (ICD) region, representing a specialized junctional area between cardiomyocytes (Rodriguez-Sinovas et al., 2012).

Three different types of connexins, Cx40, Cx43, and Cx45, are expressed in the myocardium (Alcolea et al., 1999; Kaba et al., 2001; Van Kempen et al., 1996). Cx43, the major Cx in heart and working cardiomyocytes, is predominantly expressed in the ventricles (Beyer et al., 1987), Cx40 is mostly expressed in atria and Cx45 in the conduction system, the sinoatrial node (SA node), atrioventricular node (AV node), and His-bundle (Coppen et al., 1998). In cardiomyocytes, the bulk of Cx43 is localized at the sarcolemmal membrane, although a fraction of cellular Cx43 is present at the inner membrane of mitochondria (Boengler et al., 2005)

Cx43 is a phosphoprotein that contains several phosphorylation sites at the carboxy terminal tail. These phosphorylation sites include 6 tyrosine and 21 serine residues (Lampe and Lau, 2004; Remo et al., 2012). Under physiological conditions cardiac Cx43 is found in an extensively phosphorylated state. A significant reduction of total Cx43 protein, accompanied by Cx43 dephosphorylation, is associated with several types of heart diseases (Lerner et al., 2001). Phosphorylation of Cx43 plays an essential role in Cx43 function by regulating all Cx43 properties, including intracellular assembly, trafficking, protein-protein interactions, metabolic and electrical coupling (Lampe and Lau, 2000, 2004; Solan and Lampe, 2009), and the ability of Cx43 to act as a suppressor of proliferative growth (Doble et al., 2004).

Several kinases are implicated in Cx43 phosphorylation, including protein kinase A (PKA)(Darrow et al., 1996), protein kinase B (Akt)(Shaw et al., 1998), protein kinase C (PKC)(Doble et al., 2004; Doble et al., 2000; Lampe and Lau, 2000), extracellular signal-regulated kinase (ERK)(Warn-Cramer et al., 1996), non-receptor tyrosine kinase src (Kanemitsu et al., 1997), casein kinase 1 (Cooper and Lampe, 2002) and p34cdc2 (Solan and Lampe, 2009). Changes in Cx43 phosphorylation are associated with pathologic GJ remodeling. In a transgenic mouse model of human oculodentodigital dysplasis (ODDD) which is caused by mutations in the Cx43 gene, the defects are in the phosphorylation of Cx43 at serine (S) 365, S325, S328 or S330. These ODDD mice showed significant abnormalities of cardiac impulse propagation and increased vulnerability to cardiac arrhythmias (Kalcheva et al., 2007; Paznekas et al., 2003). Another mutation in the carboxyl terminal phosphorylation sites of Cx43 (at S364) causes the cardiac malformation visceroatria heterotaxia (Britz-Cunningham et al., 1995).

The role of GJ-mediated intercellular communication (GJIC) during cell injury is not well understood, as both negative and positive effects of GJIC have been reported. During reperfusion, GJ are reported to propagate hypercontracture and cell death between connected cardiomyocytes. Spreading of hypercontracture is associated with passage of Na^+ from dying cells to adjacent cells, and subsequent influx of Ca^{2+} through secondary Na^+/Ca^{2+} exchange (Ruiz-Meana et al., 1999). Administration of the GJ uncoupler heptanol at the onset of reperfusion inhibited cell-to-cell propagation of cardiomyocyte death, resulting in a reduction of infarct size (Garcia-Dorado et al., 1997). The protective effect has been shown with other

chemically unrelated GJ uncouplers, such as 18α-glycyrrhetinic acid, palmitoleic acid and halothane (Garcia-Dorado et al., 2004; Rodriguez-Sinovas et al., 2004).

The role of GJ in the propagation of cell injury was confirmed by substituting Cx43 with Cx32 in a transgenic mouse model. Cx32 is a main connexin isoform in liver, oligodendrocytes, Schwann cells, but not in the heart. Replacement of Cx43 by Cx32 in these animals caused lower intercellular permeability and channel conductivity, associated with increased cardiac resistance to I-R injury in isolated hearts (Rodriguez-Sinovas et al., 2010). On the other hand, treatments that increase GJIC, such as peptide Gap134 or the antiarrhythmic peptide rotigaptide (ZP123) decreased infarct size and incidence of ventricular arrhythmias after regional I-R in animal models (Haugan et al., 2006; Hennan et al., 2006; Hennan et al., 2009). The beneficial effects of GJIC are proposed to reflect spreading of survival signals between cells or diluting lethal insults within a larger cell mass during reperfusion (Rodriguez-Sinovas et al., 2012)

Connexin hemi-channels are unopposed channels located in the plasma membrane outside of GJ plaques. Cx43 hemi-channels contribute to the release of mediators to the extracellular space that can activate specific receptors on the plasma membrane of adjacent cells (Kang et al., 2008; Saez et al., 2010). Under physiological conditions, Cx43 hemi-channels are predominantly in a closed state to prevent loss of essential molecules, maintain cellular homeostasis and prevent dissipation of ion gradients, such as Ca^{2+}, Na^{+} and K^{+}. Hemi-channel gating is strictly regulated by various factors, including transmembrane voltage, protein phosphorylation, osmolarity, intracellular pH, and concentration of extracellular

Ca^{2+} (Saez et al., 2005; Saez et al., 2010). Conditions that increase the open probability of hemi-channels result in membrane depolarization and reduction of cytoplasmic metabolites, causing cell death (Bukauskas and Verselis, 2004). Gap26, a specific Cx43 hemi-channel inhibitor peptide that mimics a 13 amino acid sequence in the first extracellular loop of Cx43 (Braet et al., 2003), improved cell viability in rat neonatal cardiomyocytes subjected to ischemic treatment (Shintani-Ishida et al., 2007), and reduced infarct size in isolated rat heart submitted to 40 min of ischemia and reperfusion (Hawat et al., 2010).

Connexin hemi-channels have been implicated in cell volume regulation. Cell swelling ('oncosis') is a hallmark of ischemic cell death (Jennings et al., 1990). Studies using a variety of cell types expressing connexins have shown significant and reversible increases in volume if extracellular calcium is reduced; these changes did not occur in cells lacking connexins, but could be restored after the transient or stable transfection of Cx43. (Quist et al., 2000).

I-2. Connexin 43 and heart disease

Alterations in Cx43 expression and GJ remodeling are a feature of several cardiac pathologies. GJ remodeling is characterized by a significant reduction in GJ, which includes a reduction in Cx43 at the intercalated disks and "laterization" which is redistribution from the junctional region to the lateral periphery of the cardiomyocyte, leading to structural changes and the reduction of electrical stability. It is believed that remodeling of Cx43-constituted GJ cause an irregular impulse propagation and lethal arrhythmia in several forms of heart disease,

including cardiomyopathy, cardiac hypertrophy, and heart failure (Severs et al., 2008).

Ischemic cardiomyopathy (or ischemic heart disease) is a condition where there is a loss or weakening of the heart muscle due to a narrowing of the blood vessels that deliver blood and oxygen to the heart (coronary artery disease). Blockage of the coronary artery causes major changes in formation and propagation of the cardiac impulse. Acute ischemia is associated with closure of GJ channels, leading to a reduction of intercellular and electrical coupling. Cx43 is rapidly dephosphorylated (within 30 minutes)(Jain et al., 2003; Jozwiak and Dhein, 2008; Schulz et al., 2003) and relocated to the lateral sides of the plasma membrane (Beardslee et al., 2000; Huang et al., 1999). The lateralized Cx43 is in a dephosphorylated form due to a deficiency in ATP (Verrecchia et al., 1999), the decreased thermodynamic driving force for Cx43 phosphorylation (Beardslee et al., 2000) and the action of protein phosphatases (PP1, PP2A, calcineurin) (Jeyaraman et al., 2003; Li et al., 2002a). In an isolated adult rat heart model of ischemia-reperfusion (I-R) injury, a progressive dephosphorylation of Cx43 during ischemia was observed together with a significant reduction in the total Cx43 immunofluorescent signal as well as electrical uncoupling (Beardslee et al., 2000). In a neonatal rat ventricular cardiomyocyte I-R model, a slower conduction velocity was detected after a slow recovery from Cx43 dephosphorylation at the onset of reperfusion. This Cx43 re-phosphorylation (recovery from the dephosphorylated state) has been suggested to act as a primary factor for formation of arrhythmogenic substrate by prolonging slow conduction after recovery of the membrane

excitability (de Diego et al., 2008). Additional studies have shown that serine sites, such as S297, 325, 328, 330, or 365, are being phosphorylated in normal heart conditions, but dephosphorylated during ischemia (Axelsen et al., 2006; Lampe et al., 2006; Solan et al., 2007). However, the functional outcomes of (de) phosphorylation at these serine sites are not well understood.

The chronic phase of ischemia refers to healing or healed infarcts associated with the recovering state after myocardial infarction. After the acute infarction, formation of infarct scar surrounded by a border zone (BZ), which separates the injured from normal tissues, is clearly observed. The BZ contains damaged cells with viable muscle fibers and abnormal physiological properties. The last stage of the chronic phase is associated with alterations in Cx43-constituted GJ channel expression and/or intercellular trafficking (Saffitz et al., 1992). The BZ of human healed infarcts presents a heterogeneous redistribution of Cx43 to the lateral sides of cardiomyocytes, adjacent to the normal tissue area (Kostin et al., 2003). Although the normal tissues showed regular Cx43 distribution, a reduction of total Cx43 and changes of cell size distribution were observed. Abnormal Cx43 expression and redistribution/laterization occurs before the increase in fibrosis, indicating an early remodeling post-infarction (Fontes et al., 2012; Severs, 1994).

Hypertrophic cardiomyopathy (HCM; or concentric hypertrophy) is defined as thickening of the left ventricular wall without the dilation of the LV chambers usually associated with pressure overload due to aortic stenosis or chronic hypertension (Lips et al., 2003). In LV tissue from HCM patients, up-regulation of Cx43 expression in the early compensation stage of hypertrophy is reflected as

increased numbers of GJs per ICDs (Kostin et al., 2004). Similar findings occur in the compensation stage of the pressure-overloaded guinea pig and volume overloaded pig hearts (Formigli et al., 2003). In spite of an upregulation of Cx43 in the compensated stage of the pressure overloaded rat heart, hypertrophic cardiomyopathy, and the border zone of human, canine, and rat myocardial infarcts, there is redistribution of Cx43 from ICDs to the lateral sides of cardiomyocytes. Several studies have indicated that Cx43 lateralization is associated with changes in conduction properties of myocardium. (Peters et al., 1993; Salameh et al., 2009; Sepp et al., 1996).

Decompensated cardiac hypertrophy is usually characterized by a progression of myofibril disarray, and fibrosis, leading to contractile dysfunction and heart failure. Down-regulation of Cx43 expression and heterogeneous distribution of GJs are key features of the progression from compensated to decompensated stage of cardiac hypertrophy, as seen in a guinea pig model with chronic aortic stenosis (Kostin et al., 2004; Wang and Gerdes, 1999). A transgenic mouse model with 50% reduction in Cx43, as seen in the HCM patients, shows slow ventricular conduction velocity, and unidirectional conduction block, leading to lethal arrhythmias (Cooklin et al., 1997; Kostin et al., 2004). A marked reduction of Cx43 in the decompensated stage is frequently associated with the heterogeneity of Cx43 distribution. In addition, a large reduction of total Cx43 content in the left ventricle but increase of Cx40 at the endocardial surface were found in idiopathic cardiomyopathy (Dupont et al., 2001). In the rat model of pressure overload induced by aortic banding, the reduction of Cx43 levels, increased dephosphorylated

Cx43 and slowed conduction velocity were observed in the late decompensated stage of hypertrophy (Jin et al., 2010). Taken together, up-regulation of total Cx43 content in compensated hypertrophy is considered to represent an immediate adaptive response to elevated heart workload, whereas the reduction and heterogeneous Cx43 distribution in decompensated hypertrophy play a detrimental role as an arrhythmogenic substrate in hypertrophied and failing hearts (Kostin et al., 2003; Peters et al., 1993). End-stage heart failure due to multiple causes (ischemic heart disease, aortic stenosis, dilated cardiomyopathy, and calreticulin overexpression (Lee et al., 2013) is characterized by a significant reduction in Cx43 levels, disruption of the distribution of GJs between cardiomyocytes, and increased Cx43 dephosphorylation (Kostin et al., 2003; Severs et al., 2008).

Dilated cardiomyopathy (DCM; eccentric hypertrophy) is defined as a thickening of the LV wall in concurrence with an increase in the diameter of the LV chambers, and is usually associated with volume overload from aortic or mitral valve regurgitation, anemia, muscle dysfunction (Lips et al., 2003). Down-regulation of Cx43 expression and laterization are features of DCM consistently observed in patients and experimental animal models with heart failure (Kostin et al., 2003). Collectively, these DCM studies in human and experimental animal models have shown the substantial evidence that alterations of Cx43 expression and distribution are a major cause of cardiac functional block and unstable impulse reentry, leading to ventricular arrhythmias. (Formigli et al., 2003).

I-3. Cardiac Cx43 and cardioprotection

It is increasingly accepted that Cx43 plays an essential role in the development of a cardiac injury-resistant phenotype. Isolated cardiomyocytes (Schwanke et al., 2002), as well as hearts from heterozygous Cx43 deficient ($Cx43^{+/-}$) mice, expressing 50% of the normal Cx43 content, are incapable or deficient in developing an ischemic preconditioning (IPC) cardioprotective response (Heinzel et al., 2005). IPC reduces the ischemia-induced Cx43 dephosphorylation and electrical uncoupling in rat (Jain et al., 2003), rabbit (Miura et al., 2004), and pig hearts (Schulz et al., 2003). Preservation of Cx43 phosporylation status after IPC may be the result of an increase in the interaction of Cx43 with kinases, such as PKC or p38MAPK, and reduced co-localization with phosphatases. The mechanism by which Cx43 mediates cytoprotection is not fully understood, and the role of intercellular communication via GJs in the protective effect is controversial. Heptanol, a GJ inhibitor which dissolves Cx43 from plasma membrane totally eliminates the reduction of infarct size by IPC (Li et al., 2002a), suggesting that intercellular communication is required for IPC-induced cardioprotection in mouse (Li et al., 2002a), rat (Miura et al., 2004), and canine (Papp et al., 2007) hearts and that Cx43 is a key mediator of the signaling cascade of IPC. On the other hand, isolated cardiomyocytes (which do not form GJ) are still capable of an IPC response, unless they have reduced Cx43 content, suggesting that Cx43 can mediate cytoprotection in the absence of GJs. It is possible that Cx43 can regulate the IPC response by both GJ-dependent and independent mechanisms.

Co-localization of Cx43 with protein kinase Cε (PKCε), a known mediator of IPC, suggests a role for Cx43 and its phosphorylation in the cytoprotective mechanism (Doble et al., 2000; Ping et al., 2001; Schulz et al., 2003). In the ischemic pig heart, phosphorylation of Cx43 is well preserved in the preconditioned but not in non-preconditioned hearts (Schulz et al., 2003). These results were confirmed in isolated rat (Jain et al., 2003) and rabbit hearts (Miura et al., 2004).

I-3.1. Cardioprotection by fibroblast growth factor-2 (FGF-2) and Cx43

Several studies from our laboratory, as well as studies from other investigators, have demonstrated the cardioprotective effect of low molecular weight (18 kDa) FGF-2 (Kardami et al., 2007b; Manning et al., 2013). FGF-2 protects neonatal cardiomyocytes from both hydrogen peroxide and serum starvation-induced damage (Padua et al., 1998). Administration of FGF-2 to isolated adult rat heart prior to ischemia results in resistance to ischemia reperfusion injury (Padua et al., 1998; Padua et al., 1995). Post-ischemic (post-conditioning) treatment of isolated adult rat heart with FGF-2 reduces ischemia reperfusion-induced cell death and loss of function (Jiang et al., 2002; Jiang et al., 2004). In addition, intramyocardial administration of FGF-2 provides acute and long-term cardioprotection from functional loss and tissue damage in irreversible coronary ligation *in vivo* (Jiang et al., 2002; Jiang et al., 2004). In mouse hearts, endogenous overexpression of FGF-2, or FGF-2 administration by perfusion, stimulates increased resistance to ischemia-reperfusion injury (Sheikh et al., 2001). FGF-2 administration also protects against doxorubicin-induced cardiotoxicity (Wang et al., 2013).

The cardioprotection afforded by FGF-2 requires fibroblast growth factor receptor 1 (FGFR1) and activation of the PKC signaling cascade (Jiang et al., 2002; Jiang et al., 2004; Padua et al., 1998). Chronic overexpression of FGF-2 results in elevation of activated PKCε and PKCα consistent with the protective effect these PKC isoforms (Sheikh et al., 2001). The downstream target of survival kinases by FGF-2 activation, such as ERK1/2 and Akt, may also contribute to the protective response (Kardami et al., 2007b; Matsunaga et al., 2009).

FGF-2 increases the interaction of Cx43 and PKCε in cardiomyocytes in culture (Doble et al., 2000), resulting in further phosphorylation of Cx43 at specific PKCε target sites, S262, and S368 (Doble et al., 2004). Similar findings were obtained in the adult heart: FGF-2 administration to the non-ischemic rat heart causes increased cardiac Cx43 phosphorylation at S262 and S368 (Srisakuldee et al., 2006). Cx43 is known to act as a suppressor of proliferative growth (Kardami et al., 2007a). The FGF-2-induced phosphorylation of Cx43 at S262 cancelled the anti-proliferative effect of Cx43, enabling stimulation of DNA synthesis in cardiomyocytes and non-myocytes in vitro (Dang et al., 2006; Doble et al., 2004). A causative link between cardiac Cx43 phosphorylation at S262 and the ability of FGF-2, PKCε, and IPC to protect cardiomyocytes from simulated ischemia-induced cell death has also been reported (Jeyaraman et al., 2012; Srisakuldee et al., 2009).

I-3.2. Mitochondrial connexin 43

In addition to Cx43 localization at the plasma membrane, Cx43 was localized in the mitochondria of human umbilical vein endothelial cells, where its levels were upregulated following homocysteine-induced cellular stress (Li et al., 2002b). In

2005, Boengler and colleagues reported for the first time that IPC caused translocation of Cx43 to cardiac mitochondria (Boengler et al., 2005). The same group went on to document that cardiac mitochondrial Cx43 was localized exclusively in the SSM mitochondrial population, at the inner mitochondrial membrane, with its carboxy terminus directed towards the intermembrane space (Boengler et al., 2009; Miro-Casas et al., 2009; Rodriguez-Sinovas et al., 2006). Cardiac mitochondrial Cx43 has been detected in additional experimental models, including mouse, rat, pig, and human left ventricular tissue (Boengler et al., 2005; Rodriguez-Sinovas et al., 2006).

Cx43 protein has no leader sequence for mitochondrial targeting. Studies have shown that Cx43 is transported into the inner mitochondrial membrane by heat-shock protein 90 (HSP90) and the translocase of outer membrane (TOM) complex (Rodriguez-Sinovas et al., 2006). Furthermore, mitochondrial Cx43 is exclusively present in its phosphorylated form, indicating that Cx43 phosphorylation could play an important role in the regulation of mitochondrial Cx43 content (Rodriguez-Sinovas et al., 2006).

There is evidence that mitochondrial Cx43 may play a significant role in the mitochondrial respiration, since mitochondria from Cx43-deficient mice show a reduction of ADP-stimulated respiration and respiratory control ratio compared to wild-type mice (Boengler et al., 2012)

Cx43 is required for cardiac mitochondria to activate cardioprotective mechanisms by IPC (Boengler et al., 2009). Recent studies have shown that IPC protection against reperfusion–induced SSM respiratory failure and oxidative

damage may be independent of cytosolic signaling, since it can be triggered in the isolated mitochondria. The IPC effects are not associated with either mPTP or mitoK_{ATP} channel, but appear to require the presence of mitoCx43 (Ruiz-Meana et al., 2014). Furthermore, normal levels of mitoCx43 are essential for diazoxide-mediated protection (Boengler et al., 2005). The protective action of diazoxide is exerted by stimulating opening of the mitochondrial K_{ATP} channel and the resulting downstream ROS formation (Forbes et al., 2001; Pain et al., 2000). Diazoxide is no longer protective in cardiomyocytes from $Cx43^{+/-}$ mice that present reduction in ROS (Heinzel et al., 2005).

The hemi-channel structure and function of mitochondrial Cx43 may play a significant role in IPC. Low concentration of glycyrrhetinic acid (GE), a GJ uncoupler agent, prevents formation of mPTP induced by supraphysiological Ca^{2+} concentrations in rat heart mitochondria (Battaglia et al., 2008). Isolated heart mitochondria from Cx43KI32 transgenic mice, where endogenous Cx43 is absent and replaced by Cx32, show an inhibitory effect on mitochondrial K^+ influx in the presence of ATP, suggesting that mitochondrial Cx43 contributes to mitochondrial K^+ flux by forming hemi-channel-like structures with a very low conductance or by changing ion-transport in the inner mitochondrial membrane (Miro-Casas et al., 2009)

Presence of carbenoxolone, an inhibitor of Cx43 channels and hemi-channels, or of the peptide Gap19, which acts as a specific Cx43 hemi-channel blocker (Boengler et al., 2013), or genetic Cx43 deficiency, result in suppression of mitoK_{ATP} activation (Miro-Casas et al., 2009; Ye et al., 2003), supporting the notion that

mitochondrial Cx43 hemi-channel function is required to enable mitoK_{ATP} opening, and downstream protective effects.

II. MITOCHONDRIA AND THE HEART

II-1. Energy Production

Cardiac mitochondria generate over 90% of the energy required by cardiomyocytes in the form of the high-energy molecule, adenosine triphosphate (ATP) (Harris and Das, 1991). Approximately 30-40% of the cardiomyocyte volume is made up of mitochondria. Regular cardiac contractile function depends on a high rate of ATP utilization, requiring a high rate of cardiac metabolism (Balaban, 1990; Balaban et al., 1986).

Under physiological conditions, 60-90% of total generated ATP for the heart comes from oxidative phosphorylation (Ox-Phos) of fatty acids. The balance of the remaining 40-10% of the ATP production is from glucose and carbohydrate metabolism via glycolysis (Ashrafian and Frenneaux, 2007; Opie, 1968). Generally, the heart has the metabolic flexibility to switch fuel sources between fatty acids and glucose in order to provide adequate ATP production at a constant rate and amount in the face of varied physiological conditions and substrate availabilities. The contribution of glucose catabolism in the normal heart occurs postprandially and during exercise (Ardehali et al., 2012; Ashrafian et al., 2007; Ingwall, 2009). In the immature heart, glucose or lactate is the main energy substrate, which will be switched to the mature fatty acid metabolic program around 1 week of age (Porter et al., 2011). In the normal adult heart, fatty acid is rapidly esterified to fatty acyl-CoA in the cytosol, then converted to fatty acylcarnitine by carnitine palmityl transferase I (CPT-I) for transport to mitochondria via the carnitine shuttle system. Once inside the mitochondrial matrix, fatty acylcarnitine is converted back to fatty

acetyl-CoA, which undergoes β-oxidation. Then, acetyl-CoA enters the Kreb's cycle (citric acid cycle or tricarboxylic acid cycle: TCA cycle) and is further oxidized by mitochondrial dehydrogenases. During the Krebs cycle, every molecule of acetyl Co-A generates three molecules of reduced nicotinamide adenine dinucleotide (NADH) and one molecule of reduced flavin adenine dinucleotide ($FADH_2$), along with one molecule of ATP. NADH and $FADH_2$ are required for the electron transport chain (ETC) by conveying their electrons to the ETC, which is involved with the electron transfer between an electron donor (NADH) and electron acceptor (O_2) with the transfer of protons across the inner mitochondrial membrane. The ETC is composed of a number of protein complexes that reside in the IMM. Each membrane protein complex has a specific electronegativity (affinity for electrons). The electron transferring through complex I, III, and IV of ETC results in the extrusion of protons from the mitochondrial matrix, generating a mitochondrial membrane potential ($\Delta\Psi m$, negative in matrix) and a pH gradient (ΔpH; alkaline in the matrix). Together, $\Delta\Psi m$ and ΔpH produce the proton-motive force (Δp). The extruded protons re-enter the mitochondria via the F_1F_0 ATPase, which couples the proton transfer down an electrochemical gradient generating ATP to support the cardiac electrical and mechanical activities (Stanley, 2004).

ATP generated in the mitochondria is transferred to the cytosol via transporter pumps. ADP and Pi, from ATP hydrolysis in the cytosol, are returned to the mitochondria to be used for ATP production. Normally, the rates of ATP synthesis and breakdown are well balanced, and associated with the rate of

myocardial oxygen consumption (MVO_2) and generation of NADH by the oxidation of carbon substrates.

II-2. Regulation of cell metabolism

Mitochondria are involved in calcium (Ca^{2+}) homeostasis, the β-oxidation of fatty acids, steroid biosynthesis and ketogenesis.

Cytosolic Ca^{2+} becomes elevated under conditions of increased heart workload. Ca^{2+} enters the mitochondria via mitochondrial Ca^{2+} uniporters and is removed via a sodium calcium exchanger (mNCX). The concentration of mitochondrial calcium ($[Ca^{2+}]_m$) is one of the fundamental factors regulating mitochondrial function and ATP generation. It is required for activation of Krebs cycle enzymes, including pyruvate dehydrogenase, isocitrate dehydrogenase, and α-ketoglutarate dehydrogenase. Physiological elevation of calcium in mitochondria leads to a coordinated upregulation of the Ox-Phos machinery, resulting in increased respiration and ATP output. Mitochondria, together with the endoplasmic reticulum, are one of the main storage compartments for intracellular calcium and as such have a major impact on bioenergetics and anabolic metabolism as well as activation of programmed cell death (Campanella et al., 2004).

In the process of β-oxidation, fatty acids are broken down and imported to mitochondria by the fatty acyl-coenzyme A synthase and carnitine shuttle to generate acetyl-coA, which then enters the Krebs cycle (Houten and Wanders, 2010). In steroid biosynthesis, the mevalonate pathway (HMG-CoA reductase pathway) is processed in the mitochondria and requires some mitochondrial enzymes to convert cholesterol into mineralocorticoids, androgens and estrogens

(Miller, 2011). In conditions where there is a high rate of β-oxidation or low activity level of Krebs cycle (such as the shortage of intermediates during fasting), acetyl-coenzyme A is totally converted to ketone bodies, i.e acetoacetate, acetone, and β hydroxybutyrate, which can be used efficiently by the heart for energy production (Kodde et al., 2007).

Besides being the host for several metabolic processes, the ultrastructure of mitochondria also provides an optimal microenvironment as well as mitochondrial enzymes for multiple biosynthesis and catabolic pathways, including amino acid metabolism (Watford, 1991), the assembly of Fe/S clusters (Lill and Muhlenhoff, 2005), gluconeogenesis, and heme biosynthesis (Ajioka et al., 2006). Taken together, these examples highlight the essential roles of mitochondria in the metabolism of the cell.

II-3. Stress Sensing

Mitochondria are involved in multiple cellular mechanisms to repair damage induced by excessive reactive oxygen species (ROS) production and pathogen invasion, and re-established homeostasis (Kroemer et al., 2010).

ROS (reactive oxygen species) are oxygen-derived molecules, capable of oxidizing other molecules. Generally, the level of ROS is well maintained in the "redox state", the balance between ROS production and their antioxidant system, by the combined activity of mitochondrial, cytosolic, and peroxisomal antioxidant defense systems. Oxidative stress is defined as an imbalance between an excess ROS production and their antioxidant defense mechanisms, leading to their detrimental effects on structural integrity and function of biological tissue.

Approximate 0.2-2% of the oxygen consumed by mitochondrial respiration is converted to superoxide (O_2^-). O_2^- is detoxified to hydrogen peroxide (H_2O_2) by manganese superoxide dismustase (MnSOD), and further converted to H_2O and O_2 by catalases, peroxiredoxins (PRXs), and glutathione peroxidase (GPXs) (Giordano, 2005; Nordberg and Arner, 2001). Mutant mice lacking MnSOD die within the first 10 days of life, due to dilated cardiomyopathy (Li et al., 1995). An increase in O_2^- level, due to partially inhibition of MnSOD, causes hypertrophy and apoptosis in isolated cardiomyocytes (Siwik et al., 1999). These studies indicate the importance of SOD in the regulation of O_2^- , as a byproduct of Ox-Phos. There are 6 PRX isoforms, of which PRX3 and 5 are in the mitochondria. PRXs are responsible for scavenging H_2O_2 in nanomolar levels, due to their high rate constant and high abundance. GPXs are the enzymes that use reducing equivalents of glutathione (GSH) for converting H_2O_2 into H_2O. GPXs have similar rate of constant as PRXs, but are less abundant. GPXs can compete for substrates with PRXs only at the higher concentrations of intracellular H_2O_2 (Winterbourn and Hampton, 2008). Therefore, it is possible that PRXs are important for turning ROS signaling off, whereas GPXs are used for buffering high levels of ROS to a normal level that will not damage the cell or initiate cellular signaling stress responses. Catalase, found only in peroxisomes, has a lower affinity for H_2O_2 and catalyzes the breakdown of H_2O_2 into H_2O and O_2. Activity and expression levels of these antioxidant enzymes are regulated by wide-range of mechanisms and functions in part to control ROS levels.

In response to a mild increase in oxidative stress, mitochondria undergo multiple functional adaptations to reduce an excessive level of ROS. With a small

elevation of ROS, mitochondrial thiols are rapidly oxidized, leading to the alteration of several mitochondrial enzyme activities. Normally, adenine nucleotide translocase (ANT) mediates the exchange between ADP and ATP from the cytosol and mitochondrial matrix. This enzymatic activity is impaired by oxidation, resulting in a shortage of intramitochondrial ADP and inhibition of F_1F_0-ATP synthase. Several protective alterations are rapidly triggered, including activation of the antioxidant defense systems as well as molecular chaperones that counteract ROS-induced protein unfolding. These enzymatic and proteomic alterations maximize the ROS-buffering ability of mitochondria to allow re-establishment of cellular. In contrast, if elevation of ROS persists and is associated with molecular damage (mutation of mitochondrial DNA, protein misfolding, lipid peroxidation) that is beyond recovery, the mitochondrial adaptive response will be changed to the activation of cell death.

Excessive levels of ROS can be triggered in several conditions including hyperglycemia, and ischemia-reperfusion. Importantly, de-regulated ROS production contributes to the pathogenesis of cardiovascular diseases, such as left ventricular hypertrophy, coronary heart disease, congestive heart failure, and cardiac arrhythmias, in conditions with or without the presence of cell death induction (Afanas'ev, 2011).

II-4. Dynamic changes

Mitochondria are dynamic organelles continually changing their morphology through the combined actions of fusion (the interconnected lengthened phenotype), and fission (the discrete fragmented mitochondrial phenotype) (Chen and Chan,

2010; Liesa et al., 2009). The process of fission and fusion in the adult heart was first observed in 1972 (Tandler and Hoppel, 1972). Under normal conditions, the balance of these opposing processes maintains the overall shape, size, number, and function of mitochondria. Disruption of fission and/or fusion causes cellular dysfunction and apoptosis-induced cell death. At the cellular level, mitochondrial fusion and fission are involved in the maintenance mitochondrial morphology, and respiratory capacity, as well as cell division, autophagy, and embryonic development, indicating that mitochondrial dynamics play a key role in quality control of mitochondria. For recent reviews please see (Dorn, 2013; Ong et al., 2013)

II-5. Cell Survival and Cell Death

In response to cellular stress, mitochondria become the main mediator of "programmed cell death" (PCD), an active process of signal transduction leading to cellular demise. PCD can be the result of apoptosis or necrosis, and can also be associated with autophagy (Kroemer et al., 2009; Shaw and Kirshenbaum, 2008). Under physiological conditions, both apoptosis and necrosis are essential for prenatal development and postnatal homeostasis (Fuchs and Steller, 2011). Autophagy, a highly regulated physiological process involved in cell survival and homeostasis, removes excess or damaged organelles, and degrades cellular protein (Klionsky and Emr, 2000). Deregulated PCD is associated with several pathological conditions, including heart diseases, cancer, diabetes mellitus, sepsis, and neurodegenerative disorders.

Apoptosis: Apoptosis-induced cell death is characterized by rounding up of the cell (apoptotic bodies), reduction of cell volume (cell shrinkage), chromatin

condensation, nuclear fragmentation, plasma membrane blebbing, minimal inflammatory response, and no significant alteration of cellular ultrastructure. Cell integrity is preserved until the last stage of the process. Total ATP levels in apoptotic cells are well maintained because of continued production and reduced expenditures (Soldani and Scovassi, 2002; Sun et al., 2004). In mammalian cells, apoptosis is typically mediated by the "extrinsic" and "intrinsic" apoptotic pathways. The extrinsic pathway involves death receptor-mediated apoptosis, while the intrinsic pathway is mitochondrial-induced. These two pathways are highly overlapping by convergence of activation of executioner caspases, such as caspase 3 and 7 (Broughton et al., 2009; Kroemer et al., 2007; Whelan et al., 2010).

The intrinsic pathway is the canonical mitochondrial death pathway that can be initiated by a wide range of cardiotoxic stimuli, such as oxidative stress, DNA damage, cytosolic Ca^{2+} overload, and endoplasmic reticulum (ER) stress. The main regulators of the mitochondrial-based apoptotic pathway are the Bcl-2 family proteins that consist of both anti-apoptotic (i.e. Bcl-2, Bcl_{XL}), and pro-apoptotic proteins (i.e. Bax, Bak, Bad, etc) (Chipuk et al., 2010). In healthy cells, Bax is localized mainly in the cytosol. However, apoptotic stimuli activate conformational changes of Bax causing translocation to the outer mitochondrial membrane (OMM) (Walensky and Gavathiotis, 2011) as well as conformational changes in Bak at the OMM (Cheng et al., 2003). The activation of Bax and Bak induces mitochondrial outer membrane permeabilization (MOMP). In most cases, MOMP is an irreversible point for cell survival. MOMP causes loss of mitochondrial integrity, resulting in the release of pro-apoptotic proteins from the mitochondrial intermembrane space

(IMS) to cytosol, such as cytochrome C, second mitochondria-derived activator of caspase/ direct IAP (inhibitor of apotosis proteins) binding protein with low isoelectric point (Smac/DIABLO), Omi/high temperature requirement protein A2 (Omi/HTRA2), apoptosis-inducing factor (AIF), and endonuclease-G (endo G).

The extrinsic pathway is initiated by the binding of death receptors to their respective ligands, which recruits adaptor proteins, such as FAS-associated death domain protein (FADD), resulting in the assembly of cytosolic death-mediating signal complex. This signal complex triggers activation of an initiator caspase, caspase 8. Active caspase 8 can directly cleave and activate the executioner caspases, caspase 3 and 7, leading to apoptotic cell death (Muzio et al., 1996; Robaye et al., 1991; Suda et al., 1993).

Necrosis: Necrosis was originally believed to be an uncontrolled or accidental form of cell death in response to excessive cellular stress. Recently significant evidence has introduced the concept of programmed necrosis, termed "necroptosis". Unlike apoptosis, necrosis is characterized morphologically by swelling of cells and their organelles (oncosis), lack of nuclear fragmentation, rupture of the plasma membrane, and loss of the intracellular contents, leading to mitochondria dysfunction. Cellular stress or activation of death receptors stimulates a group of serine/threonine kinases, termed "receptor-interacting proteins" (RIPs), and RIP1 and 3 are mediators of necrosis. Activation of RIPs1 and 3 elevate levels of ROS production either through NADPH oxidase (Morgan et al., 2008) or increased mitochondrial oxidant production (Vandenabeele et al., 2010).

A major mitochondrial target of RIP-mediated necrosis is the mitochondrial permeability transition pore, mPTP (described in the following paragraph). While apoptosis is characterized by permeabilization of the OMM, IMM permeabilization and mPTP opening are the main features of necrosis (Krysko et al., 2008; Kung et al., 2011). Opening or formation of mPTP is proposed to activate the apoptotic process when ATP levels are still sustained. A sudden or severe loss of ATP, during prolonged ischemia and in myocardial infarction, will then activate the necrotic death process, due to the loss of electrochemical gradient across the IMM (Lemasters et al., 1999). This ultimately results in matrix swelling and subsequent rupture of the OMM, with release of mitochondrial proteins into the cytoplasm. Later, rupture of the plasma membrane causes release of cytoplasmic proteins, i.e. lactate dehydrogenase and troponin-T, at the site of injury (Krysko et al., 2008). A unique characteristic of necrosis, but not apoptosis, is an inflammatory response from the neighboring cells, due to the release of intercellular contents, proteins and enzymes (Mughal et al., 2012; Whelan et al., 2010).

II-6. Mitochondrial permeability transition pore (mPTP)

The mitochondrial permeability transition pore (mPTP) is the result of a sudden opening of large, non-specific channels that lead to a significant change in permeability of the IMM (Hunter et al., 1976). Opening of mPTP allows communication between cytosol and the mitochondrial matrix. The transient opening of mPTP is essential physiologically in regulating calcium homeostasis (Korge et al., 2011; Saotome et al., 2009). Under pathological conditions, prolonged mPTP opening permits free transport of water and solutes of molecules up to 1.5

kDa into the mitochondrial matrix, leading to mitochondrial swelling and dysfunction. Analysis of mitochondria membrane channel activity in response to Ca^{2+} revealed that mPTP is a voltage-dependent and large conductance (~ 1.2 nS) megachannel (Petronilli et al., 1989; Zoratti and Szabo, 1994; Zorov et al., 1992). mPTP can be stimulated by either direct molecular effects , i.e. $[Ca^{2+}]_m$ elevation, $\Delta\Psi_m$ fall, increase in ROS, inorganic phosphate (Pi), long- chain fatty acids (Schonfeld et al., 2000), Bax (Marzo et al., 1998), Bid (Zamzami et al., 2000), sirtuin-3 (Sadoshima, 2011), p53 (Vaseva et al., 2012), or pathological mechanisms, including ischemia-reperfusion, and drug cardiotoxicity (Marcil et al., 2006; Martel et al., 2012). It should be noted that high concentrations of Mg^{2+}, protons and adenine nucleotides (particularly ADP) are antagonists of mPTP opening, suggesting that the mPTP is an intrinsic and well controlled process (Di Lisa et al., 2009).

There are several methods used to assess the mPTP. In *in vitro* studies, the mPTP can be assessed spectrophotometically by measuring the absorbance/ turbidity of isolated mitochondrial suspensions, which decreases upon mitochondrial swelling caused by the mPTP (Ruiz-Meana et al., 2006). An enzymatic assay can be used to measure the accessibility of mitochondrial enzymes, such as citrate synthase (Belzacq-Casagrande et al., 2009). mPTP can be examined *in situ* using fluorescent probes, calcein/cobalt (Petronilli et al., 1999).

In spite of essential roles for the mPTP in both physiological and pathological conditions, the molecular composition of proteins forming the mPTP remains unknown. Based on biochemical and pharmacological studies, the mPTP was proposed to be a result of a protein complex forming between the voltage-

dependent anion channel (VDAC) in the OMM, the adenine nucleotide translocase (ANT) in the IMM, and cyclophilin-D (Cyp-D) in the matrix (Halestrap et al., 2004; Weiss et al., 2003). In the closed state, Cyp-D is detached from ANT, the IMM component, while hexokinase II (HKII) is attached to VDAC, the OMM component. Opening of the mPTP, which is regulated by both Ca^{2+} and inorganic phosphate (Pi), is facilitated by the binding of Cyp-D to ANT. However, recent studies using gene-targeted mice for each of the components of the mPTP failed to confirm this model. In fact, mitoplasts (mitochondria without OMM) and cells lacking all three isoforms of VDAC are susceptible to mPTP opening in response to Ca^{2+} overload, indicating that VDAC is dispensable and therefore no longer included in the model as an essential component of mPTP structure (Baines et al., 2007). ANT, another key candidate of the mPTP, consists of different isoforms. ANT1, the main isoform in cardiac and skeletal muscle, interacts with Cyp-D at the contact sites between the inner and outer mitochondrial membrane. Studies using targeted expression of ANT1 in rat heart showed a cardioprotective effect in a model of cardiomyopathy (Wang et al., 2009). In liver mitochondria lacking both ANT1 and 2, mPTP opening still occurred in response to Ca^{2+} overload. These experiments suggest that although ANTs are non-essential structural component of the mPTP, they may act as a peripheral regulatory protein associated with sensitivity to adenine nucleotides and ANT ligands (Kokoszka et al., 2004).

Another promising candidate as an essential component of the mPTP is cyclophilin D (Cyp-D). Cyclosporine A (CsA), an immunosuppressant, inhibits mPTP opening by binding to Cyp-D in mitochondria (Davidson and Halestrap, 1990;

Griffiths and Halestrap, 1991). Unlike VDAC and ANT, Cyp-D consists of only one gene, the *Ppif* gene. Cyp-D-null mice show a higher level of cardiac resistance to ischemia-reperfusion injury than their wild type counterparts (Baines et al., 2005; Nakagawa et al., 2005). Mitoplasts from Cyclophilin D-deficient mitochondria, however, could still display calcium-induced mPTP, consistent with the notion that Cyclophilin D is a regulator of mPTP opening, if not an essential structural component of the pore (Basso et al., 2005; De Marchi et al., 2006).

Several proteins have been proposed to regulate mPTP opening. The mitochondrial phosphate carrier (PiC) interaction with Cyp-D can be enhanced by mPTP-inducing agents, whereas the interaction is reduced with compounds that inhibit the mPTP. Inhibition of mitochondrial Pi transport can block mPTP formation in isolated mitochondria (Leung et al., 2008). Using an RNA interference approach in HeLa cells, reduction of PiC expression by 65-80% did not prevent either mitochondrial calcium accumulation or mPTP formation (Varanyuwatana and Halestrap, 2012). Further genetic analysis is required to determine how PiC is involved in the mPTP. Creatine kinase, hexokinase, translocator protein, and Bcl-2 family members have also been proposed as key candidates for the mPTP. However, genetic deletion studies are required to show the exact identity of the mPTP protein components (Baines et al., 2007; De Marchi et al., 2004).

Opening of the mPTP does not occur during ischemia due to intracellular acidosis (low pH) with high concentrations of Mg^{2+}, ADP and low ROS production. Permeability transition occurs after 2 min of reperfusion when the pH has returned to normal (Halestrap et al., 2004). Prolonged opening of mPTP mediates cell death

in response to ischemia-reperfusion. Upon reperfusion, the recovery of normal pH with a burst of ROS formation in the presence of high $[Ca^{2+}]_m$ and Pi appears to be the perfect condition for opening of mPTP. The large pore size (1.5 kDa) permits H^+ ions to enter the matrix and causes dissipation of the $\Delta\Psi_m$, uncoupling of the electron transport chain (ETC) and inhibition of ATP synthesis (Baines, 2010). Pharmacological inhibitors of Cyp-D, such as cyclosporine-A, sangliferine-A, Debio-025, have a beneficial effect against ischemia-reperfusion-mediated cell death in all tissues tested, such as small bowel (Puglisi et al., 1996), liver (Saxton et al., 2002), heart (Clarke et al., 2002; Di Lisa et al., 2009), kidney (Singh et al., 2005), and brain (Muramatsu et al., 2007). A hypothetical model of the formation of the mPTP is included in Figure 1.

Figure 1 Mitochondrial permeability transition pore

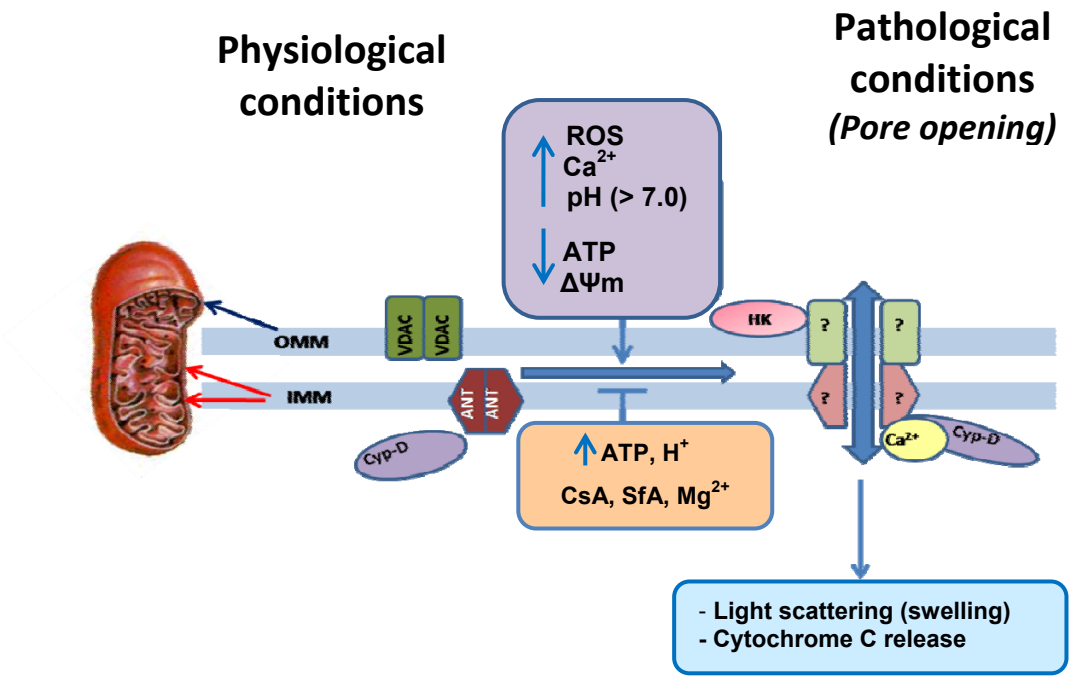

The mitochondrial permeability transition pore (mPTP) is a large, non-specific pore, that allows free movement of solutes across the inner (IMM) and outer (OMM) mitochondrial membranes. The molecular composition of mPTP is unknown, but it is believed to be a multi-protein complex forming at the IMM. Proteins implicated in pore formation or regulation include the voltage-dependent anion selective channel (VDAC; an OMM protein) the adenine nucleotide transferase (ANT) at the IMM and cyclophilin D (Cyp-D) in the mitochondrial matrix (Baines et al., 2007). Hexokinase (HK) is also implicated in pore regulation. The pore forms/opens under pathological conditions, such as accumulation of mitochondrial Ca^{2+}, a burst of ROS production, and depletion of ATP. Formation/opening of the mPTP results in loss of ionic homeostasis, dissipation of membrane potential, matrix swelling, and membrane rupture, causing release of apoptogenic proteins, such as cytochrome c, from the intermembrane space. In isolated mitochondria, measurements of mitochondrial matrix swelling, and release of cytochrome C are used to monitor the activity of mPTP. Elevation of ATP, an acidic environment, and pharmacological blockers of cyclophilin D, such as cyclosporine A (CsA) and sanglifehrin (SfA), results in the inhibition of mPTP opening.

II-7. Cardioprotection and mitochondria

Ischemic and pharmacological preconditioning

It is well established that brief periods of ischemia and reperfusion elicit a potent self-defense response ('ischemic preconditioning', IPC) that can protect the heart from cell death and contractile dysfunction caused by subsequent prolonged ischemia and/or reperfusion (Murry et al., 1986). It is now known that several substances can simulate some or all aspects of the IPC response, causing pharmacological preconditioning. Several signaling pathways have been identified as playing important roles in preconditioning. Preconditioning is associated with the activation of G_i-protein –coupled receptors (GPCRs), and/or tyrosine kinase receptors at the plasma membrane of cardiomyocytes. This is followed by downstream phosphorylation/activation of key kinases such as, PKCε, AKT, and ERK1/2, that can target several subcellular domains to affect a protective response. For example, activated AKT is released from the plasma membrane to the cytosol, and cytosolic Akt transmits a signal from PI3K to the ERK1/2-endothelial nitric oxide (eNOS)-protein kinase G pathway, which stimulates mitochondria and causes opening of the mitochondrial ATP-sensitive K^+ channel (mitoK_{ATP}). Opening of mitoK_{ATP} induces low levels of ROS generation, leading to activation of mitochondrial-based cardioprotective mediators, such as PKCε, ERK1/2 and Akt (Downey et al., 2007).

Mitochondrial entities linked to cardioprotective/survival signaling include the mitoK_{ATP} channel, and mPTP. Inhibition of mPTP opening is an ideal target for cardioprotective interventions and/or manipulations aimed at maintaining

cardiomyocyte viability. Cyclosporin A, which inhibits mPTP opening by binding to cyclopillin D (Fournier et al., 1987), shows a protective effect against reperfusion injury in isolated cardiomyocytes (Griffiths et al., 2000), and intact hearts (Griffiths and Halestrap, 1993). In clinical studies, Cyclosporine A is able to reduce infarct size by 20% in MI patients (Piot et al., 2008).

Several studies have focused on a protective role for the mitoK$_{ATP}$ opening (Garlid et al., 1997; Garlid et al., 2006). Upon opening of mitoK$_{ATP}$, the influx of K^+ into the matrix causes mitochondrial depolarization along with matrix swelling and alkalinization. This type of mitochondria swelling causes an increase in efficiency of energy metabolism in normoxic cardiomyocytes and accelerates the recovery of normal ATP concentrations during post ischemia reperfusion by preventing substrate loss (Kowaltowski et al., 2001). MitoK$_{ATP}$ channel openers, such as diazoxide (Dzx), have been shown to be protective in several animal models (Grover et al., 1989). Dzx reduces the calcium-induced mPTP as measured by loss of mitochondrial calcein in adult rat cardiac mitochondria, suggesting a connection between the opening of mitoK$_{ATP}$ channel and mPTP inhibition (Hausenloy et al., 2002).

Overall, most protective mechanisms require the opening of mitoK$_{ATP}$, a mild increase of ROS production and activation of PKCε (Costa et al., 2008; Downey et al., 2007; Garlid et al., 2009). In terms of mitochondrial-based signaling, PKCε forms a complex with mitogen-activated protein kinases (ERKs, JMKs, and p38 MAPK) and mitochondrial proteins (VDAC, ANT, and HKII) (Baines et al., 2002). In mice overexpressing active PKCε, the threshold of Ca^{2+}-induced mPTP opening is

significantly increased with highly phosphorylated mitochondrial ERKs and PKCε binding to VDAC1, ANT and HKII. Phosphorylation of ERK1/2 blocks the opening of mPTP via GSK-3β phosphorylation (Rasola et al., 2010). A GST-pull-down assay *in vitro* found VDAC1 to be a direct binding partner with PKCε (Baines et al., 2003). Taken together, these findings have suggested that activated PKCε inhibits mPTP opening via the signaling of ERK-GSK.

In addition to its role in signal transduction, PKCε-mediated IPC is associated with attenuation of ATP hydrolysis and preservation of ATP levels during ischemia (Fryer et al., 2000; Kida et al., 1991; Kobara et al., 1996; Laclau et al., 2001; Murry et al., 1986; Wang et al., 2001; Yabe et al., 1997). In PKCε-overexpressing preconditioned hearts, the reduction of ATP was significantly delayed during ischemia compared to non-transgenic hearts (Cross et al., 2002).

II-8. Cardiac subsarcolemmal and interfibrillar mitochondria

Cardiac mitochondria can be divided into two distinct subpopulations based on location: subsarcolemmal (SSM), and interfibrillar (IFM) mitochondria. SSM are located beneath the sarcolemma, whereas IFM are densely distributed in parallel rows between myofilaments (Palmer et al., 1977). Despite being present within the same cell, SSM and IFM possess different functions (i.e. respiration), morphology, composition (i.e lipid and protein), and biochemical properties (i.e. metabolic enzyme activities) (Lesnefsky et al., 2001; Monette et al., 2010; Muller, 1976; Palmer et al., 1977; Riva et al., 2005). Under normal conditions, both SSM and IFM are efficient in controlling the cellular ATP-processes and maintaining ionic homeostasis of cells. IFM have a greater rate of ADP-stimulated (state III)

respiration, and oxidative phosphorylation (~150% in SSM)(Palmer et al., 1977, 1985), resulting in elevation of respiratory cytochromes and activity of electron transport chain complexes (Asemu et al., 2013), whereas the coupling of respiration is similar in both sub-populations (Lesnefsky et al., 1997). Studies on the morphology of SSM and IFM using electron microscopy and high resolution scanning electron microscopy (HRSEM) reveal that SSM are round in shape and larger in size, with predominantly lamelliform cristae, while IFM are smaller and elongated with a tubular cristae structure (Riva et al., 2005). It is not known how the difference in cristae configuration may relate to differences in function between these two sub-populations. It has been suggested that the differences in intracellular location determine the role of these two mitochondrial sub-population: SSM are involved in mediating sarcolemmal signaling pathways regulating ion homeostasis (Bell et al., 1992; Palmer et al., 1986; Riva et al., 2005), whereas IFM are the primary energy source for myosin ATPase and the contractile apparatus (Kuznetsov et al., 2009; Ritov et al., 2005; Vendelin et al., 2005).

These two sub-populations respond differently in pathologic conditions, including calcium overload (Palmer et al., 1986), cardiomyopathy (Hoppel et al., 1982), aging (Fannin et al., 1999), diabetes, and ischemia-reperfusion injury (Kajiyama et al., 1987; Lesnefsky et al., 1997; Shin et al., 1989; Ueta et al., 1990).

Ischemia reperfusion injury: During ischemia, mitochondrial ATP is reduced significantly and ionic pumps fail to maintain Na^+/K^+ gradients across the sarcolemmal membrane, resulting in accumulated cytosolic Ca^{2+}. During reperfusion, oxygen rapidly restores mitochondria membrane potential and leads to

excessive uptake of Ca^{2+} into the mitochondria, which promotes opening of the mPTP. Both SSM and IFM are affected by ischemia, but mitochondrial damage occurs more rapidly in SSM. IFM are more resistant to calcium-induced mPTP opening than SSM, as seen by their larger Ca^{2+} retention capacity and Ca^{2+}-induced cytochrome C release (Hofer et al., 2009; Khairallah et al., 2010; Palmer et al., 1986). Inhibition of electron transport at complex I by amobarbital (AMO), a short –acting barbiturate that specifically inhibits complex I of the electron transport chain (ETC), preserves respiration in SSM during ischemia, indicating the ETC itself is the source of mitochondrial damage (Chen et al., 2006; Lesnefsky et al., 2004). Prior to ischemia, cytochrome C oxidase (an electron carrier that transfers electrons between complexes III and IV) is similar in both SSM and IFM in adult heart (Lesnefsky et al., 2001). Thirty minutes of ischemia impairs the distal electron transport chain of SSM only, leading to a decrease in the rate of Ox-Phos through a decrease in cytochrome C oxidase content (Lesnefsky et al., 1997) thus limiting the capacity of SSM to generate ATP for maintaining transsarcolemmal ion pumps which are critical for homeostasis at the time of reperfusion.

Cardiolipin, an inner mitochondrial membrane phospholipid (Lesnefsky et al., 2001), is an integral component of complex III (Fry and Green, 1981; Gomez and Robinson, 1999) and IV (Fry et al., 1980; Robinson et al., 1980). Cardiolipin is susceptible to lipid peroxide formation, which is a main target of ROS production from the ETC. Decreased cardiolipin content or the presence of oxidized cardiolipin lead to increased inner membrane permeability (Hoch, 1998; Sparagna and Lesnefsky, 2009). During ischemia, the cardiolipin content in SSM decreases without

alteration in composition, while the content of other phospholipids is preserved. In IFM, the cardiolipin content is unchanged during ischemia. Therefore, cardiolipin in SSM is an early target of the ischemia-induced mitochondrial damage.

Studies by Holmuhmedov *et al* (2012) have shown that diazoxide, a mitochondria ATP-sensitive K^+ channel opener with cardioprotective properties, protects SSM against excessive Ca^{2+} overload by inducing inner membrane depolarization, decreased Ca^{2+} uptake, and release of accumulated Ca^{2+}, resulting in preservation of ATP production. Diazoxide restores excessive mitochondrial Ca^{2+}-inhibited state III respiration in both SSM and IFM, but the magnitude of protection is more prominent in SSM, indicating that SSM is a preferential target for cardioprotective agents in the setting of I-R heart (Holmuhamedov et al., 2012).

Aging: Mitochondria isolated from aged animals have greater rates of oxyradical production (Barja, 1998; Kwong and Sohal, 1998), which are responsible for oxidative damage to mitochondria, including protein sulhydryl oxidation, lipid peroxidation, and mitochondrial DNA damage (Floyd et al., 2001; Van Remmen and Richardson, 2001). Both SSM and IFM are affected by aging. SSM from aged mice (>13 months old) show a 40% decrease in Cx43 protein content compared to SSM from young mice (< 3 months old), while there is no change in the expression levels of PKCε and endothelial nitric oxide synthase (eNOS). The lack of IPC cardioprotection in aged mice is associated with a decreased in Cx43. The reduction of mitoCx43 in aged heart may contribute to the loss of protection by IPC, since normal levels of Cx43 are required for IPC protection (Boengler et al., 2007).

IFM from aged rat hearts (24 months old) show a marked decrease in mitochondrial protein content (~25%), rate of Ox-Phos (25-30%)(Lakatta et al., 1987; Lesnefsky et al., 1994; Wei, 1992), as well as defects in electron transport complex III (Lesnefsky et al., 2001) and cytochrome oxidase complex IV, but not complexes I and II (Fannin et al., 1999). A defect within the ubiquinol-binding site (Q_o) of cytochrome b in complex III of IFM causes an increased in ROS production (Moghaddas et al., 2003) and increased vulnerability to Ca^{2+}-induced membrane permeabilization (Fannin et al., 1999; Hofer et al., 2009; Riva et al., 2006). Defects in oxidative metabolism of IFM in aged heart are associated with impaired heart performance.

The aged heart is more vulnerable and sustains greater damage to ischemia and reperfusion, both in experimental (Lesnefsky et al., 1994; Lucas and Szweda, 1998) and clinical (Lesnefsky et al., 1996) settings. Aging alone does not alter the cardiolipin content or cytochrome C oxidase in either SSM or IFM (from both adult 6 months old and aged 24 months old hearts) (Lesnefsky et al., 2001). However, aged hearts subjected to 25 minutes ischemia, followed by 30 min reperfusion (I-R) show a 3-fold increase in oxidized cardiolipin content in both SSM and IFM. This increase in oxidized cardiolipin content perseveres during reperfusion in the aged heart, suggesting that a markly increased oxidative modification to cardiolipin takes place during ischemia (Lesnefsky and Hoppel, 2008; Lesnefsky et al., 2009). An increased level of oxidized cardiolipin causes a functional defect in the inner mitochondrial membrane and reduction in cytochrome C content, while release of cytochrome C

activates caspase cascades and predisposes the heart to programmed cell death (Ott et al., 2002).

Diabetes: In streptozotocin (STZ)-induced type 1 diabetes, there is a greater stress on cardiac IFM compared to SSM, as indicated by increased superoxide production and oxidative damage, impaired ETC function (decrease in state I and III respiration), and decreased mitochondrial-specific phospholipid cardiolipin content (Dabkowski et al., 2009). IFM from type 1 diabetic hearts are also associated with enhanced apoptotic susceptibility. They have a lower resistance to oxidative-stress induced mPTP opening, decreased cytochrome C and Bcl-2 levels, but increased Bax levels, when compared with IFM from control hearts. However, there is no apparent change in SSM from diabetic hearts (Baseler et al., 2011; Dabkowski et al., 2009; Williamson et al., 2010).

Pressure overload: Chronic pressure overload in a rat model decreased the respiratory capacity of both SSM and IFM but the effect was more pronounced in IFM. The magnitude of change in IFM respiration correlated with loss of contractile function, and supports the notion that IFM are producing ATP for contraction (Schwarzer et al., 2013).

Chronic 'physiological' hypoxia: In rats exposed to chronic hypoxic conditions, both SSM and IFM displayed decreased mitochondrial respiration, associated with down-regulation of different pathways. SSM exhibited a reduction of ETC activity (complex I, II, and IV), linked to a protected phenotype such as decreased ROS production and decreased vulnerability to mPTP. Chronic hypoxia

decreased aconitase activity in IFM, without affecting resistance to stress stimuli (Heather et al., 2012).

In conclusion, the differences in the responsiveness between SSM and IFM to the physiological and pathological states suggest that these two mitochondrial sub-populations are regulated and affected by different cellular pathways.

III. RATIONALE AND HYPOTHESES

There is strong evidence that the membrane protein Cx43, an interacting partner and cellular target of PKCε, is required for cardioprotection. The PKCε-mediated phosphorylation of Cx43 at serine (S) 262 has, furthermore, been shown to regulate the ability of Cx43 to modulate cardiomyocyte proliferative growth, downstream of growth factor (FGF-2) stimulation. In my Masters studies, I showed that administration of the cardioprotective agent FGF-2 to the normal isolated adult rat heart promoted cardiac Cx43 phosphorylation at PKCε-target sites S262 and S368, suggesting the possibility that Cx43 phosphorylation at these sites is a 'marker' of the injury-resistant phenotype.

In the first series of studies, I examined **main hypothesis 1:** several PKCε-mediated cardioprotective manipulations (pre- and post-ischemic FGF-2 treatment, ischemic preconditioning, diazoxide administration) are associated with (a) acute increases in cardiac Cx43 phosphorylation at PKCε-target sites (S262, S368), (b) prevention of ischemia and/or reperfusion-induced Cx43 remodeling.

In addition to its localization at the intercalated disks, Cx43 is present at cardiac subsarcolemmal mitochondria where it is reported to mediate cardiomyocyte resistance to injury. It is currently not known whether the cardioprotective effects of FGF-2 administration extend to protective effects at the mitochondrial level, and/or effects on mitochondrial Cx43 phosphorylation. In a second series of studies, I addressed **main hypothesis 2:** FGF-2 administration to the isolated heart exerts protective effects on cardiac subsarcolemmal and interfibrillar mitochondrial populations; the protective effect on subsarcolemmal

mitochondria (a) is linked to mitochondrial Cx43 phosphorylation at S262 and S368, and (b) is dependent on mitochondrial Cx43 channel function.

FGF-2, which is found in the exracellular matrix, is considered to exert potent cytoprotective effects by activating plasma-membrane receptors, and downstream signaling pathways. FGF-2 is also present in cytosolic and nuclear subcellular sites where it is believed to activate intracrine signaling pathways. There is no information if FGF-2 can exert direct effects on cardiac mitochondria. In a third series of studies, I examined **hypothesis 3**: FGF-2, added to cardiac mitochondrial suspensions, can raise resistance to calcium-induced mPTP, by a mechanism activating a mitochondria-located FGF-2-receptor.

CHAPTER 2. MATERIALS AND METHODS

VI. Methods corresponding to Results section 1

Animals

Adult male Sprague-Dawley rats (250-280 g) were provided by the Central Facility at the University of Manitoba and used as approved by the local Animal Care Committee of the National Research Council of Canada, according to the Guide for the Care and Use of Laboratory Animals of the US National Institutes of Health. Adult male rats were deeply anesthetized with ketamine (90 mg/kg body weight) and xylazine (10 mg/kg body weight); once there was complete lack of reflex response, hearts were excised and used for Langendorff perfusion.

Materials

Recombinant 18 kDa FGF-2 produced in *Escherichia coli* was purified to homogeneity as published previously (Jiang et al., 2002), and used within one month of preparation. Complete list of all antibodies used and their source is shown in Methods Table 1M. All Cx43 antibodies have been fully characterized and validated. In-house rabbit polyclonal anti-Cx43 antibodies (P.AB), recognizing all phosphorylated and non-phosphorylated Cx43 forms (41-45 kDa), were raised against residues 367-382 (Doble et al., 2000). Mouse monoclonal antibodies (#13-8300), recognizing cardiac dephosphorylated (D) 41 kDa Cx43 was raised against residues 360-376, as previously described (Beardslee et al., 2000; Nagy et al., 1997). Rabbit polyclonal anti-P-S262-Cx43 antibodies, recognizing Cx43 phosphorylated at S262, have been validated in several reports (Dang et al., 2003; Doble et al., 2004; Solan and Lampe, 2007, 2008). Briefly, it was demonstrated that anti-P-S262-Cx43

can only recognize Cx43, or the C-terminal tail of Cx43 in cell lysates following PKC stimulation (Dang et al., 2006; Doble et al., 2004). By mutating S262 to alanine, the recognition site for anti-P-S262-Cx43 is abolished, and the antibody no longer recognizes Cx43 in lysates from PKC stimulated cells with this mutation, confirming its specificity (Dang et al., 2006). Rabbit polyclonal anti-P-S368-Cx43, which recognizes Cx43 phosphorylated at S368, has been characterized and validated by several groups (Ek-Vitorin et al., 2006; Miura et al., 2007; Solan et al., 2003; Srisakuldee et al., 2006). Protease inhibitor cocktail (PIC#P8340) was obtained from Sigma – Aldrich. Phosphatase inhibitor cocktails 1 and 2 (Cocktail set II and IV) were obtained from Calbiochem.

Langendorff whole heart perfusion

As previously described (Jiang et al., 2007; Jiang et al., 2002; Jiang et al., 2004; Padua et al., 1998), Kreb-Henseleit perfusion solution (K-H; in mM 118 NaCl, 25 $NaHCO_3$, 4.7 KCl, 1.2 KH_2PO_4, 1.2 $MgSO_4.7H_2O$, 1.25 $CaCl_2.2H_2O$, 11.1 glucose) was freshly made and filtered (1.2µm, Millipore) before use. Adult rats were anesthetized and killed by decapitation. Hearts were rapidly removed, and washed in cold buffer. The atria, extraneous fat, and connective tissue were trimmed off. A short cannula was inserted in the aorta and hearts perfused with oxygenated K-H solution, at 37°C, at a constant pressure of 80 mmHg under non-recirculating conditions. During perfusion, the K-H solution (pH 7.4) was constantly gassed with 95% O_2 and 5% CO_2, and maintained at a temperature of 37 °C.

Cardiac functional measurement

As previously described (Jiang et al., 2007; Jiang et al., 2002; Jiang et al., 2004; Tanguy et al., 2006), a water-filled balloon connected to a pressure transducer was inserted into the left ventricle and inflated to impose an end diastolic pressure of 5 mmHg. Left ventricular end diastolic and systolic pressures were recorded for up to 60 minutes of reperfusion. Left ventricular developed pressure (LVDP) was calculated from diastolic and systolic pressure values.

Heart tissue extraction

At the end of each experiment hearts were frozen in liquid nitrogen and stored at -80°C for no longer than one week. Ventricular tissue (50 mg) was powdered using a mortar and pestle with liquid nitrogen then transferred to a 15 ml tube containing 500 µl (approximate 10 volumes/ weight) cold TNM buffer (10 mM Tris-HCl pH 7.4, 100 mM NaCl, 300 mM sucrose, 2 mM $MgCl_2$, 1% thiodiglycol, 60 mM β-glycerophosphate, and 10 mM NaF) with 0.25% NP40. Protein Inhibitor Cocktail (PIC;Sigma # P8340), and Phosphatase Inhibitor Cocktails 1 and 2 (PPIC1; Sigma #P2850;PPIC2; Sigma#P5726) at dilutions of 1:100 were added to all buffers. All subsequent procedures were done at 4°C. Following homogenization with a glass homogenizer, the homogenate was filtered using Nitex in a Swinnex filter to remove large insoluble material. An equal volume of 2x SDS buffer (20% glycerol, 100 mM Tris-HCl pH 6.8, 2% SDS, 60 mM β-glycerophosphate, 5 mM EDTA, 5 mM EGTA, 2 mM NaOV, 1mM NaF) with inhibitors was added and the samples sonicated at 40 Hz for 3x5 seconds. The extract was boiled for 5 minutes and centrifuged at 21000 g for

15 min at 4°C, to remove residual debris. Supernatants were used for further analysis.

SDS-PAGE and Western blotting

Cardiac lysates (20 μg of protein per lane) or cardiomyocyte culture lysates (5 μg of protein per lane) were analyzed in 10% or 15% polyacrylamide gels, as required. Broad range molecular weight markers (BioRad; range 6.5-200 kDa), or Kaleidoscope molecular weight markers (BioRad; 10.0-250 kDa) were used. Following electrophoresis, protein was transferred to PVDF (Polyvinylidene difluoride) membrane (Roche). For immunodetection, all steps were done at room temperature unless otherwise indicated. To block non-specific binding, membranes were incubated for 1 hour in 3-5% bovine serum albumin (BSA; Sigma) or 10% skim milk (depending on the antibody, as per manufacturer's instruction, in Tris-buffered saline (TBS; 137 mM NaCl, 2.7 mM KCl, 25 mM Tris) with TWEEN-20 (TBST). Following blocking, membranes were rinsed briefly with TBST before adding the primary antibody. Membranes were washed with either 0.1% BSA or 1% milk in TBST between primary and secondary antibodies. Antigen-antibody complexes were detected by enhanced chemiluminescence (ECL$^+$ plus; Amersham Biosciences) and exposure to Kodak X-omat. Immunoblot band density was measured using the Bio-Rad Model GS-800 densitometer with Molecular Analyst software (Bio-Rad).

Immunofluorescence

Transverse 7 μm thick cryosections were obtained using a Microm HM550 cryostat. Tissue sections were fixed with 1% cold paraformaldehyde for 15 minutes.

Cardiac sections were incubated overnight with primary antibodies diluted in 1% BSA in PBS (2.7 mM KCl, 1.5 mM KH_2PO_4, 137 mM NaCl, 8 mM Na_2HPO_4). Antigen-anitobody complexes were visualized after incubation with secondary antibodies: biotinylated anti-rabbit IgG (Amersham Biosciences) at 1:20 dilution in 1% BSA/PBS followed by Streptavidin-Fluorescein (Amersham Biosciences) at 1:20 dilution. Sections stained with mouse primary antibodies were incubated with Texas Red conjugated-anti-mouse IgG (Jackson Laboratories) at 1:100 in 1% BSA/PBS. Nuclei were labeled with 2.5 mM Hoechst dye 33342 (Calbiochem) for 1 min and rinsed thoroughly. Coverslips were mounted with Prolong Antifade Kit (Invitrogen). Images were captured in a Zeiss Axiovert 3.0 epifluorescence microscope.

Experimental design

Various treatments of isolated perfused hearts are described in Figure M1. All groups were subjected to 20 min perfusion with oxygenated K-H (stabilization) before the following treatments: IPC, diazoxide, and FGF-2.

(1) IPC was induced by 3 cycles of 3 minutes global ischemia (complete interruption flow) followed by 5 minutes reperfusion (complete re-establishment of flow).

(2) Diazoxide (Sigma): A stock solution of diazoxide (0.5 M in 0.1 N NaOH) was added to oxygenated K-H to a final concentration of 150 μM. Diazoxide–containing K-H was perfused into hearts for 10 minutes. An equivalent volume of vehicle solution in K-H was used for perfusion of the control group.

(3) Pre-ischemia administration of FGF-2: After equilibration with pre-gassed K-H for 20 minutes, FGF-2 (10μg FGF-2 dissolved in 12 ml K-H) or non-supplemented K-H was infused with a peristaltic pump directly into the main line entering the heart, at 1 ml/min for 12 minutes. This was followed by an additional 8 minutes perfusion with K-H, before either tissue extraction, or global ischemia for 30 min, under normothermic conditions, followed by tissue extraction.

(4) Post-ischemic administration of FGF-2: After 30 minutes global ischemia, FGF-2 supplemented (10 μg FGF-2 dissolved in 12 ml of K-H) or non-supplemented K-H was infused with peristaltic pump directly into the main line of K-H solution re-entering the heart, at 1 ml/minutes for the first 12 minutes of reperfusion period, followed by reperfusion with K-H for another 48 minutes. This procedure results in approximately 4-fold increases (Padua et al., 1995) in heart–associated FGF-2, distributed around cardiomyocytes in a basement-membrane-like pattern.

Statistical analysis

The data are presented as mean ± SD. Statistical significant of differences between 2 groups were compared using unpaired student's t-test analysis. One way analysis of variance (ANOVA) was used when more than 2 groups (one treatment) were compared. Two way ANOVA was used, as needed. All statistics was calculated with software Graph-Instat. The level of significance level was defined as *$P<0.05$, **$P<0.01$, ***$P<0.001$, respectively.

Figure 1M Experimental design for the perfused heart groups

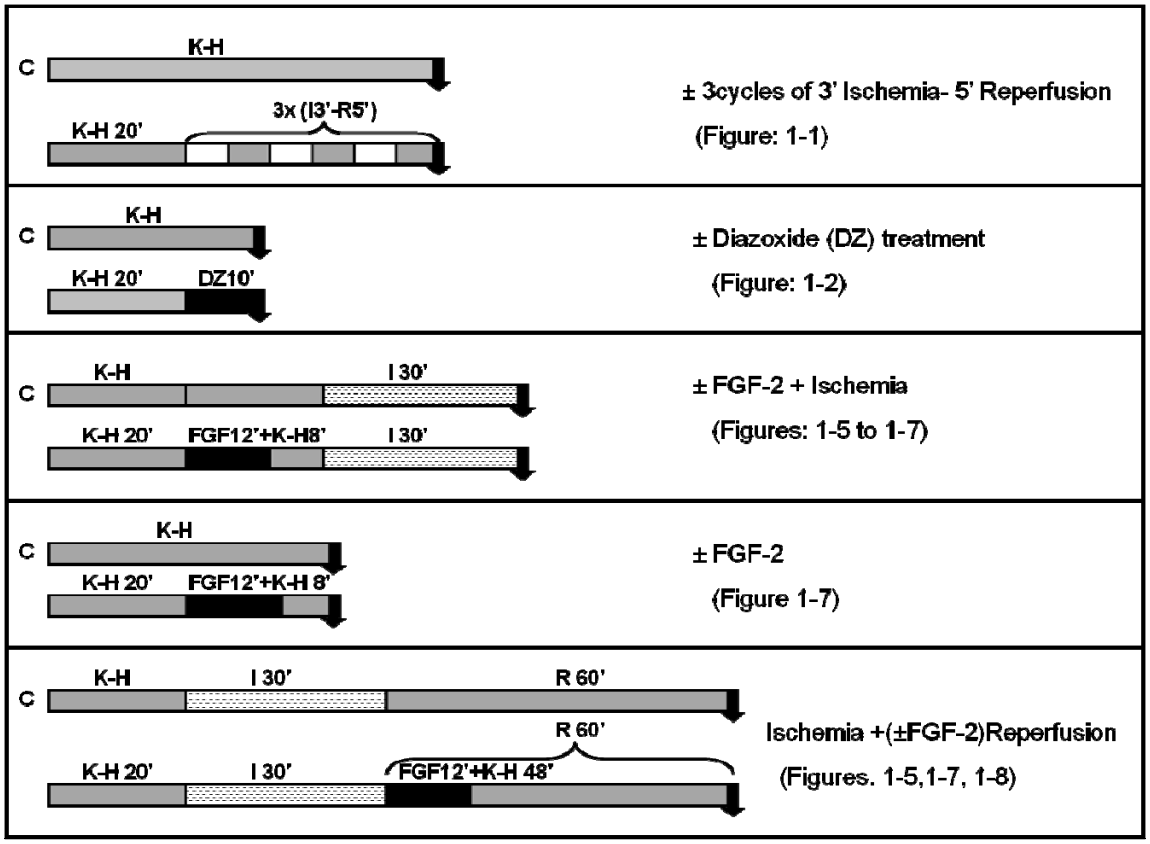

Five groups of isolated perfused heart experiments, each with its own controls (C) were used to determine the effects of specific treatments on Cx43, as indicated. Duration of each treatment is indicated in minutes. (‘). K-H denotes perfusion with Krebs- Henseleit buffer. “I” denotes ischemia, and “R” denotes reperfusion. Arrows mark termination of experiment.

V. Methods corresponding to Results section 2

Materials and methods not described in preceding sections are included here.

Material

The PKCε specific inhibitor peptide ($\varepsilon V_{1\text{-}2}$; EAVSLKPT; #539522) and its inactive scrambled control peptide (Scr; LSETKPAV; #539542) were obtained from EMD Millipore. Both peptides were dissolved in DMSO and used at a final concentration of 0.5μM (Costa et al., 2006a). The Cx43 channel blocker Gap 27 (SRPTEKTIFII), a mimetic peptide corresponding to the sequence of the first extracellular loop region of Cx43, and the inactive, scrambled peptide of Gap27 (REKIITSFIPT), were >95% pure, and obtained from Anaspec Inc. (catalogue # 62642 for Gap 27; #64765 for scrambled Gap27). The peptides were dissolved in DMSO and used at a final concentration of 250 μM. A complete list of antibodies can be found in table 1M.

Isolation of subsarcolemmal (SSM) and interfibrillar (IFM) mitochondria

SSM and IFM were isolated from freshly obtained vehicle-, or IPC-, or FGF-2 perfused hearts by differential centrifugation using filtered (1.2 μm) ice-cold isolation buffer (225 mM Mannitol, 75 mM Sucrose, 1 mM EGTA, 10mM MOPS, 10 mM Tris-HCl (pH 7.2), 0.1% (w/v) fatty acid-free bovine serum albumin (BSA) with both phosphatase (PPIC II and IV; Calbiochem) and protease inhibitors added, unless otherwise specified. Briefly, ventricular heart tissue minced with scissors was homogenized using a polytron tissue homogenizer (PT 3000, Brinkmann Instruments, Mississauga, ON, Canada), and the homogenate centrifuged at 550 x g for 5 minutes. For isolation of SSM, the supernatant was filtered through 2 layers of

cheesecloth and centrifuged at 8,800 x g for 10 min. For isolation IFM, pellets from the first centrifugation were re-suspended with isolation buffer (without protease and phosphatase inhibitors) in the presence of 8 U/g of the protease nagarse (Sigma-Aldrich; P8038) and incubated for 1 min on ice (Boengler et al., 2009). The suspension was homogenized using a glass homogenizer with a Teflon pestle and centrifuged at 550 x g for 10 min. The crude mitochondrial pellets from either SSM or IFM were further fractioned by centrifugation through a discontinuous step gradient of 15%, 26%, and 40% Percoll in isolation buffer for 20 min at 31,000 x g. After centrifugation, the mitochondria were separated into four bands, according to quality and intactness. The lowest (heaviest) band contained intact mitochondria and was used in all the mitochondrial experiments. After removal from the gradient, mitochondrial suspensions were washed twice with isolation buffer and re-suspended in 250 mM sucrose, 10 mM MOPS pH 7.2. The mitochondrial protein content was determined by the Bradford method using the Pierce Coomassie Kit (Biolynx, Brockville, ON, Canada).

Citrate synthase activity, measured spectrophotometrically (A_{412}) and calculated as per the manufacturer's instructions (ScienceCell™), was similar between IFM and SSM, at 10 units/mg protein. Citrate synthase measurements in the absence and presence of Triton X-100 indicated that 97% of mitochondria in SSM as well as IFM suspensions had intact inner mitochondrial membrane.

Removal of the outer mitochondrial membrane by digitonin

SSM were re-suspended at 20 mg/ml in buffer D (220 mM mannitol, 70mM sucrose, 2 mM HEPES pH7.4, 0.5 mM EGTA), containing 0.05% (w/v) BSA. An equal

volume of buffer D (no BSA) containing 0.3 mg digitonin (Sigma #D141) per mg of mitochondrial protein was added to the mitochondrial suspension and sample incubated on ice. At time point of 0, 15, 30 minutes, a portion of the sample was removed, diluted 10x with buffer D and centrifuged at 12,000 x g for 10 minutes at 4°C (Hovius et al., 1990). The pellet was washed three times with buffer D (centrifuged at 10,000 x g for 10 minutes at 4°C). Pellets were re-suspended in 1X SDS buffer (10% glycerol, 50 mM Tris-HCl 6.8, 2% SDS, 30 mM β-glycerophosphate, 2.5 mM EGTA, 1 mM NaOV, 0.5 mM NaF), boiled for 5 minutes, sonicated and centrifuged to remove any insoluble material prior to SDS PAGE and Western blotting.

Electron microscopy

SSM were prepared for routine electron microscopy as previously described (Palmer et al., 1986) with slight modifications. Equal volumes of mitochondrial suspension and 3% glutaraldehyde in 0.1 M phosphate were mixed, allowed to stand at room temperature for one hour and then centrifuged. The resulting pellets were washed with 5% sucrose in 0.1 M phosphate buffer, and fixed in 1% osmium tetraoxide in 0.1 M phosphate buffer for one hour at room temperature. After hydrating in ascending concentrations of alcohol, the pellets were embedded in epon, sectioned, stained with uranyl acetate and lead citrate, viewed and photographed in a Phillips CM-10 electron microscope (Collaboration with Dr. J.A. Thliveris, University of Manitoba).

Immuno-electron microscopy

Adult rat heart ventricles were rinsed in warm PBS and minced into 2 x 2 mm pieces before fixing overnight in a 4% paraformaldehyde/0.5% glutaraldehyde in 0.1 M sodium cacodylate buffer. The fixed tissue was then processed for immune-electron microscopy, as previously described (Zhang and Pasumarthi, 2007). Purified mitochondria were fixed under similar conditions for 2 hours at 4°C. Ultrathin sections (~80 nm) placed on nickel grids were blocked with Tris-buffered saline (pH 8.1) containing 1% skim milk and 1% BSA for 45 min and either incubated with primary antibodies specific to Cx43 (610061, BD Transduction Laboratories), or without primary antibodies, overnight and subsequently incubated with anti-mouse IgG antibodies coupled to 5 nm gold particles (Sigma, ON). After immunolabeling, the grids were stained with uranyl acetate and lead citrate and viewed using a JOEL JEM 1230 Transmission Electron Microscope at 80 kV. Images were captured by a Hamamatsu ORCX-HR digital camera (Collaboration with Drs F. Zhang and K.B. Pasumarthi, Dalhousie University).

Mitochondrial matrix swelling

Mitochondrial matrix swelling is a standard technique for assaying induction of the mitochondrial permeability transition pore (mPTP). Swelling of the mitochondrial matrix is reflected by changes in the optical density (absorbance, A) of the mitochondrial suspension. The changes were measured at 545 nm (A_{545}), at constant temperature of 30°C, using a Molecular Devices Spectra max 384 plus spectrophotometer. Briefly, mitochondria (0.5 mg/ml in a final volume of 2.0 ml) in incubation buffer (125 mM KCl, 10 mM NaCl, 0.5 mM $MgCl_2$, 1 mM KH_2PO_4, 5 mM

MOPS, pH 7.2) were added to a 2.0 ml cuvette at 30°C. ADP (75 μM) and Oligomycin (2 μg/ml) were added before mitochondria were energized by addition of 20 mM glutamate and 2mM malate for 2 min. 50 mM $CaCl_2$ was added in 5 μl aliquots every 1 min (increases Ca^{2+} by 125 μM each step) until there was no further change in absorbance (about 10 min in total). The optical density before Ca^{2+} addition was considered 0% swelling; maximum swelling (100%) was determined at the end of experiment by adding alamethicin (15 μg/ml), a bacterial antibiotic that forms a large conductance pore. All buffers were between 275-280 mosM. Calcium capacity or tolerance was defined as the amount of calcium that could be added to the mitochondrial suspension until a drop in A_{545} is observed. Experiments were also conducted in the presence of the mPTP inhibitor Cyclosporine A (CsA; 0.5 μM), which was added before $CaCl_2$, to confirm that the change in absorbance was due to mPTP. In select experiments, mitochondrial suspensions were supplemented with Gap27, or scrambled Gap27 peptides at 250 μM (De Vuyst et al., 2011; Wang et al., 2012), prior to the addition of calcium.

Mitochondrial respiration assay

Mitochondrial respiration was measured polarographically using a Clark-type electrode in a sealed chamber (Quibit System, ON, Canada) containing 1 ml incubation medium (120 mM KCl, 10 mM NaCl, 2 mM $MgCl_2$, 2mM KH_2PO_4, 20 mM MOPS, 0.7 mM $Calcl_2$, and 1 mM EGTA, pH 7.2) with magnetic stirring at 30°C. The concentration of Ca^{2+} in the incubation buffer was calculated to yield free a Ca^{2+} concentration of <1 μM using WebMaxC software (Patton CW, Stanford University). Experiments were initiated by adding 0.5 mg of mitochondria to the incubation

medium. Substrates for respiration were 20 mM glutamate/2 mM sodium malate. ADP (150μM) was used for activation of state III respiration. Respiration control index (RCI) was calculated as the ratio of state III to state IV respiration. ADP/O ratio and oxidative phosphorylation rate (ADP/O ratio x state III oxygen consumption) were calculated as described previously (Makazan et al., 2007).

Cytochrome C release assay

Using conditions similar to the mitochondrial swelling assay, mitochondria (0.5 mg/ml) with 75 μM ADP were energized for 5 min with 20 mM glutamate, 2mM malate and 2 μg/ml oligomycin before aliquoting (100 μl) into 1.5 ml tubes. Samples were subjected to increasing concentrations of calcium (0-1000 μM) in the presence or absence of CsA at 30°C. After a brief centrifugation, mitochondrial pellets and supernatants were collected for SDS-PAGE and Western blotting analysis.

Phorbol 12-myristate 13-acetate (PMA) stimulation

SSM from non-stimulated hearts were suspended at a concentration of 4 mg/ml in suspension buffer (120 KCl, 10 mM HEPES pH 7.4, 10 mM succinate, 5mM KH_2PO_4, 0.5 mM $MgCl_2$, containing 1:100 dilution of PIC, PPIC II, IV) supplemented with 0.67 μM Oligomycin and 50 μM ADP before dividing into four groups: (1) control+ Scr (0.5 μM), (2) control+$\varepsilon V_{1\text{-}2}$ (0.5 μM), (3) stimulated with PMA (0.2 μM) + Scr (0.5 μM), (4) stimulated with PMA (0.2 μM) + $\varepsilon V_{1\text{-}2}$ (0.5 μM)(Costa et al., 2006a) for 2 minutes. Mitochondrial pellets were used for Western blot analysis.

Experimental design

Three mitochondrial groups were studied (Figure M2). The “control” group, where hearts were perfused with oxygenated K-H solution (pH 7.4; 37°C) under

non-recirculating conditions at a constant pressure of 80 mmHg, as previously described. (2) The "FGF-2" group, where after a stabilization period of 20 min perfusion, FGF-2 supplemented K-H (10 μg FGF-2 in 12 ml) was infused with a peristaltic pump directly into the main line entering the heart, at 1 ml/min for 12 min, followed by an additional 8 min of perfusion with K-H. (3) The "IPC" group, where hearts were subjected to 3 cycles of 3 minutes of global ischemia, followed by 5 minutes reperfusion. SSM preparations are obtained from all three groups. IFM preparations were obtained from the 'control' and 'FGF-2' groups.

Statistical analysis

The data are presented as mean ± SD. Statistical significant of differences between 2 groups were compared using unpaired student's t-test analysis. One way analysis of variance (ANOVA) was used when more than 2 groups (one treatment) were compared. Two way ANOVA was used, as needed. All statistics was calculated with software Prism 6. The level of significance level was defined as *$P<0.05$, **$P<0.01$, ***$P<0.001$, respectively.

Figure 2M Experiment design for mitochondrial groups.

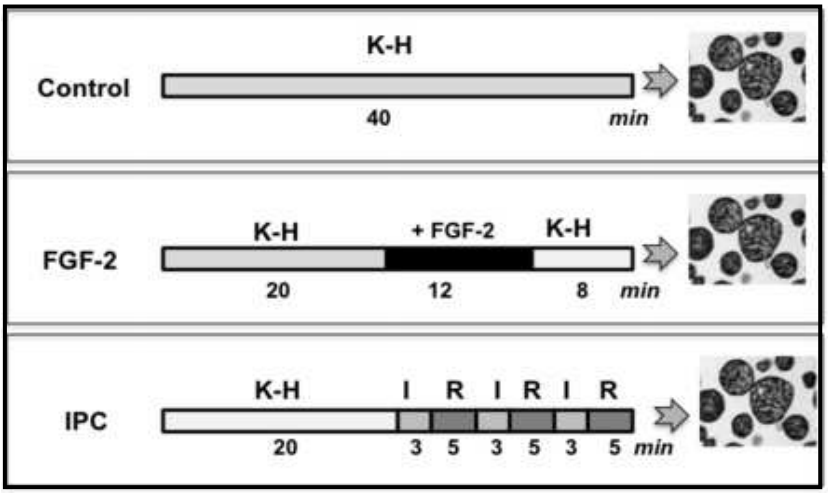

Three groups of hearts were used to isolate mitochondria. The 'control' and 'FGF-2' groups consisted of hearts perfused, respectively, with Kreb-Heinseleit (K-H) solution, or with FGF-2 supplement K-H. Perfusion duration is indicated in minutes (min). Hearts were also subjected to an IPC protocol, composed of three cycles of 3 min global ischemia and 5 min reperfusion. At the end of these manipulations, hearts were used immediately for mitochondrial isolation

VI. Methods corresponding to Results section 3

Materials and methods not described in preceding sections are included here.

Materials

The pharmacological FGFR inhibitor, SU5402 (2-[1, 2-Dihydro-2-oxo-3H-idol-3-ylidene) methyl]-4-methyl-1*H*-pyrrole-3-propanoic acid) was obtained from Tocris Bioscience, #3300. Anti-FGFR1 neutralizing antibody (Neu-Ab) was obtained from EMD Millipore (MAB 125). A complete list of antibodies can be found in table 1M.

The cDNA for mouse FGFR1 was a gift from Dr. P. Cattini (Physiology, University of Manitoba. Human embryonic kidney cells (HEK203) were purchased from Stratagene, and subjected to transient gene transfer exactly as described previously (Dang et al., 2006).

Experimental Design

In all experiments, mitochondria (SSM) were isolated from normal, untreated heart, as previously described in the section 2. The first set of experiments measured the calcium retention capacity by the mitochondrial matrix swelling assay, of SSM treated with or without FGF-2 (25 ng/ml) in the presence of either a PKCε-specific inhibitory peptide ($\varepsilon V_{1\text{-}2}$; 0.5μM) or scrambled peptide (Scr; 0.5μM). Six groups were studied: (1) control SSM, (2) SSM treated with FGF-2 alone, (3) control SSM+ Scr, (4) control SSM+ $\varepsilon V_{1\text{-}2}$, (5) FGF-2 treated SSM + Scr, (6) FGF-2 treated SSM + $\varepsilon V_{1\text{-}2}$.

The second set of experiments was aimed to examine cytochrome c release in SSM that were either treated with or without FGF2, in the presence of either εV_{1-2} or Scr peptides, prior to calcium overload (625 μM). Following the addition of calcium, the mitochondrial suspension was centrifuged to give a pellet (mitochondria) and a supernatant (soluble material released by the mitochondria), which were then analyzed by Western blotting. The pellet fraction was also analyzed for Cx43 as well as Cx43 phosphorylation at S262 and S368.

The third set of experiments was aimed to examine the presence of an FGF receptor in cardiac mitochondria using control as well as FGF2 treated SSM. Two techniques using antibodies to FGFR, anti-FGFR, and phospho FGFR1 (pY-653/654 and pY677) were used: electron microscopy with immunogold labeling and Western blotting. Additional experiments used a pharmacological FGF receptor inhibitor, SU5402, or a neutralizing antibody prior to FGF treatment to block its effect on cytochrome C release.

Statistical analysis

The data are presented as mean ± SD. Statistical significant of differences between 2 groups were compared using unpaired student's t-test analysis. One way analysis of variance (ANOVA) was used when more than 2 groups (one treatment) were compared. Two way ANOVA was used, as needed. All statistics was calculated with software Prism 6. The level of significance level was defined as $*P<0.05$, $**P<0.01$, $***P<0.001$, respectively.

Table 1M: List of antibodies

Antibodies to	Species	Dilutions	Companies, catalogue number
ANT	Goat	1:1000	Santa Cruz Biotechnology; sc-929
Calreticulin	Rabbit	1:1000	Abcam; Ab4
Caveolin	Goat	1:300	Santa Cruz Biotechnology; sc9154
Cx43	Rabbit	1:10000	In-house antibody; (Doble et al., 2000)
Cx43, P-S262	Rabbit	1:2000	Santa Cruz Biotechnology; sc-17219-R
Cx4, P-S368	Rabbit	1:1000	Millipore; AB 3841
Cyclophillin D	Mouse	1:5000	MitoSciences; MSA04
Cytochrome C	Mouse	1:5000	BD Biosciences Pharmigen; 556433
FGFR1	Rabbit	1:2000	Santa Cruz; SC121
FGFR1,pY653/654	Rabbit	1:500	Santa Cruz; 30262-R
FGFR1,pY766	Rabbit	1:500	Santa Cruz; 16309-R
GAPDH	Mouse	1:5000	Abcam; ab8245-100
58K Golgi	Rabbit	1:1000	Abcam; ab5820
GSK-3β	Rabbit	1:1000	Cell Signalling Technology; 9315
GSK-3β, pS9	Rabbit	1:1000	Cell Signalling Technology; 9336
HRP-rabbit	Donkey	40 ng/ml	Jackson Immuno Res. Lab. 711-035-152
HRP-mouse	Donkey	40 ng/ml	Jackson Immuno Res. Lan. 715-035-150
HRP-goat	Donkey	40 ng/ml	Jackson Immuno Res. Lab. 705-035-147
Lamin B	Goat	1:200	Santa Cruz Biotechnology; sc-6217
Lamp1	Mouse	1:1000	Abcam; 13523
Na^+/K^+ATPase	Mouse	1:10000	Millipore; #05-369
N-Cadherin	Rabbit	1:300	Santa Cruz Biotechnology; sc7939
PKCε (nPKCε)	Rabbit	1:1000	Santa Cruz Biotechnology; sc-214R
PKCε, pS729	Rabbit	1:1000	Abcam; ab5811
SERCA2 ATPase	Mouse	1:1000	Affinity BioReagents; MA3-919
Tom20 (FL-145)	Rabbit	1:800	Santa Cruz Biotechnology; sc11415
VDAC	Rabbit	1:1000	Cell Signalling; 4866

CHAPTER 3. RESULTS

Results section 1. PKCε-mediated cardioprotection and Cx43 phosphorylation *(Published in Cardiovascular Research (2009) 83, 672-681)*

In the first series of studies, the effect of various PKCε-mediated cardioprotective manipulations on the phosphorylation pattern of Cx43 in perfused hearts was examined. Methods Figure M1 outlines the experimental design used to obtain the various perfused heart groups. Cx43 phosphorylation was assessed by Western blotting and antibodies detecting: all Cx43 phosphorylation states, at 41–45 kDa (P.AB); only dephosphorylated (D-) Cx43, at 41 kDa (#13-8300); only P-S262-Cx43; only P-S368-Cx43. Cx43 migrating at 43–45 kDa, representing Cx43 phosphorylated at several sites, will be referred to as P-Cx43. Please note that the term P*Cx43 signifies Cx43 populations with enhanced levels of P-S262-Cx43, and P-S368-Cx43.

1.1 Effect of ischemic preconditioning (IPC) and diazoxide

In lysates from normal perfused hearts analyzed under non-saturating protein loading conditions (20 μg/lane), P.AB detected mainly a Cx43 band at 45 kDa (Figure 1-1A). Under protein overload conditions, P.AB also detected a band at 41 kDa (inset, Figure 1-1A). IPC did not affect total Cx43 levels (Figure 1-1A and A-i). Normal hearts showed very faint or no staining for P-S262-Cx43 and some staining for P-S368-Cx43, as expected (Miura et al., 2007; Srisakuldee et al., 2006) (Figure 1-1B, C). IPC hearts displayed significant increases in both P-S262-Cx43, and

P-S368-Cx43 (P*Cx43) compared with controls (Figure 1-1B and C, respectively, and B-i and C-i).

The P-S368-Cx43 migrated predominantly near 41 kDa (Figure 1-1C), as reported (Miura et al., 2007; Solan and Lampe, 2007). The P-S262-Cx43 migrated mainly at and/or just above 45 kDa (Figure 1-1B), indicating that it belongs to Cx43 population(s) phosphorylated at several other residues, but not S368. Slower migration of P-S262-Cx43, corresponding to extensively phosphorylated Cx43 (P2) has been reported previously (Dang et al., 2006; Doble et al., 2004; Solan and Lampe, 2007). Differences in migration of P-S262-Cx43 and P-S368-Cx43 suggest that phosphorylation at these sites may be mutually exclusive, and that they belong to distinct Cx43 sub-populations (Srisakuldee et al., 2006).

Lysates from hearts perfused briefly with diazoxide, a treatment shown by others to be cardioprotective by a mechanism requiring PKCε (Costa and Garlid, 2008) displayed elevated levels of both P-S262-Cx43, as well as P-S368-Cx43 compared with vehicle-perfused controls (Figure 1-2A and B). There is no significant difference between control and diazoxide-treated groups (data not shown).

In parallel studies, it was confirmed that IPC hearts were indeed cardioprotected as they displayed improved recovery of contractile function after 30 min of global ischemia and 60 min of reperfusion; the experiments were done in collaboration with Dr. Stéphane Tanguy (France) (Srisakuldee et al., 2009), and results are shown in Figure 1-3.

Hearts subjected to IPC followed by 30 min global ischemia were also examined by immunofluorescence for Cx43 distribution. Corresponding heart lysates were also probed by Western blotting for total Cx43. Ischemia elicited Cx43 redistribution away from intercalated disks (Figure 1-4 B), as well as Cx43 dephosphorylation, as expected (Figure 1-4) (Beardslee et al., 2000). IPC prevented the ischemia-induced Cx43 changes (Cx43 dephosphorylation and lateralization (Figure 1-4 A, C).

Figure 1-1 IPC promotes Cx43 phosphorylation at PKC sites.

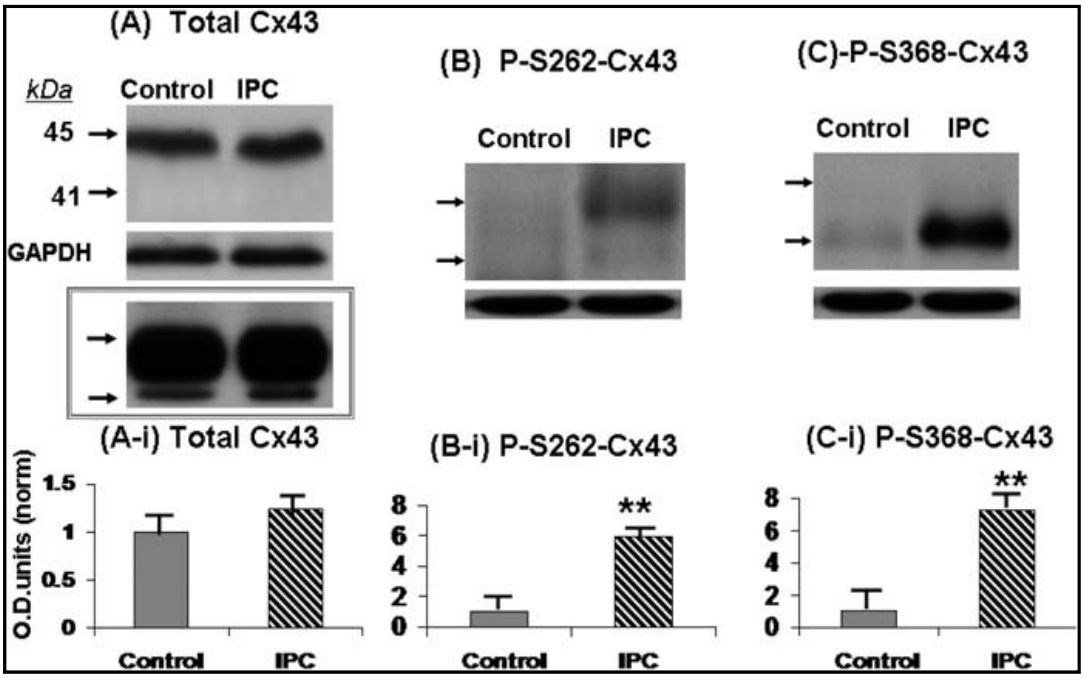

Panels (A-C) representative Western blots of cardiac lysates of control hearts and hearts subjected to ischemic preconditioning (IPC), and probed with antibodies recognizing total Cx43 (P.AB), P-S262-Cx43, and P-S368-Cx43. Lysates were analyzed at 20 µg/lane, except in (A), inset, at 50 µg/lane. Staining for anti-glyceraldehyde 3-phosphate dehydrogenase (GAPDH), indicative of equal loading, was included. (A-i, B-i, C-i) Quantitative data from densitometry measurements corresponding to (A-C). Optical density (O.D. units) was normalized against control values, defined arbitrarily as 1. Migration of molecular weight markers is indicated in kDa. **P<0.01, n=6

Figure 1-2 Diazoxide promotes Cx43 phosphorylation at S262, S368.

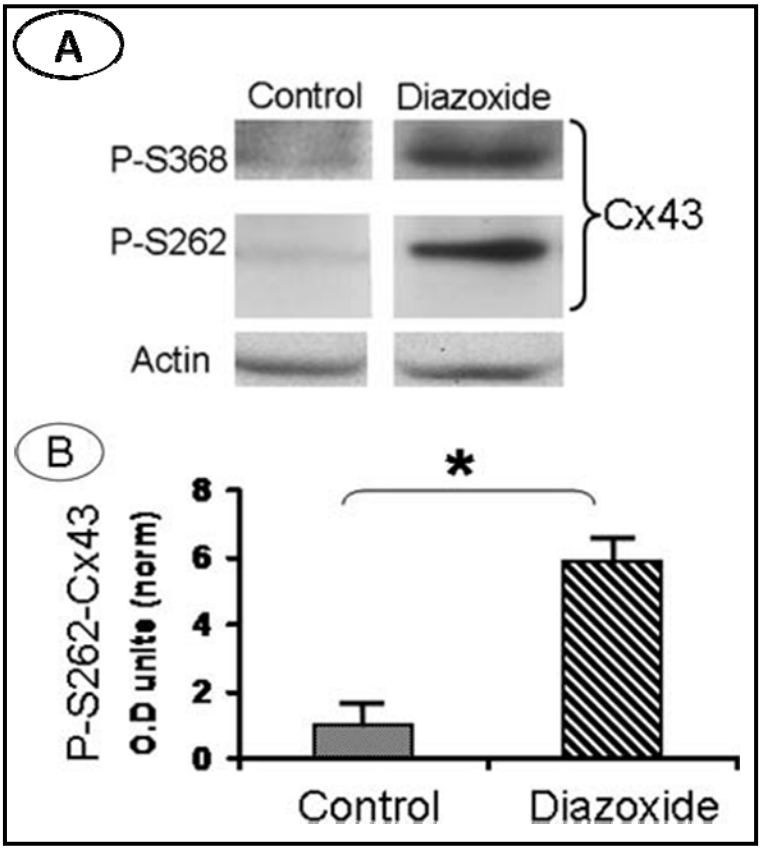

Panel (A) Representative Western blots of cardiac lysates from control and diazoxide –treated hearts, probed for P-S262-Cx43, P-S368-Cx43, and pan-actin, as indicated. P-368-Cx43 images are representative of n=2. **Panel (B)** Corresponding quantitative data for P-S262-Cx43 (O.D units) normalized against control values. *P<0.01, n=4. There is no difference in total Cx43 from both groups (data not shown).

Figure 1-3 Effect of ischemic preconditioning (IPC) on myocardial function under pre-ischemic conditions of perfusion and after global ischemia (30 min) and reperfusion (60 min) *(These experiments were done by Stéphane Tanguy.)*

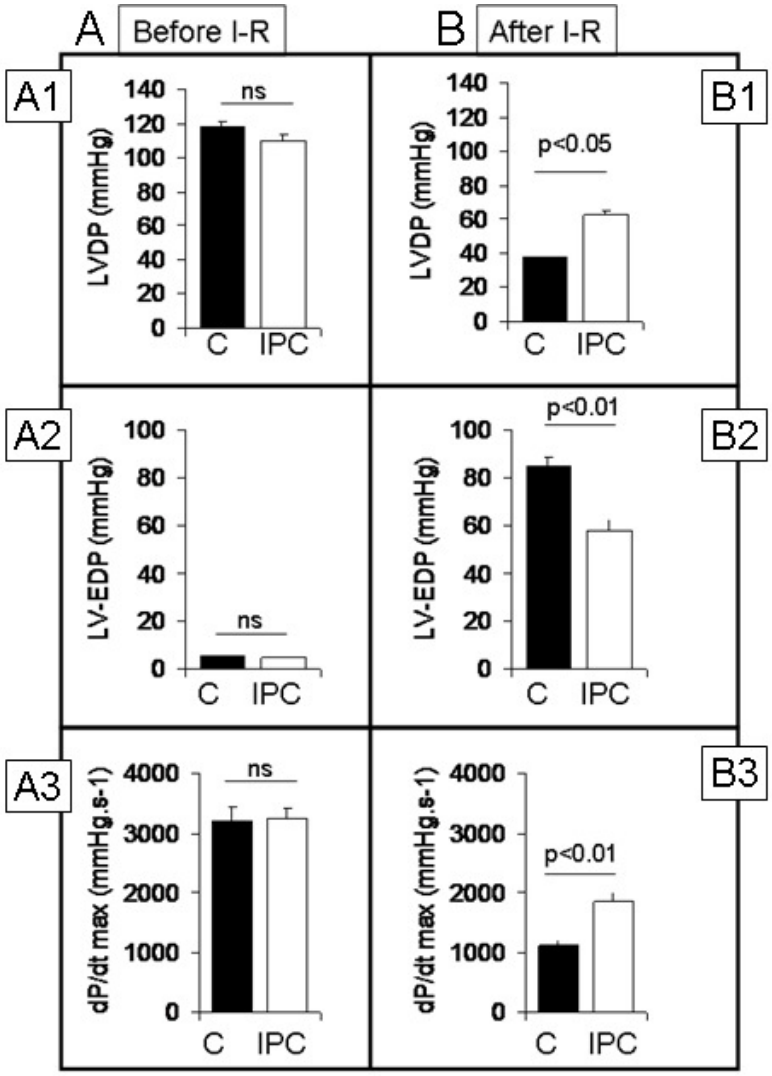

There were no significant differences in LVDP (left ventricular developed pressure), LV-EDP (left ventricular end diastolic pressure), dp/dt max (rate of contraction) between control and IPC groups, as indicated in A1-3. The IPC-treated group showed significantly increased values for LVDP and dP/Dt max, compared to the control groups, B1 and 3. The elevated LV-EDP seen in the non-treated groups after ischemia-reperfusion is significantly decreased in the IPC group, as shown in B2. Results were means ± SD, n=6.

Figure 1-4 Ischemic preconditioning (IPC) prevents ischemia-induced Cx43 dephosphorylation

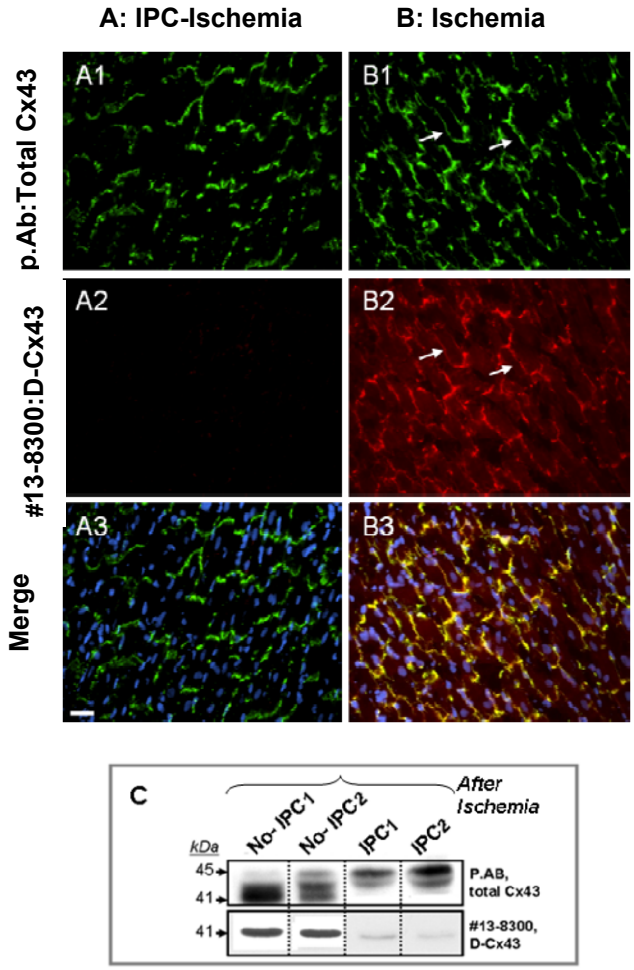

Panels (A and B) show representative immunofluorescence images from hearts subjected or not to IPC, followed by 30 minutes of global ischemia. (A1, A2 or B1, B2) show the same cardiac section field stained for total Cx43 (P.AB), or dephosphorylated Cx43 (D-Cx43, #13-8300). (A3 or B3) show the merging of A1, A2 or B1, B2 images, counterstained with Hoechst stain to visualize nuclei. The IPC-treated ischemic hearts do not show the ischemia-induced staining for D-Cx43 (compare A2 with B2), nor do they show evidence of Cx43 laterization; the latter is observed clearly in non-IPC treated ischemic hearts (see arrows in B1 and B2). **Panel (C)** shows Western blots from two-IPC treated ischemic hearts (IPC1, IPC2) and two non-IPC-treated ischemic hearts (no-IPC1, no-IPC2, as indicated), stained for total Cx43 (P.AB), and then stained for D-Cx43 (#13-8300). Staining with P.Ab shows that Cx43 in non-IPC ischemic hearts migrates mostly at 41-42 kDa, while Cx43 in IPC-treated hearts migrates at 43-45 kDa, consistent with protection from ischemia-induced Cx43 dephosphorylation. Similarly, the prominent staining for D-Cx43 seen in non-IPC ischemic hearts is substantially reduced in the IPC-treated ischemic hearts. All lanes were loaded with 30 µg protein lysate/lane.

1.2 Effect of ischemia (± FGF-2), and ischemia-reperfusion (± FGF-2) on relative levels of phosphorylated (P) Cx43 and dephosphorylated (D) Cx43

The results are shown as representative Western blots (Figure 1-5A-C) and corresponding quantitative data (Figure 1-5A1 and 2; B1 and 2; C1 and 2). Probing with the rabbit polyclonal anti-Cx43 antibodies (P.AB) showed that relative levels of total Cx43 were similar between non-ischemic controls and hearts subjected to ischemia (± FGF-2 pre-treatment; Figure 1-5A, B, A1), or hearts subjected to ischemia and reperfusion (± FGF-2), Figure 1-5A, C, A2. Taken together, the data indicated there was no net Cx43 loss (degradation) during the experiments.

Probing with P.AB showed that pre-ischemic hearts are composed of P-Cx43 (Figure 1-5A). Ischemia resulted in disappearance of P-Cx43 and accumulation of 41-42 kDa Cx43 (Figure 1-5B). This was partially prevented by FGF-2 pre-treatment, resulting in 78% P-Cx43 despite global ischemia (Figure 1-5B and B1). Hearts subjected to ischemia-reperfusion accumulated mainly 41 kDa Cx43 after 60 min of reperfusion, with minimal recovery (15% of total) of P-Cx43 (Figure 1-5C and C1). In contrast, FGF-2-reperfused hearts accumulated 80% P-Cx43 (Figure 1-5C and C1). FGF-2- reperfusion of ischemia hearts therefore reversed the effects of ischemia and re-established prominence of P-Cx43.

Confirming results with P.AB, the #13-8300 antibodies detected a prominent 41 kDa band, D-Cx43, in ischemic hearts (Figure 1-5B) and hearts subjected to ischemia-reperfusion (Figure 1-5C). D-Cx43 was significantly decreased in the FGF-2 pre-treated ischemic group (Figure 1-5B and B2); and the FGF-2-perfused group (Figure 1-5C and C2), compared with their non-FGF-2-treated counterparts.

Immunofluorescence staining was used to examine the effect of FGF-2 pre-treatment on total and D-Cx43 localization after ischemia. Representative images are shown in Figure 1-6. As expected, non-ischemic hearts showed Cx43 (P.AB) immunostaining at intercalated disks (arrows, Figure 1-6A), and lacked of staining for D-Cx43 (Figure 1-6 A–i).

Ischemia caused Cx43 redistribution to lateral cardiomyocyte surfaces (Figure 1-6B, double arrows), as well as strong immunoreactivity for #13-8300 (D-Cx43; Figure 1-6B–i). Morphological examination of several tissue sections, from several ischemic hearts, indicated that most myocytes stained positive for #13-8300, and displayed some Cx43 lateralization. These changes were not observed in the FGF-2 pre-treated hearts (Figure 1-6, c/c-i).

Figure 1-5 Effects of pre- or post-ischemic FGF-2 on total (41-45 kDa) Cx43

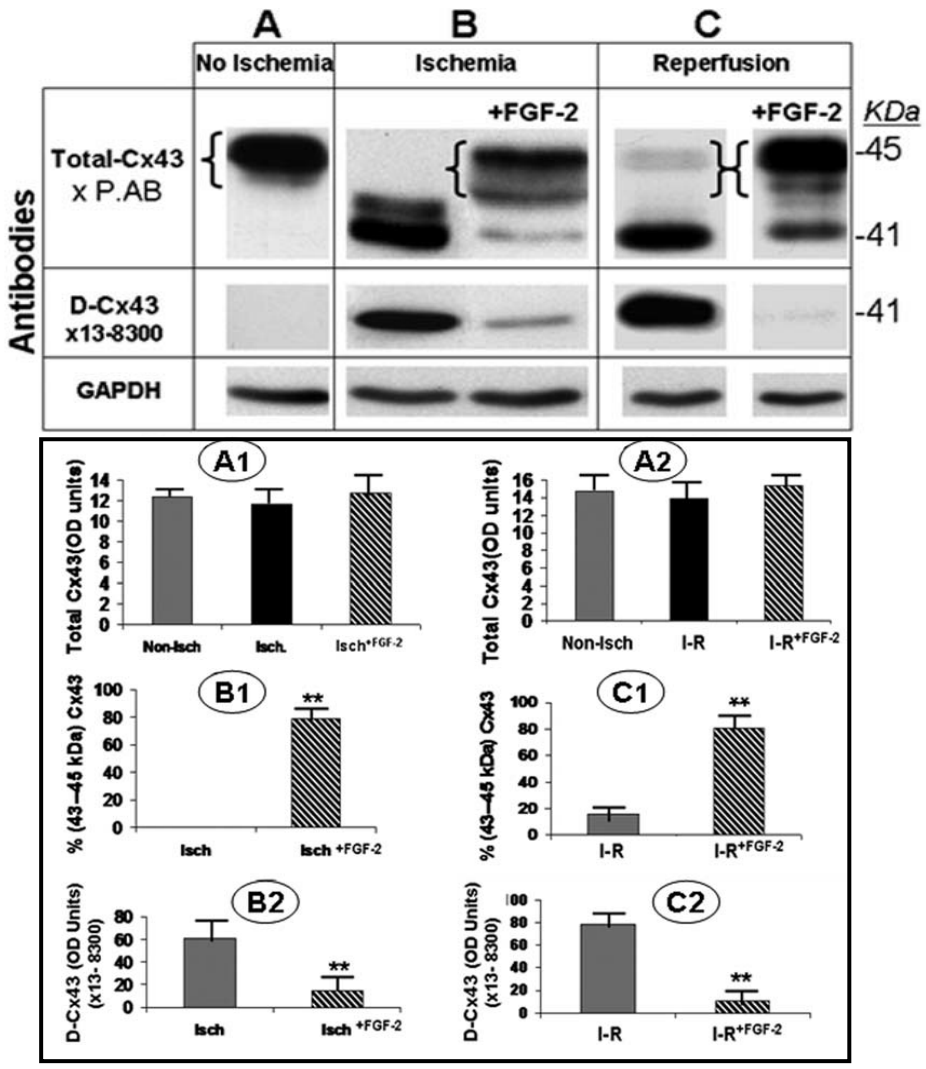

Representative Western blots from (A) non-ischemic hearts, (B) ischemic hearts ±FGF-2 pre-treatment, (C) hearts subjected to ischemia followed by reperfusion in the presence or absence of FGF-2. Blots were probed with antibodies for total Cx43 (P.AB), D-Cx43 (#13-8300), and GAPDH, as indicated. Brackets denote 43-45 kDa P-Cx43. A1 and A2 showed the relative levels of total Cx43 (P.AB, O.D. units) in non-ischemic hearts (No-Isch), and (A1) ischemic heart ± FGF-2 pre-treatment (Isch, Isch^{FGF-2}), (A2) hearts subjected to ischemia (± FGF-2) reperfusion (I-R, I-R^{FGF-2}). (B1) and (C1) Percent 43-45 kDa P-Cx43 (P.AB) in ischemic hearts ± FGF-2 pre-treatment and hearts subjected to ischemia and reperfusion ± FGF-2. (B2) and (B3) relative levels of D-Cx43 (#13-8300) in respectively, ischemic heart ± FGF-2 pre-treatment, and hearts subjected to ischemia and (± FGF-2) reperfusion. (n=6; **P<0.01)

Figure 1-6 FGF-2 pre-treatment prevents ischemia-induced Cx43 changes.

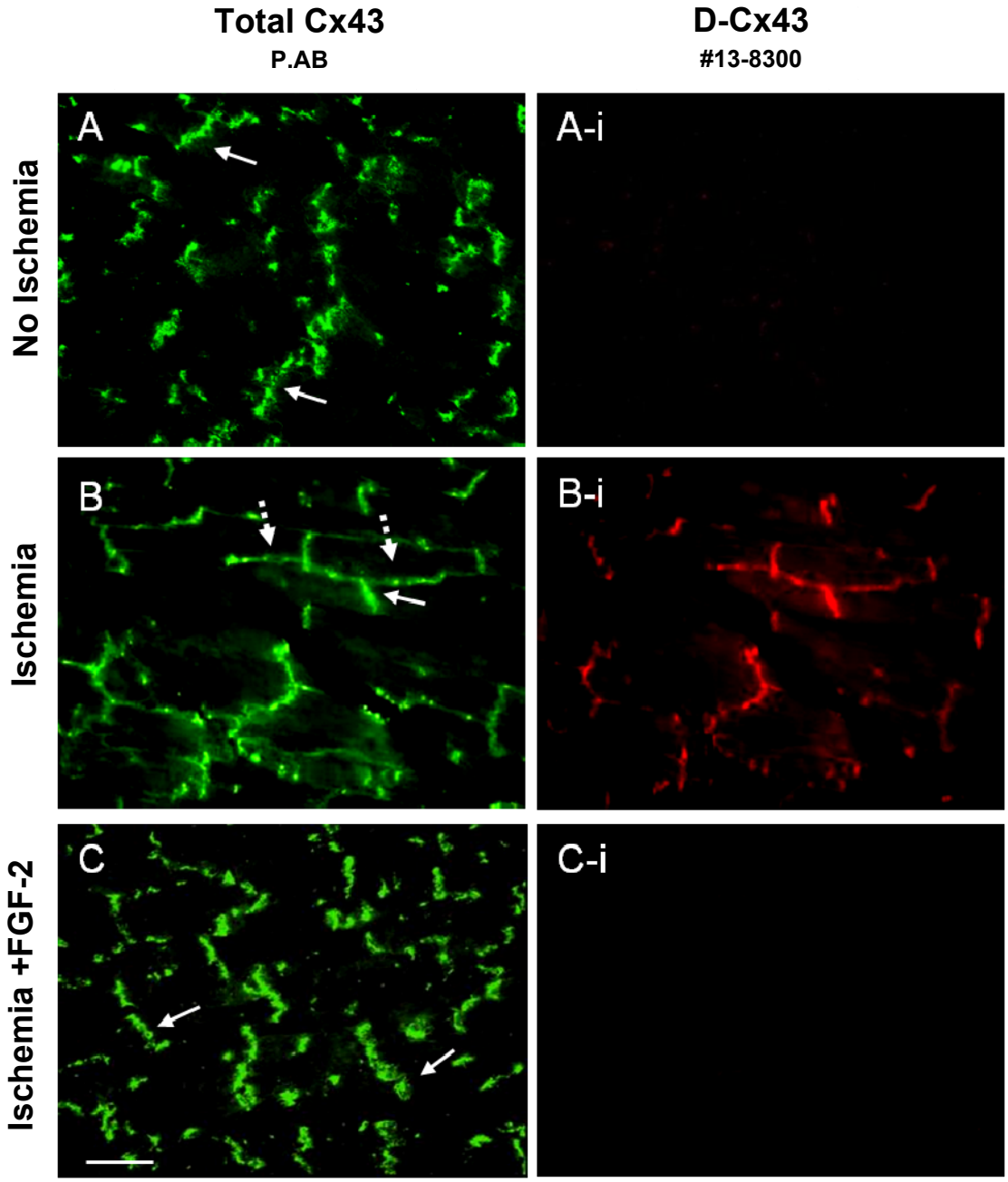

Panels (A, A-i) Representative double-immunofluorescence images of sections from control, non-ischemic hearts; **panels (B, B-i)**, hearts subjected to 30 min global ischemia, **panels (C, C-i)** FGF-2 pre-treated hearts subjected to 30 min global ischemia. Sections were probed for, panels (A-C), total Cx43 (P.AB), and (A-i, B-i, C-i), for D-Cx43 (#13-8300). Solid arrows point to intercalated disks, while 'dot' arrows point to lateral myocyte surfaces.

1.3 Effect of ischemia (± FGF-2), and ischemia-reperfusion (± FGF-2) on relative level of P*Cx43

As previously shown (Srisakuldee et al., 2006), and repeated here for comparison, FGF-2 pre-treatment increased P-S262- and P-S368-Cx43 above baseline levels, thus inducing a P*Cx43 state before ischemia (Figure 1-7A1 and B1). After ischemia, FGF-2 pretreated hearts had significantly higher levels of P-S262-Cx43 or P-S368 Cx43 compared with non-treated hearts, as seen in Figure 1-7A2 and A3 or Figure 1-7B2 and 3, respectively. Within the FGF-2-treated groups (Figure 1-7C), total levels of P-S262- or P-S368-Cx43 were not significantly affected by ischemia, as seen in Figure 1-7C1, 2 and Figure 1-7C3 and 4, respectively.

A P*Cx43 state was also induced after ischemia, during reperfusion with FGF-2 (Figure 1-8A). Significant up-regulation of anti-P-S262-Cx43 (Figure 1-8A and A1) and anti P-S368-Cx43 (Figure 1-8A and A2) immunoreactive bands were observed in the FGF-2-reperfused compared with the K-H reperfused group. Reperfusion-associated P-S262-Cx43 migrated mostly at ~45 kDa, but diffuse immunoreactivity was also seen at ~42 kDa (Figure 1-8A). Reperfusion- associated P-S368-Cx43 migrated mostly at 41-42 kDa, but some anti-P-S368-Cx43 bands were also detected at ~45 kDa (Figure 1-8A). The data indicate that phosphorylation patterns in Cx43 subpopulations after reperfusion are different to those of non-reperfused hearts; and that Cx43 phosphorylations at S262 and S368 may not be mutually exclusive in reperfusion-associated Cx43.

As expected (Jiang et al., 2002; Jiang et al., 2004), treating hearts with FGF-2 during reperfusion improved contractile functional recovery; e.g. systolic pressure

was increased by 35% compared with K-H only reperfused hearts, measured at 60 min of reperfusion. Functional measurements from hearts used to analyze Cx43 (Figure 1-5 and 1-8) have been described in (Jiang et al., 2009) and are not included in the current studies.

Figure 1-7 The effect of ischemia, ± FGF-2 pre-treatment, on P*Cx43

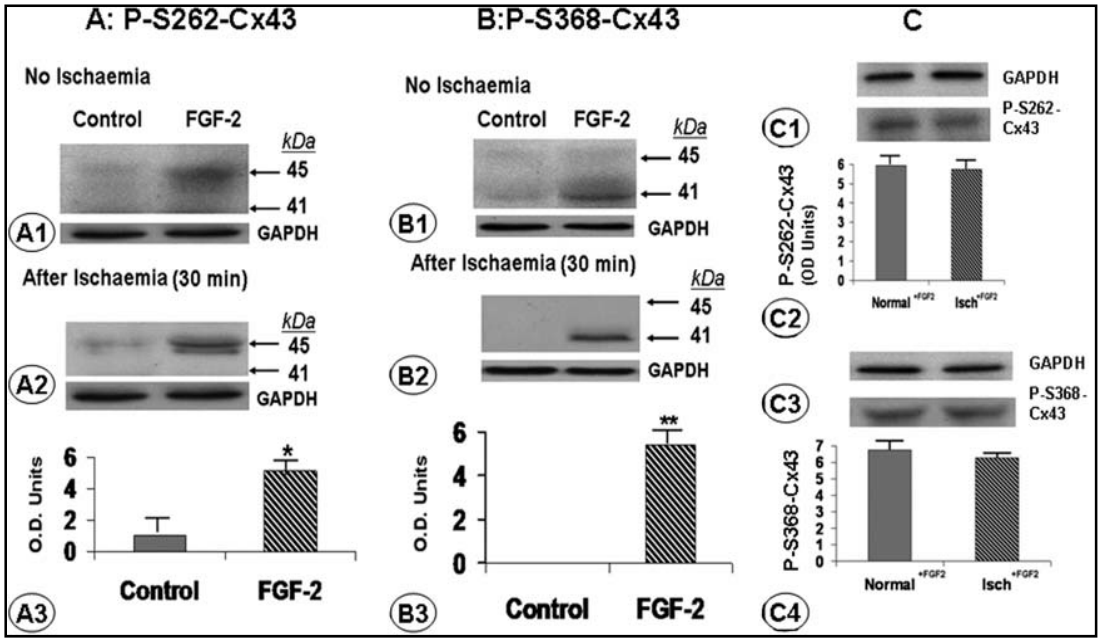

Panels (A1, B1) ('no ischemia') show representative Western blots from lysates of hearts perfused with oxygenated K–H (± FGF-2), probed for P-S262- and P-S368-Cx43, respectively. Corresponding GAPDH bands are included. Panels A2 and B2 ('after ischemia') show representative Western blots from ischemic hearts (± FGF-2 pre-treatment) probed, respectively, for P-S262- and P-S368-Cx43. **Panels (A3, B3)** show quantitation of relative P-S262- and P-S368-Cx43, respectively, corresponding to **panels (A2 and B2)**, in O.D. units. **Panels (C1, C3)** Representative Western blots and corresponding quantitative data (O.D. units) for P-S262-Cx43 in FGF-2 pre-treated hearts before ischemia (normal^{+FGF-2}), and after ischemia (Isch^{+FGF-2}). Panels (C3 and C4): representative Western blots and corresponding quantitative data for P-S368-Cx43 in FGF-2 pre-treated hearts before and after ischemia. In all cases n=6, *P<0.05, **P<0.01.

Figure 1-8 P*Cx43 is induced by FGF-2 during reperfusion.

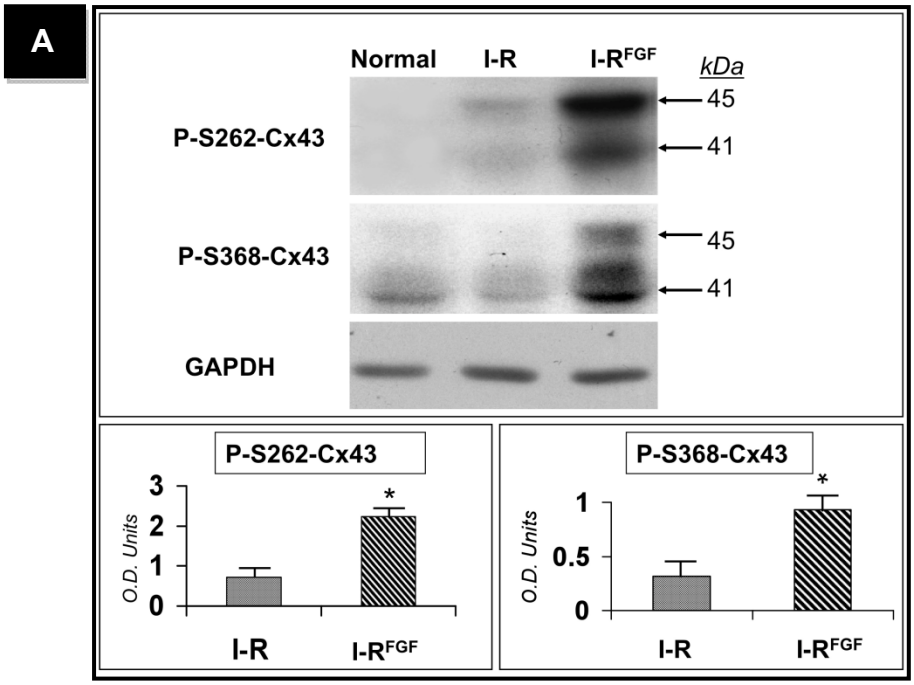

Panel (A) shows representative Western blots from non-ischemic hearts (normal), and hearts subjected to ischemia followed by reperfusion ± FGF-2 (I-R, I-R^{FGF-2}) that were probed for P-S262-, P-S368-Cx43, and GAPDH, as indicated. A1 and A2 show corresponding quantitative data (O.D units) for relative P-S262-or P-S368-Cx43; n=6, *P<0.05

1.4 The role of Cx43 phosphorylation at the S262 site in regulating cardiomyocyte resistance to injury.

In this section, we will briefly summarize work done by Maya M. Jeyaraman, as published in (Srisakuldee et al., 2009). This work is an extension of, and complements, the heart perfusion studies described in the preceding sections. Primary cultures of neonatal rat cardiomyocytes, subjected to simulated ischemia, were used to test whether the ability of Cx43 to become phosphorylated at S262 contributes to the cytoprotective effect of the FGF-2/PKCε axis. Cardiomyocytes were subjected to adenovirally mediated gene transfer, to achieve moderate overexpression of either wild type Cx43, or mutant Cx43 unable to become phosphorylated at S262 due to a serine–to-alanine (S262A) substitution. It was shown that while modest overexpression of wild-type Cx43 exerted a protective effect against ischemia-induced cellular damage and cell death, expression of S262A-Cx43 exacerbated the deleterious effects of ischemia in vitro. In addition, expression of S262A-Cx43 abolished the ability of either FGF-2 stimulation, or PKCε overexpression to elicit cardiomyocyte protection from ischemia-induced cell death (Jeyaraman et al., 2012; Srisakuldee et al., 2009). It was concluded that phosphorylation of cardiomyocyte Cx43 at S262 contributes to development of cytoprotection.

Results section 2: The effects of FGF-2 perfusion on cardiac mitochondria *(Published in Cardiovascular Research 2014, in press)*

In this series of studies the effects of FGF-2 administration on cardiac mitochondrial SSM and IFM populations were examined. Specifically, we asked if FGF-2, administered to the isolated heart by perfusion, would affect calcium tolerance of cardiac mitochondria, in relation to mitochondrial Cx43 presence, phosphorylation, and mitochondrial Cx43 function.

2.1 Validation of subsarcolemmal mitochondria (SSM) preparation

To address the role of mitoCx43 and potential changes in mitoCx43 levels or phosphorylation in response to FGF-2 treatment, it was important to confirm the presence of Cx43 in mitochondria as well as establish the integrity and relative purity of the SSM preparations (Makazan et al., 2007; Rodriguez-Sinovas et al., 2006; Totzeck et al., 2008). As seen in Figure 2-1A, SSM preparations appeared structurally intact and free of contamination by other organelles or debris when examined by electron microscopy (EM). Western blot analysis (Figure 2-1B) showed enrichment of SSM for mitochondrial proteins (cytochrome C, adenine nucleotide transferase, ANT) compared to total heart lysates, and lack of contamination by markers of sarcolemmal (Na^+/K^+ ATPase, caveolin 1, N-cadherin), cytosolic (GAPDH), sarcoplasmic reticulum (SERCA2), nuclear (lamin B), Golgi (58 k Golgi), and lysosomal (Lamp 1) subcellular compartments, while these markers were present in total heart lysates. Cx43 (43-45 kDa) was clearly detected in SSM. When SSM were subjected to digitonin to remove the outer mitochondrial membrane, the voltage-dependent anion channel (VDAC), an outer mitochondrial membrane

protein, gradually disappeared while mitoCx43 immunoreactivity remained unchanged, as did that of ANT, an inner mitochondrial membrane protein (Figure 2-1C). Immuno-EM of SSM, or rat heart ventricular sections showed the presence of immune-gold-labeled Cx43 at mitochondria, likely mitochondrial cristae, in both cases (Figure 2-1D, E). Incubation in the absence of the anti-Cx43 antibody did not elicit any immunogold-labeling (Figure 2-1F). Functional analysis of state III and state IV respiration, and the ratio of state III/state IV respiration showed similarity to those published previously (Makazan et al., 2007), and indicative of well-coupled mitochondria (Table 2-1).

Figure 2-1 Characterization of subsarcolemmal mitochondria (SSM) preparations:

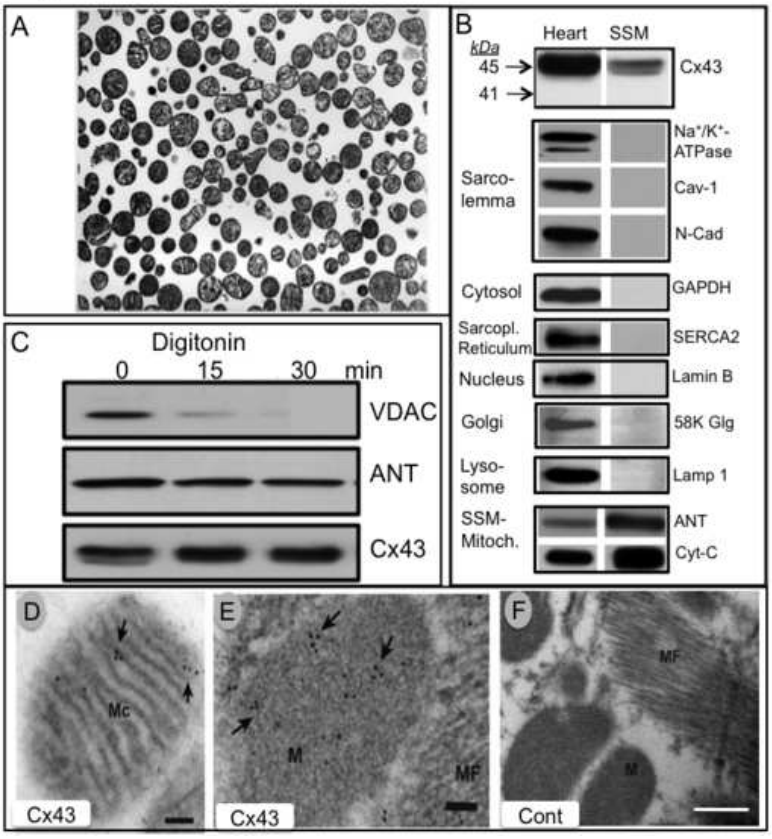

Panel (A) Electron microscopy image of SSM; **Panel (B)** Western blot analysis of total lysates (heart), and mitochondrial lysates (SSM) for Cx43 and for proteins present in sarcolemma (Na^+/K^+ ATPase, Caveolin 1, N-Cadherin), cytosol (GAPDH), sarcoplasmic reticulum (SERCA2), nucleus (Lamin B), Golgi (58 K Golgi), and mitochondria (ANT, cytochrome C), as indicated. **Panel (C)** Westernblot analysis of mitochondrial pellets after treatment with digitonin for 0, 15, and 30 min, and probed for proteins present at the inner mitochondrial membrane (ANT) or the outer mitochondrial membrane (VDAC), as well as for Cx43. **Panels (D, E, F)** Immuno-electron microscopy images; (D) SSM incubated with anti-Cx43 antibodies show immunoreactivity (immune-gold dots, arrows) in mitochondrial christae (Mc); in (E) Heart sections incubated with anti-Cx43 anitobodies shows immunoreactivity (immune-gold dots, arrows) within mitochondria (M) but not myofibril (MF); (F) Heart sections incubated in the absence of primary antibody (control) show lack of immune-gold staining. Size bars in (D, E) or (F) correspond to 100-500 nm.

Table 2-1 Respiratory activity of isolated rat heart subsarcolemmal mitochondria

Rate of Respiration (ng O2 /min/mg protein)		**RCI** (State III/State IV)	**ADP/O_2** (nmol ADP/ng O2)	**OPR** (nmoles ATP/min/mg protein)
State III	State IV			
381±18	65±3	5.89±0.38	3.02±0.07	1159±29

•State III: the rate of ADP-stimulated mitochondrial respiration (active state).
•State IV: the rate of mitochondrial respiration when added amount of ADP was utilized (resting state).
•RCI (respiratory control index): ratio between state III and state IV respiration, which represents the status of coupling between the rate of oxygen consumption by mitochondria and oxidative phosphorylation.
•OPR (rate of oxidative phosphorylation): Oxygen consumption was measured polarographically using a Clark-type electrode in a 1-ml sealed chamber (Quibit Systems, Canada) mixed with a magnetic stirring bar at 30°C.
•Each experiment was initiated by adding 0.5 mg mitochondrial protein. For activation of state III respiration 150 nmol of ADP was added. With glutamate and malate as a substrate, purified mitochondrial fraction had a RCI of 5.89±0.38 that points out that mitochondria were well coupled.

2.2 SSM. Effect of FGF-2 perfusion on calcium –induced swelling or cytochrome C release

SSM from hearts perfused with either vehicle (control), or vehicle with FGF-2 (FGF-2), or subjected to an ischemic preconditioning (IPC)-inducing protocol (3 cycles of 5 global ischemia followed by reperfusion, as in (Srisakuldee et al., 2009), were compared regarding their calcium capacity (tolerance), defined as the total amount of $CaCl_2$ that can be added to the mitochondrial suspension before a drop in A_{545} (an indicator of swelling) was observed spectrophotometrically. The IPC group was used as a positive control for our experimental system, as mitochondrial from hearts subjected to ischemic preconditioning have increased calcium capacity (Argaud et al., 2004). Measurements were obtained in the absence or presence of ADP; and in the absence or presence of CsA, a potent inhibitor of mPTP. Results are summarized in Table 2-2, and some representative tracings are include in Figure 2-2A, B. Regardless of the absence or presence of ADP, SSM from FGF-2-treated hearts had a significant higher calcium capacity compared to those from vehicle-treated hearts. As expected (Halestrap and Davidson, 1990; Lapidus and Sokolove, 1994), ADP itself raised calcium tolerance of both control-heart derived and FGF-2- heart derived SSM preparations. Calcium tolerance of SSM from IPC-hearts was also significantly higher than those from control hearts. In the presence of CsA, $CaCl_2$ failed to induce swelling (drop in A_{545}) in either control, FGF-2-, or IPC-mitochondria, unless it was added in excessive amounts (Table 2-2). These studies, by showing the expected increase in calcium tolerance of IPC mitochondria,

validated our experimental system. In addition, it was observed that FGF-2 treatment raised SSM resistance to calcium-induced mPTP.

The effect of FGF-2 on SSM was also examined by determining the effect of increasing $CaCl_2$ on cytochrome C release. Opening of mPTP is accompanied by release of cytochrome C into the extramitochondrial space. *In vitro*, released cytochrome C is present in the supernatant fraction obtained after centrifugation of mitochondrial suspensions (Baines et al., 2005). In control SSM, increasing calcium (starting at 300 μM) caused cytochrome C release to the supernatant and a corresponding decrease in the pellet (Figure 2-2C). Cytochrome C release was completely prevented by CsA, indicating that it was the result of mPTP. SSM from FGF-2-hearts did not show any cytochrome C release, indicating that they were resistant to calcium-induced mPTP under our experimental conditions (Figure 2-2C). The mitochondria swelling approach was used in all subsequent experiments assessing resistance to calcium-induced mPTP.

Table 2-2 Effect of FGF-2 perfusion on calcium capacity/tolerance of SSM suspensions

Conditions	**Calcium Capacity** ($\mu M\ Ca^{2+}$/mg of protein) **Control**	**Calcium Capacity** ($\mu M\ Ca^{2+}$/mg of protein) **FGF-2**	**Calcium Capacity** ($\mu M\ Ca^{2+}$/mg of protein) **IPC**
No ADP	**183±28**	**363±37***	**300±23***
+ ADP	**342±28**	**700±78***	**642±61**
+ ADP, +CsA	**6875±361**	**8205±500***	**7125±468**

Calcium capacity or tolerance was defined as the amount of added $CaCl_2$ capable of eliciting a drop in A_{545}, and was assessed in mitochondria from control (vehicle treated), FGF-2-perfused hearts, or hearts subjected to "ischemic preconditioning" (IPC; positive control), incubated with or without ADP, and in the absence or presence of cyclosporine A (CsA), as indicated. Asterisks (*) indicate significant difference ($P<0.05$, one way ANOVA) compared to corresponding controls; n=5

Figure 2-2 Effect of FGF-2 perfusion on calcium-induced mitochondrial swelling and cytochrome C release

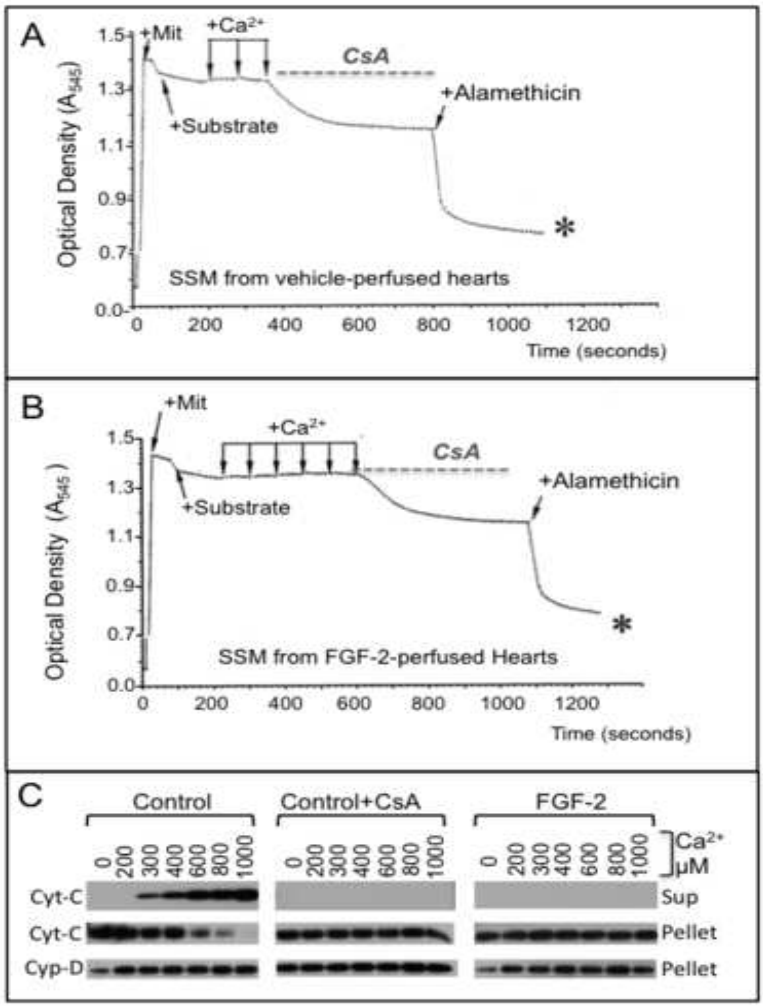

Panels (A, B) show representative tracings of changes in A_{545} (optical density) of mitochondria from (A) control or (B) FGF-2-treated hearts during titration with calcium in the presence of ADP. Calcium was added in increments of 125 µM/minute until a drop in A_{545} was observed. Number of arrows corresponds to number of increments required to cause a decrease in A_{545}. The broken line illustrates the lack of an A_{545} change when cyclosporine A (CsA) was added before calcium titration. Alamethicin, an mPTP opener, was added to obtain the maximal amplitude of swelling, indicated as asterisk (*). **Panel (C)** Mitochondria from control or FGF-2-treated hearts were subjected to increasing calcium (as indicated), ± CsA. Western blots of mitochondrial supernatant (released) and pellet fractions, were probed for cytochrome C (Cyt-C); pellets were also probed for cyclophilin D (Cyp-D), a mitochondrial matrix protein which serves as loading control.

2.3 The effect of FGF-2 perfusion on calcium-induced swelling of IFM versus SSM suspensions ± Gap27

To examine if the protective effect of FGF-2 on mitochondria was SSM-specific, and to determine the role of a mitoCx43 channel function, a second series of experiments comparing calcium tolerance (swelling) of IFM and SSM suspensions from vehicle- or FGF-2-perfused hearts were done in the presence of either Gap27 peptide or its inactive scrambled peptide. Individual SSM and IFM preparations were obtained from the same heart and tested immediately after isolation. IFM from control or FGF-2 perfused hearts expressed very low levels of Cx43 (Figure 2-3A), were devoid of plasma membrane contamination, and were enriched in mitochondrial markers such as VDAC, ANT1, cytochrome C and cyclophilin D, similar to SSM (Figure 2-3B). The scrambled Gap27 peptide had no effect on calcium tolerance of either SSM or IFM preparations, under all conditions tested (Figure 2-4).

FGF-2 administration to the heart resulted in significantly increased resistance to calcium-induced swelling in both IFM and SSM isolated from these hearts compared to IFM and SSM from control hearts (Figure 2-5). The FGF-2-induced increase in calcium tolerance of SSM was, at 2.9-fold (±0.33 SD, n=6), significantly more pronounced than the FGF-2-induced increase in calcium tolerance of IFM, at 1.7-fold ($\pm$0.12 SD, n=6). We conclude that FGF-2 administration protects both types of cardiac mitochondrial populations from calcium overload, but SSM are more responsive to the protective effect.

In SSM from control hearts, incubation with Gap27 peptide significantly decreased calcium capacity, by 44% compared to those incubated with scrambled peptide. In SSM from FGF-2- treated hearts Gap27 decreased calcium capacity by 77%, eliminating the FGF-2-induced increased calcium tolerance (Figure 2-5). In the presence of Gap27, calcium capacity was minimal and similar between SSM from FGF-2-or control-perfused hearts. In contrast, Gap27 had no effect on calcium capacity of IFM from either control- or FGF-2-hearts (Figure 2-5). IFM from FGF-2 hearts retained higher calcium tolerance compared to IFM from control hearts regardless of Gap 27. Representative tracings are included in Figure 2-6. The data indicate that mitoCx43 channel function is mediating both baseline (control) as well as the FGF-2-induced resistance to calcium overload in SSM (Figure 2-7). Absence of an effect of Gap27 on IFM is consistent with negligible levels of Cx43 in this mitochondrial population.

Control heart-derived IFM displayed significant higher calcium capacity (by 2.2-fold), compared to control heart-derived SSM (Figure 2-5). FGF-2 heart-derived IFM also displayed higher calcium capacity than FGF-2- heart-derived SSM, but the magnitude of the difference (at 1.3- fold) was less pronounced than in the control mitochondrial populations.

Figure 2-3 Interfibrillar cardiac mitochondria (IFM)

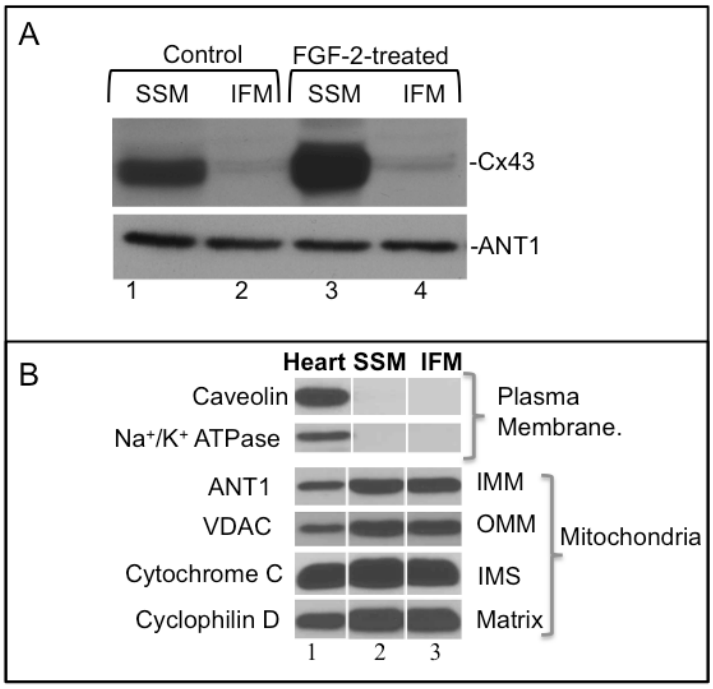

Panel (A). Connexin 43 in SSM versus IFM. Representative (n=3) Western blots of SSM (lanes 1 and 3) and IFM (lanes 2 and 4) mitochondrial from untreated control hearts (Control, lane 1 and 2) or FGF-2 perfused hearts (FGF-2-treated, lane 3, 4), and probed for Cx43 or ANT1, as indicated. Unlike SSM, IFM preparations from either control of FGF-2-treated hearts display only a weak signal for Cx43. **Panel (B).** Representative Western blots of, lane 1, total lysates (heart), lane 2, SSM lysates (SSM), lane 3, IFM lysates (IFM), all loaded at 30 µg/ml, showing absence of plasma membrane markers (Caveolin, Na^+/K^+ ATPase) from both IFM and SSM, and similar enrichment in mitochondrial proteins of the inner mitochondrial membrane (IMM) such as ANT1, the outer mitochondrial membrane (OMM) such as VDAC, inter-mitochondrial membrane space (IMS) such as cytochrome C, and mitochondrial matrix (Matrix) such as cyclophilin D, as indicated.

Figure 2-4 Lack of effect of scrambled Gap27 peptide on calcium-induced swelling of cardiac mitochondria

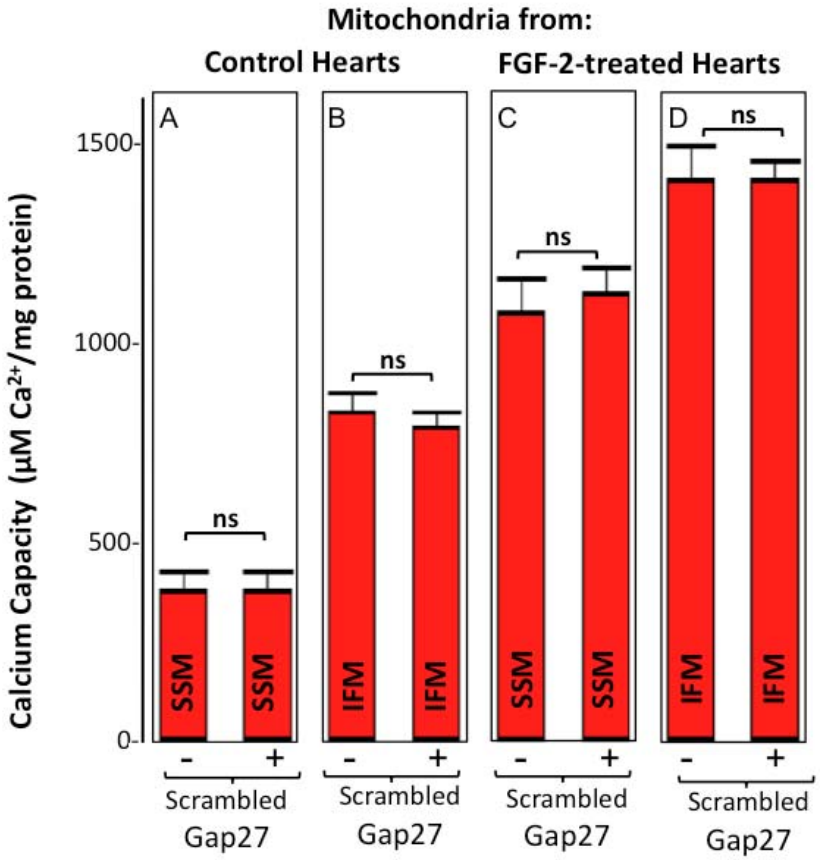

Panels (A-D) show mitochondrial calcium capacity (µM Ca^{2+}/mg protein, means ± SEM) in the absence (-) or presence (+) of a scrambled inactive Gap27 peptide (250 µM), under four different situations, represented in the four different panels. Panel A, SSM from control hearts (n=4 per group); panel B, IFM from control hearts (n=3 per group); panel C, SSM from FGF-2-treated hearts (n=4 per group); panel D, IFM from FGF-2-treated hearts (n=3 per group). Comparisons between the two groups within each panel were made using unpaired student's t test; no significant differences were seen ($P>0.05$) in any of the panels.

Figure 2-5 Effect of Gap27 peptide on calcium capacity of SSM and IFM

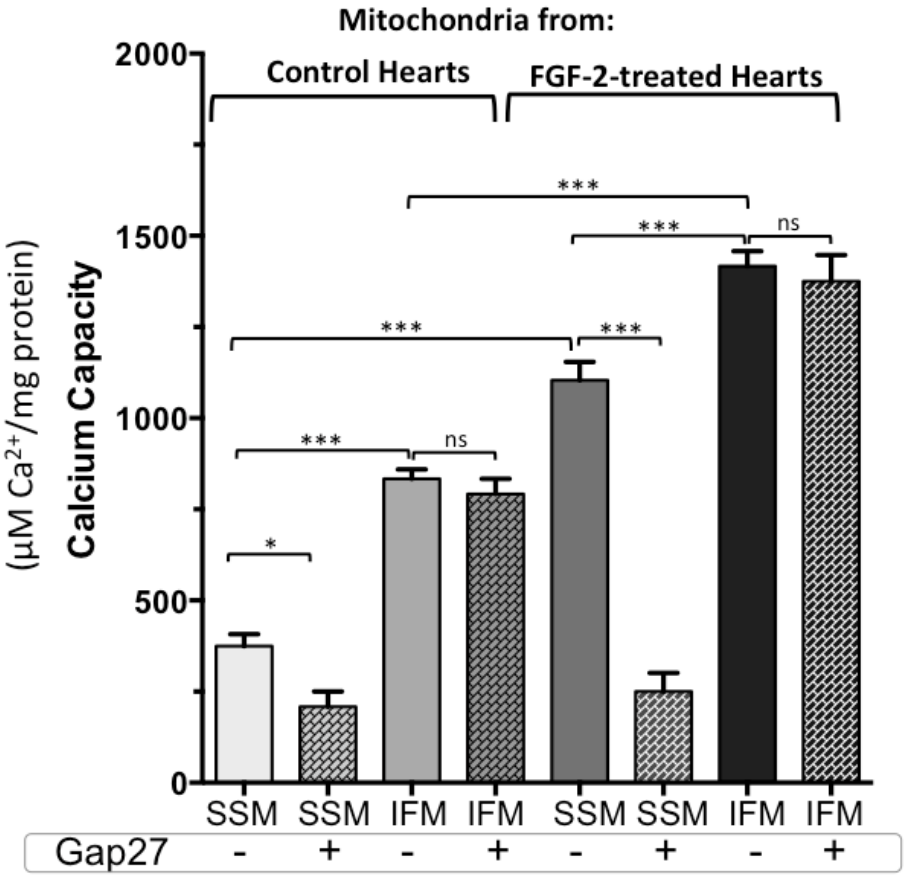

SSM and IFM preparations were obtained from control- or FGF-2-perfused hearts. Before the incremental addition of calcium, mitochondrial suspensions were supplemented with 250 μM of scrambled inactive Gap27 peptide (-), or Gap27 peptide (+), as indicated. Calcium capacity values (μM Ca^{2+}/mg protein), are shown for SSM or IFM obtained from control- or FGF-2-perfused hearts, ± Gap27. Brackets show comparisons between groups (n= 3-6), where *, **, *** correspond, respectively, to $P<0.05$, $P< 0.01$, $P< 0.001$, and ns= non significant. 2-way ANOVA analyses with Tukey's multiple comparisons test were used to separately compare values within the SSM or IFM mitochondrial groups (variables: ±FGF-2 pretreatment, ± Gap27), and also compare values between control and FGF-2 groups (variables: SSM versus IFM, ± FGF-2). Some representative tracing are shown in Figure 2-6.

Figure 2-6 Effect of FGF-2 on calcium-induced SSM or IFM in the presence of Gap27

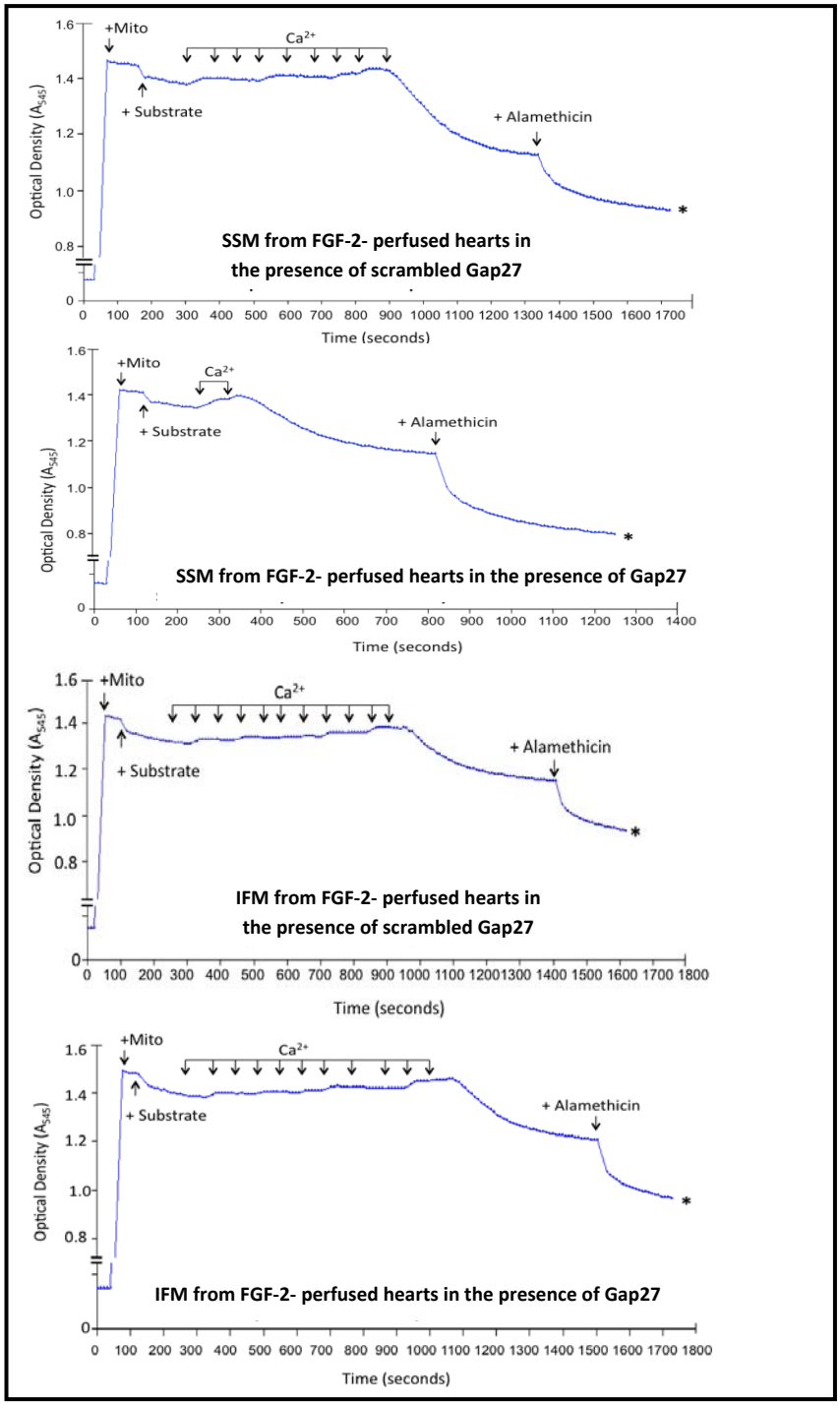

Representative tracings (n=3-6) showing optical density (A_{545}) of SSM and IFM mitochondrial suspensions obtained from FGF-2-perfused hearts, and incubated in the presence of scrambled-inactive and active peptide Gap27. Calcium was added in 125 µm increments. Presence of Gap27 diminished calcium capacity of SSM, but not IFM suspensions. Cumulative data have been shown in Figure 2-5C.

2.4 The effect of FGF-2 perfusion on mitochondrial PKCε, Cx43, P*Cx43 and Tom-20

Previous studies have shown that IPC-induced cardioprotection is associated with increased levels of PKCε and/or Cx43 in cardiac mitochondria, due to translocation via the TOM translocase complex (Budas et al., 2010; Rodriguez-Sinovas et al., 2006). To determine if FGF-2 exerted similar effects, the relative levels of mitoPKCε, mito-pPKCε, and Tom-20 in SSM and IFM from control and FGF-2-treated hearts were compared. Relative levels of total mitoCx43, as well as P-S262-, P-S368-Cx43 were also determined in SSM. As shown in Figure 2-7, Cx43, PKCε, pPKCε, and Tom-20 were clearly present in SSM from control and FGF-2 hearts, as assessed by Western blotting with specific antibodies. The FGF-2 group displayed significant 1.4-, 1.6-, 1.7- and 2.0-fold increases, respectively, in total mitoCx43, -PKCε, -pPKCε, and Tom20 compared to the control group. While immunoreactive signals for P-S262- and P-S368-Cx43 were barely above background in SSM from control hearts, significant >30-fold and 8-fold, respectively, increases were detected in SSM from FGF-2 hearts. IFM from control hearts, unlike corresponding SSM, elicited no discernible immunoreactive signal for PKCε, pPKCε, or Tom-20, Figure 2-8A. Another protein implicated in protecting mitochondria from mPTP, glycogen synthase kinase (GSK)-3β, was present in IFM from control hearts (Figure 2-8). IFM from FGF-2-treated hearts displayed presence of PKCε, pPKCε, and Tom-20. In addition, IFM from FGF-2-treated hearts showed a significant increase in mito-GSK-3β, and pS9-GSK-3β (Figure 2-8B).

Figure 2-7 Effect of FGF-2 perfusion on select SSM-associated proteins.

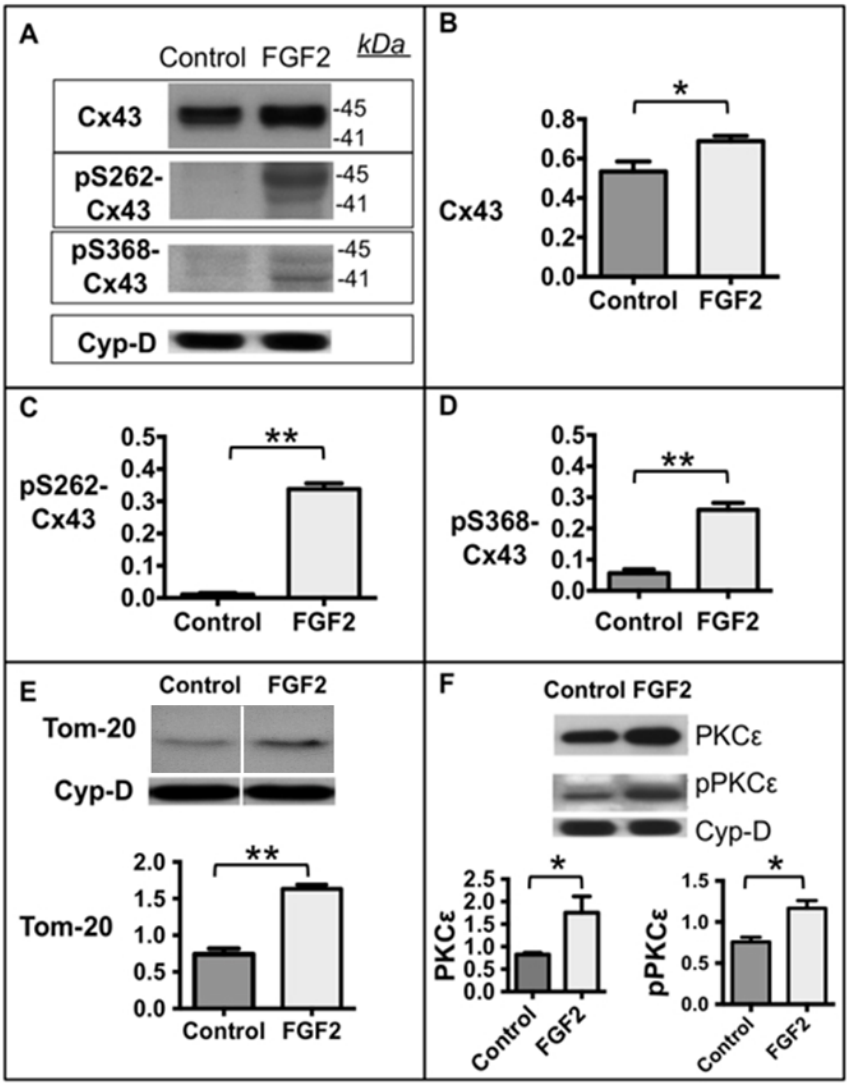

SSM from control or FGF-2-perfused hearts were analyzed by Western blotting; n=3 (independent experiments) for each group. **Panel (A)** shows representative Western blot images of SSM lysates probed for total Cx43, P-S262-, P-S368-Cx43, and cyclophilin D (Cyp-D), used as loading control. **Panels (B-D)** show the corresponding quantitative data (panel B**:** total Cx43; panel C: P-S262-Cx43; panel D: P-S368-Cx43). **Panels (E and F)** show representative Western blot images of SSM lysates probed for Tom-20 or PKCε, as well as pPKCε, as indicated; corresponding quantitative data are included within each panel. Data were analyzed using the student's t-test.

Figure 2-8 Effect of FGF-2 perfusion on IFM-associated proteins

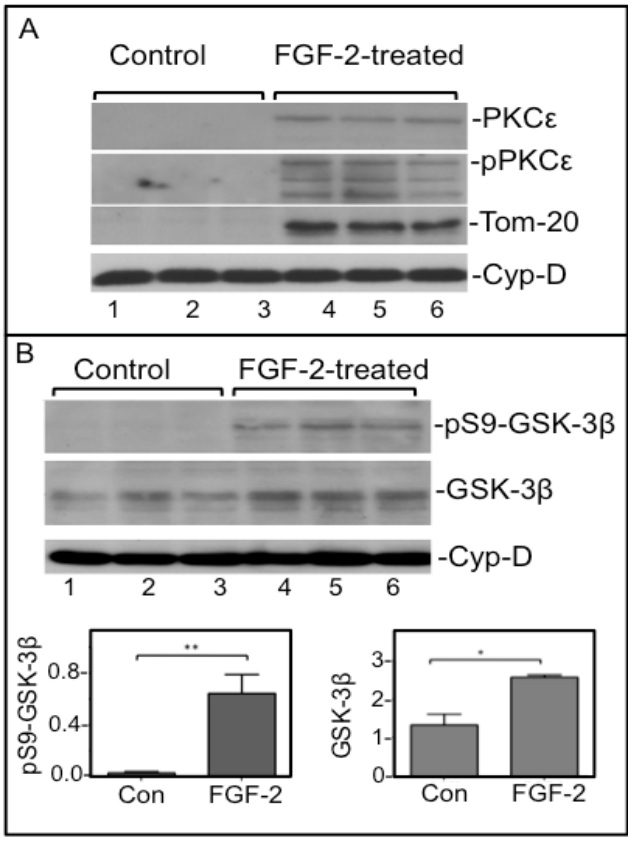

Panel (A) Western blots of IFM lysates (30 μg protein/lane), probed for PKCε, pPKCε, Tom-20, cyclophilin D (Cyp-D). **Panel (B)** Western blots of IFM lysates probed for GSK-3β, pS9-GSK-3β, and corresponding quatitative data, as indicated; comparison between two groups were made using the student's t test. The signal for Cyp-D was used for loading control. In both (A) and (B), lanes 1, 2, 3 and 4, 5, 6 contain individual IFM preparations from control and FGF-2-treated hearts, respectively.

2.5 The effect of PMA on isolated SSM

In the normal adult heart Cx43 is constitutively phosphorylated at multiple sites. Several kinases, including ERK and PKC are known to phosphorylate Cx43 at specific sites (Solan and Lampe, 2009). Previously, we demonstrated that the FGF-2 or PMA-induced Cx43 phosphorylation at S262, which occurs in addition to the constitutive phosphorylation pattern, is mediated by PKCε but not the ERK pathway (Doble et al., 2004; Doble et al., 2001; Doble et al., 2000). To determine if mitoPKCε is involved in phosphorylation of mitoCx43 at S262, and/or S368, SSM from control hearts were stimulated with the PKC activator, PMA, in the presence of either a PKCε inhibitor peptide, $\varepsilon V_{1\text{-}2}$, or its inactive control (scrambled, Scr) peptide. These reagents have been used successfully to inhibit mitochondrial PKCε (mitoPKCε) activity by others (Costa and Garlid, 2008). In the presence of scrambled peptide, PMA elicited a very significant increase in P-S262-Cx43 (14-fold) compared to control mitochondria, showing that Cx43 can be phosphorylated at S262 within the mitochondrial environment (Figure 2-9A, B). The PMA-induced increase in mitoCx43 phosphorylation at S262 was prevented by the PKCε-inhibitor peptide, indicating that mitoPKCε is responsible for phosphorylating mitoCx43 at S262 in isolated SSM (Figure 2-9A, B). PMA also increased mito-P-S368-Cx43 by 4-fold (Figure 2-9A, C), and the effect was blunted by $\varepsilon V_{1\text{-}2}$ (Figure 2-9A, C). Although, the effect of $\varepsilon V_{1\text{-}2}$ on calcium capacity in the presence of PMA was not tested, previous studies have shown that the PMA-induced increase in calcium capacity in isolated mitochondria is mediated by mitoPKCε (Costa and Garlid, 2008; Costa et al., 2006b).

Figure 2-9 Effect of PMA on mitoCx43 phosphorylation at S262/S368

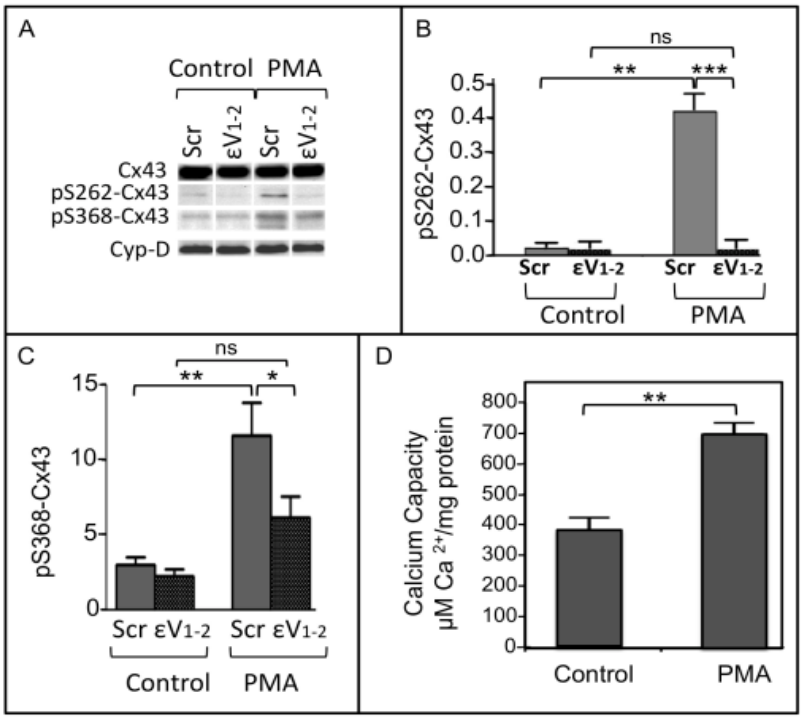

SSM isolated from non-stimulated hearts were incubated without PMA (Control) or with PMA, as indicated, in the presence of scrambled inactive PKCε peptide (Scr) or PKCε-inhibitor peptide ($\varepsilon V_{1\text{-}2}$) and analyzed by Western blotting for total Cx43, P-S262-Cx43, P-S368-Cx43 and Cyp-D (loading control). Representative images are shown in panel A, with quantitative data for P-S262- or P-S368-Cx43 shown, respectively, in panels B and C; n=4. Two-way ANOVA was used to compare groups in B and C; variables ± PMA, ± $\varepsilon V_{1\text{-}2}$. Panel D shows SSM calcium capacity, determined by the mitochondrial matrix swelling assay, in the absence or presence of PMA, as indicated. Asterisks (**) indicate significant difference (student's t test) compared to controls; n=5 (see also Figure 2-7).

Figure 2-10 Effect of PMA stimulation on calcium-induced SSM swelling

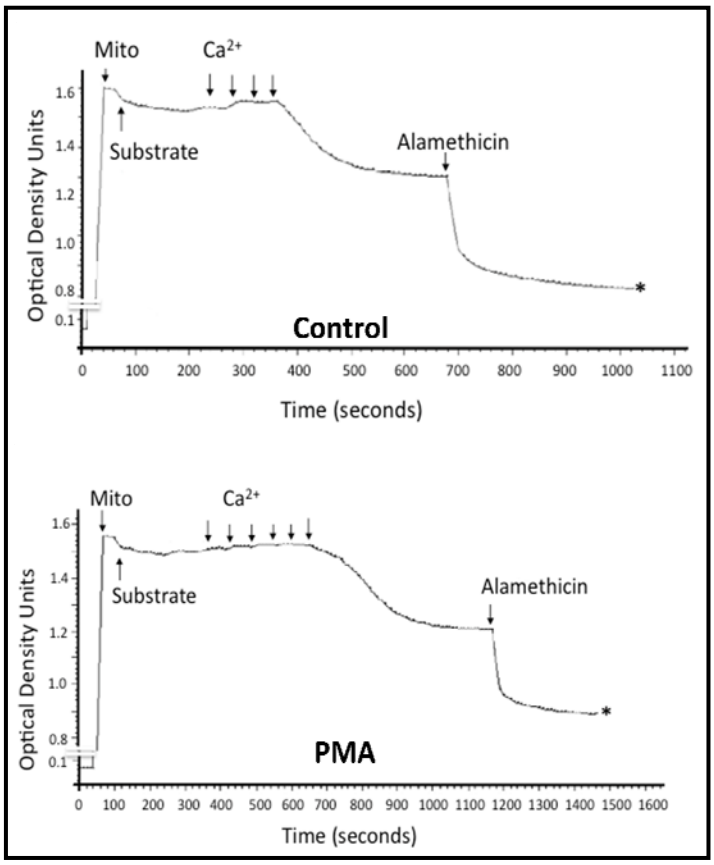

Representative tracings of changes in A_{545} (optical density) in SSM from unstimulated or PMA-stimulated hearts during titration with calcium in the presence of ADP are shown. Calcium was added in 125 μM increments. Alamethicin, an mPTP opener, was added at the end of the experiment to obtain the maximal amplitude of swelling, indicated as asterisk (*). Cumulative data have been shown in graph from in Figure 2-9D.

Results section 3. Direct effects of FGF-2 on cardiac SSM mitochondria

In the previous sections, the indirect, plasma membrane-mediated effects of extracellular-acting FGF-2 (administered to the heart by perfusion), on total and mitochondrial Cx43, and on mitochondrial calcium tolerance were examined. In addition to the extracellular space FGF-2 is present in the cytosolic and nuclear locales. Cytosolic FGF-2 may exert direct effects on subcellular organelles such as the mitochondria. This section will describe a first series of studies investigating the hypothesis that FGF-2 can directly modulate calcium tolerance of cardiac SSM mitochondria.

3.1 Cardiac SSM respiration ± FGF-2

To examine whether direct exposure of isolated mitochondria to FGF-2 would affect respiratory function, cardiac mitochondrial suspensions (0.5 mg) were treated with or without FGF-2 (25 ng/ml). Respiration in isolated cardiac SSM was assessed polarographically using glutamine and malate as oxidative substrates. The respiratory control index (RCI), normally regarded as an index of mitochondrial viability and quality, was calculated as a ratio of state III/ state IV respiration. Cardiac mitochondria preparations with RCI values of higher than 4.0 indicate well coupled mitochondria [McCarthy J et.al. 2010]. The RCIs of cardiac mitochondria in the current experiments were above 7.0. The respiration rate of isolated cardiac mitochondria incubated in presence of FGF-2 was not significantly different than controls, indicating that FGF-2 did not affect the efficiency of oxidative phosphorylation (Table 3-1).

Table 3-1 Respiratory activity of isolated cardiac mitochondria treated with FGF-2

	Rate of respiration		RCI (State 3/ State 4)	ADP/O ratio (nmol ADP/ nmoles O_2)	Rate of Oxidative Phosphorylation (nmol ATP/min/mg protein)
	State 3	State 4			
Control	154.3 ± 6.7	19.9 ± 1.2	7.79 ± 0.26	2.51 ± 0.05	387.3 ± 19.5
FGF-2	171.3 ± 10.3	20.0 ± 2.4	8.85 ± 0.87	2.56 ± 0.04	437.9 ± 25.8

State III is the rate of ADP-stimulated respiration (active state). State IV is the rate of mitochondrial respiration when the added ADP is consumed (resting state). RCI (Respiratory control index), calculated as the ratio of state III to state IV, represents the status of coupling between the rate of oxygen consumption and oxidative phoshorylation. OPR is rate of oxidative phosphorylation. Data are expressed as mean ± SEM from four independent experiments.

3.2 Direct protective effect of FGF-2 on mitoP*Cx43, resistance to mPTP, and the role of mitoPKCε

Mitochondria (SSM) were isolated from control, unstimulated hearts. SSM suspensions, incubated in the presence or absence of FGF-2 (25 ng/ml), were subjected to the calcium-induced matrix swelling (mPTP formation) assay, measuring light scattering (A_{545}) upon consecutive calcium increments. A representative series of light scattering measurements (Figure 3-1A, B) showed that FGF-2 treated mitochondria had a significantly higher calcium retention capacity compared to untreated controls.

As shown in results section 2, mitoPKCε is present in SSM from unstimulated hearts. To examine whether mitoPKCε mediates the direct protective effects of FGF-2 on mitochondria, SSM were treated with FGF-2 in the presence of a PKCε -selective inhibitory peptide (εV_{1-2}) or a scrambled control peptide (Scr), and subjected to the calcium-induced matrix swelling assay. As shown in Figure 3-2, the ability of FGF-2 to directly raise mitochondrial calcium capacity/tolerance was abolished in the presence of εV_{1-2}, but not the scrambled peptide. These results indicate that mitoPKCε activity is necessary for the direct protective effect of FGF-2 on mitochondria.

To investigate if FGF-2 can exert direct effects on mitoCx43 phosphorylation, mitochondrial suspensions from unstimulated hearts were treated with or without FGF-2 for 15 minutes, followed by Western blot analysis of mitochondrial lysates. As shown in Figure 3-3, FGF-2 did not affect total mitoCx43 (44-45 kDa, probed with P.AB) levels. FGF-2 treatment stimulated a statistically significant increase in

relative P-S262- and P-S368-Cx43 (Figure 3-3A and B, respectively). The P-S262-Cx43 band migrated at approximately 45 kDa, while the P-S368-Cx43 migrated at approximately 41 kDa.

To examine whether mitoPKCε mediated the direct FGF-2-induced phosphorylation of mitoCx43 at S262 and S368, mitochondrial suspensions were stimulated with FGF-2 in the presence of peptide $\varepsilon V_{1\text{-}2,}$ or inactive peptide, Scr. As shown in Figure 3-4, incubation with $\varepsilon V_{1\text{-}2}$ peptide prevented the FGF-2-induced upregulation in P-S262-Cx43 and P-S368-Cx43. These results indicate that FGF-2 can directly promote mitoCx43 phosphoryation by mitoPKCε.

Figure 3-1 Incubation with FGF-2 increases mitochondrial (SSM) calcium capacity

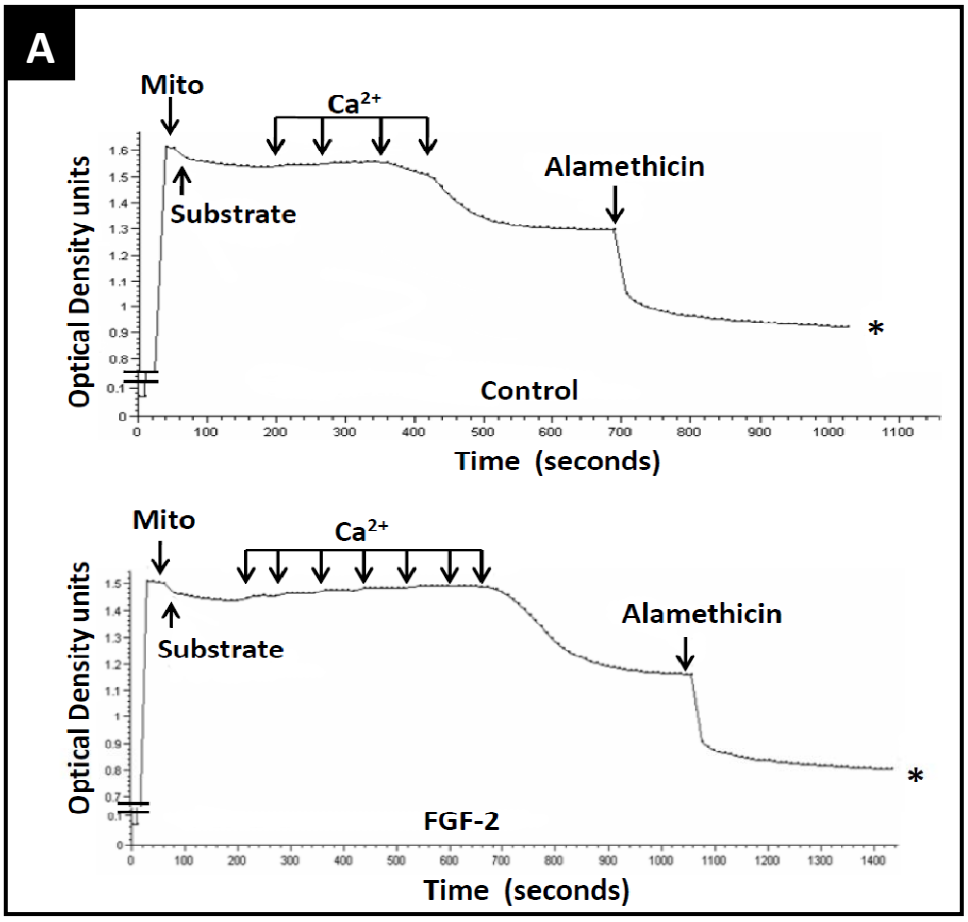

B

Calcium Retention Capacity (nM Ca^{2+}/mg of protein)	Control	FGF-2
ADP	400 ± 25	876 ±64*
CsA+ ADP	8000 ±310	9050±500*

Panel (A) shows representative tracing of changes in optical density A_{545} nm in FGF-2-treated, and untreated control SSM, during titration with calcium, as indicated. **Panel B** shows cumulative data from four independent experiments indicating a significant increase in calcium capacity in FGF-2 treated mitochondria compared to controls. Full (100%) mitochondria swelling were determined by addition of alamethicin. Ca^{2+} denotes calcium. *P<0.05.

Figure 3-2 MitoPKCε activity mediates the direct protective effect of FGF-2 on SSM

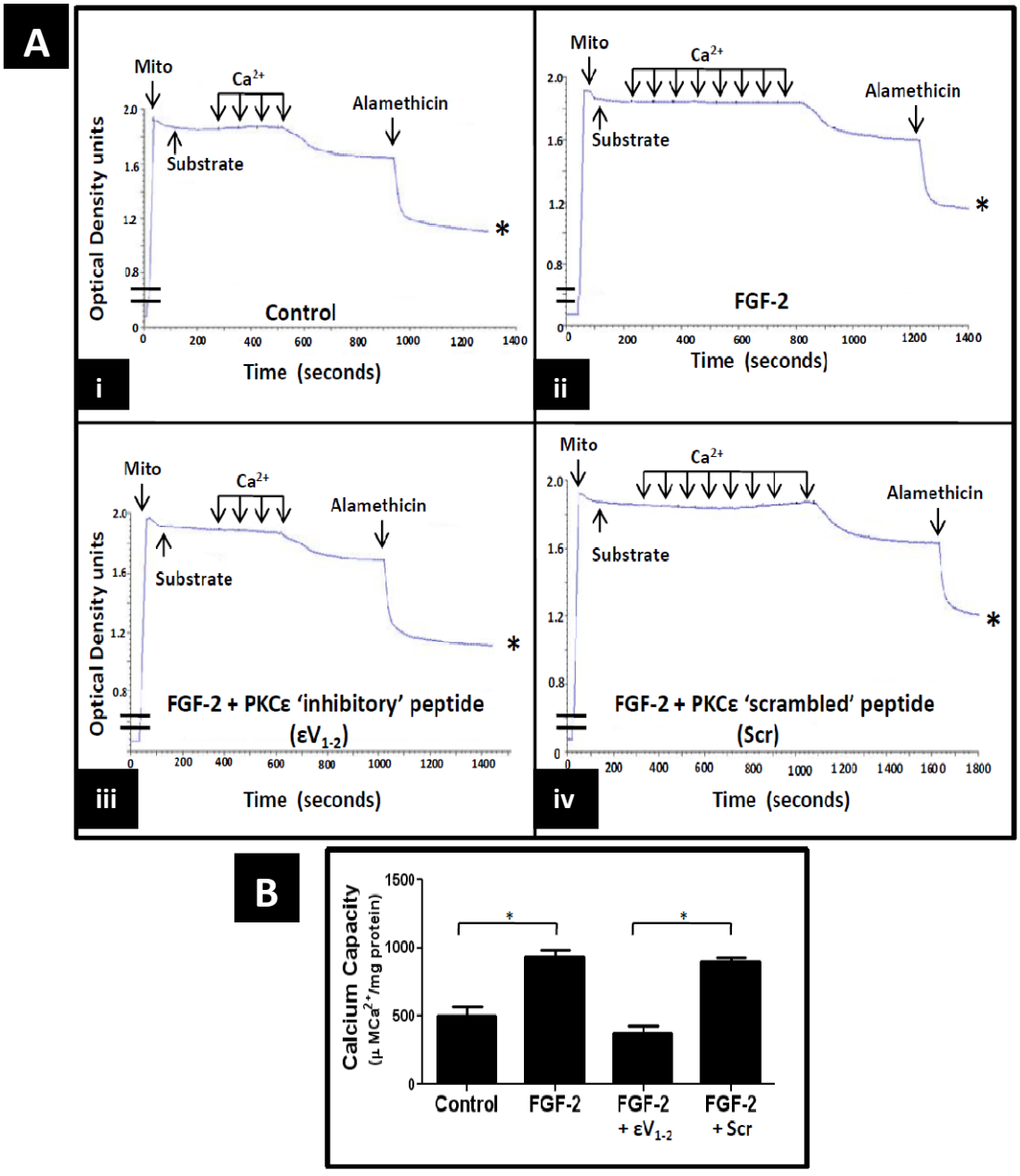

Panels A (i-iv) and B show the representative optical density (A_{545}) measurements, and corresponding quantitative data (n=4), of different SSM groups (± FGF-2; ± εV_{1-2}) subjected to the calcium-induced matrix swelling assay. Brackets in B indicate comparisons between groups, where $P<0.05$ is significant (*).

Figure 3-3 FGF-2 directly stimulates mitoCx43 phosphorylation at S262 and S368.

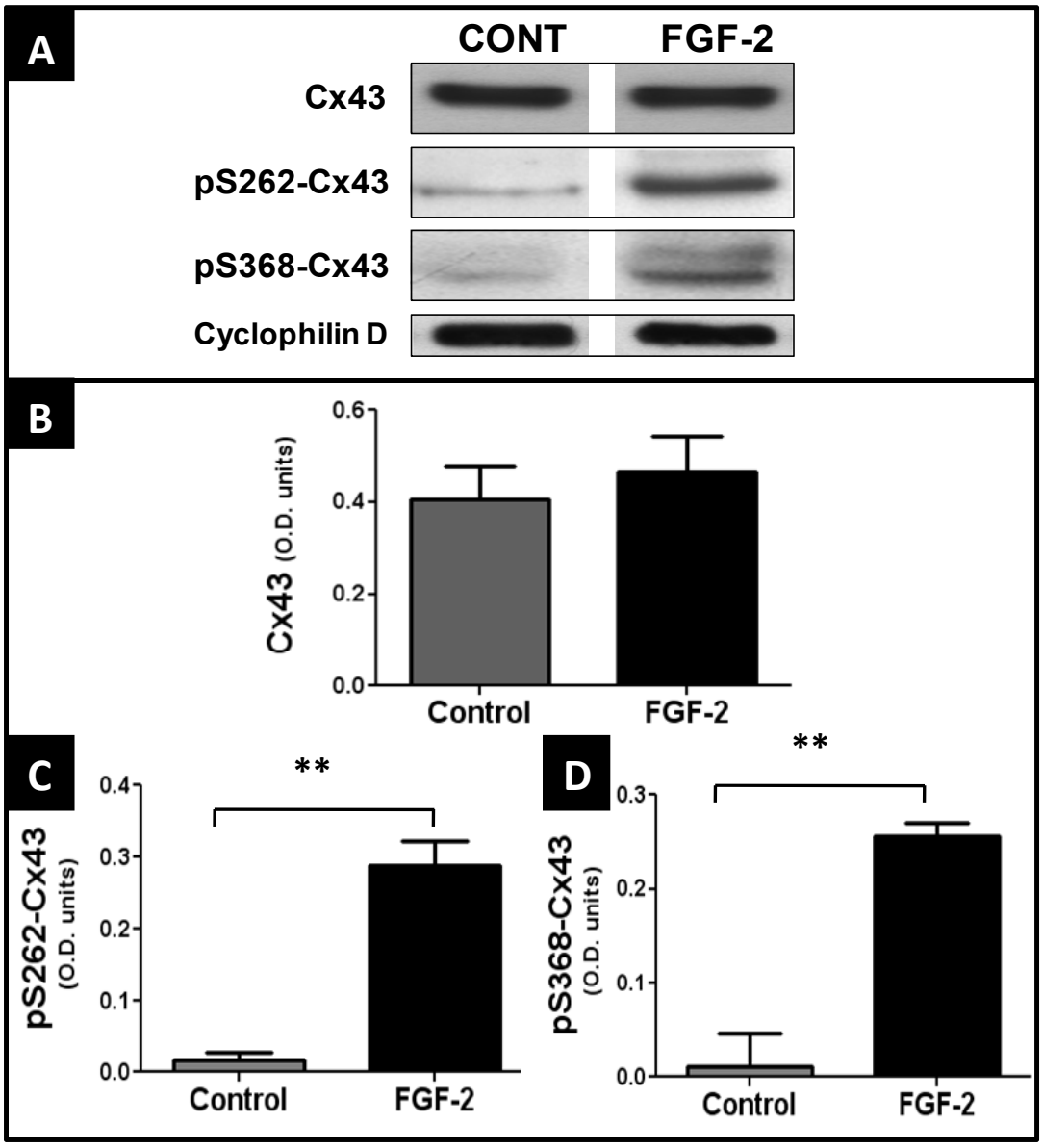

Panel (A) shows representative Western blots of unstimulated control (CONT), or FGF-2-stimulated mitochondria (FGF-2) probed for total Cx43, P-S262-Cx43, P-S368-Cx43, as indicated. Cyclophilin D was included as a control for equal loading. Corresponding quantitative data (n=4 independent experiments) are shown in panel B (total Cx43), panel C (P-S262-Cx43), and panel D (P-S368-Cx43). **P<0.01.

Figure 3-4 The direct, FGF-induced mitoCx43 phosphorylation at S262 and S368 is mediated by mitoPKCε.

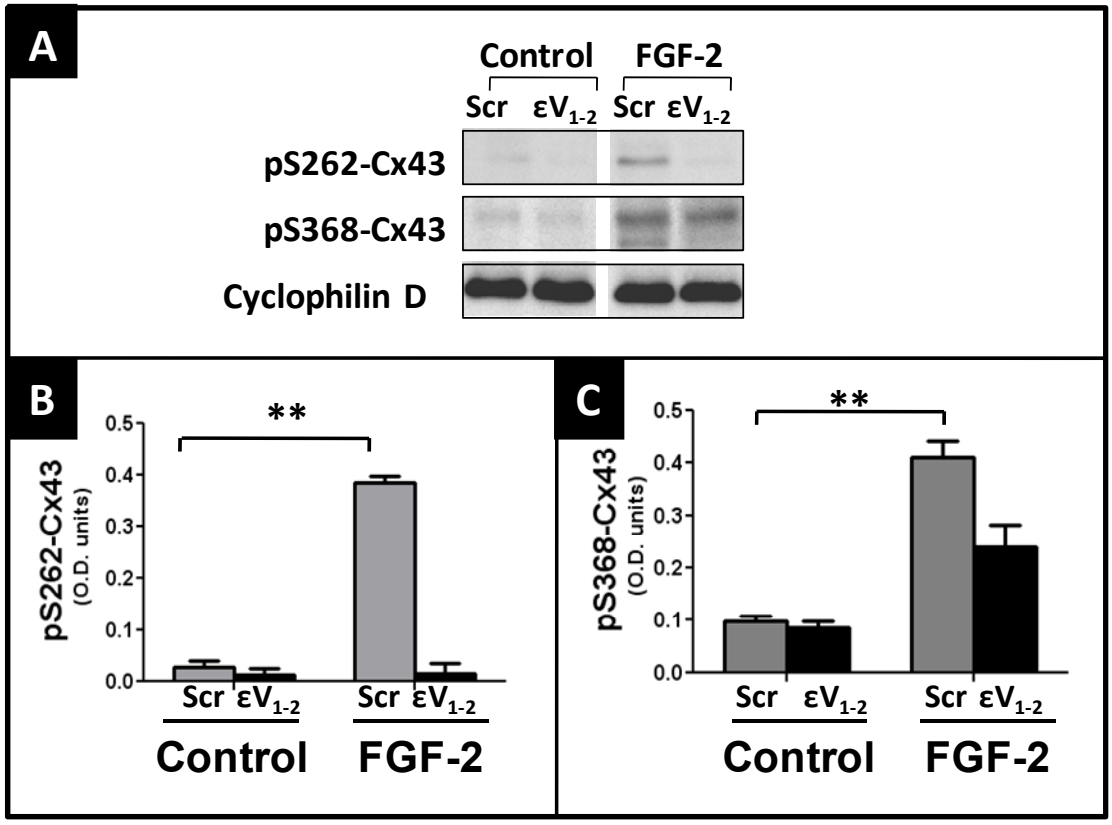

Panel (A) shows representative Western blots of untreated (Control) or FGF-2-treated (FGF-2) cardiac mitochondrial suspensions, co-incubated with either peptide $\varepsilon V_{1\text{-}2}$ or an inactive scrambled (Scr) peptide, as indicated, and probed for total Cx43, P-S262-Cx43, P-S368-Cx43, and cyclophilin D (Cyp-D). Cumulative data (n=3) are included in panel B (total Cx43), panel C (P-S262-Cx43), and panel D (P-S368-Cx43). **P<0.01.

3.3 Direct effects of FGF-2 on calcium overload-induced cytochrome C release

Calcium (625 μM) was added to cardiac mitochondrial suspensions pre-treated with or without FGF-2; after a 3 minute of incubation, suspensions were centrifuged gently to obtain pellet and supernatant fractions. The mitochondrial pellets and supernatants were analyzed by Western blotting for cytochrome C, and results presented in Figure3-6. In non- treated SSM mitochondria, calcium overload caused the appearance (release) of cytochrome C in the supernatant, accompanied by a decrease in cytochrome C in the pellet fraction. On the other hand, FGF-2-treated mitochondria remained intact in the presence of calcium, displaying no cytochrome c release to the supernatant.

Calcium overload not only caused cytochrome C release from mitochondria, but also stimulated loss of mitoCx43, presumably due to degradation. In the absence of FGF-2, calcium overload resulted in almost complete disappearance of mitoCx43 from the mitochondrial pellet (Figure 3-5A, D). ANT, an inner mitochondrial membrane protein, was used as control for protein loading (Figure 3-5A). These results indicate that FGF-2 prevented the calcium-induced degradation of mitoCx43. This protection may require the FGF-2 induced-, PKCε-mediated, phosphorylation of mitoCx43 at PKC sites S262 and 368.

Figure 3-5 FGF-2 prevents calcium induced cytochrome C release and mitochondrial Cx43 loss

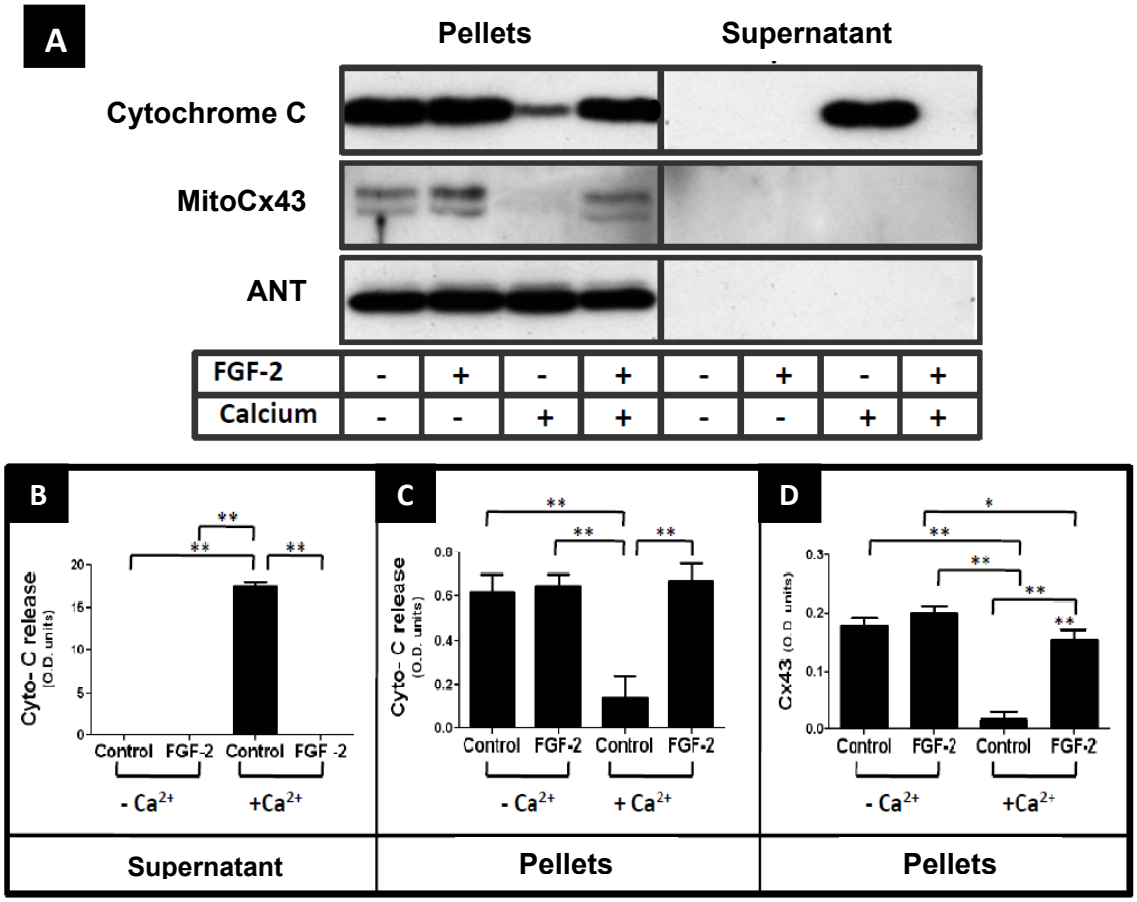

Panel (A) Isolated cardiac mitochondria were pre-treated with FGF-2, and subjected to calcium overload. At the end of experiment, mitochondrial pellet and supernatant fractions were analyzed for cytochrome C and ANT was included as a control for equal loading. **Panels (B-D)** Cumulative data from four independent experiments shows a significant loss of cytochrome C from pellets to supernatant and degradation, in the presence of calcium overload. *P<0.05 and **P<0.01.

3.4 Presence of FGFR1-like protein (s) in cardiac mitochondria

The preceding experiments showed that FGF-2 can exert direct effects on cardiac SSM, including mitoCx43 phosphorylation and protection from calcium-induced cytochrome C release. These findings suggested the presence of a FGF-2 receptor to transduce the direct effects of FGF-2 through an intra-mitochondrial pathway. It is known that tyrosine kinase FGFR1 is the major cardiomyocyte FGF-2 receptor (Sheikh et al., 1999). Therefore, we hypothesized that an FGFR1-like protein may be present at mitochondria. To address this question it was important to verify the ability of commercially available anti-FGFR1 antibodies to detect FGFR1. To this end, a cDNA coding for FGFR1 was expressed in HEK293 cells by transient gene transfer, and cell lysates were probed with the anti-FGFR1 antibodies before and after transfection. Results are shown in Figure 3-6. Untransfected cells presented a relatively weak signal in the 100-150 kDa range, corresponding to the expected size of FGFR1. Anti-FGFR1 (sc-121) antibody elicited a strong immunoreactive signal in transfected cells. Antibodies against tyrosine-phosphorylated (activated) FGFR1, PY766-FGFR1, and PY653/654-FGFR1, also detected a robust signal in transfected cells. All three different anti-FGFR1 antibodies detected similar bands in transfected cells, indicating that they were capable of detecting the introduced FGFR1. These antibodies were then used to detect potential FGFR1 in cardiac mitochondria, as well as total heart lysates, and results are shown in Figure 3-7. Two different SSM preparations presented a strong anti-FGFR1 (sc-121) signal at about 100 kDa, consistent with the expected size of FGFR1 and similar to an immunoreactive band in total heart lysates (Figure 3-8A).

We examined unstimulated and FGF-2-stimulated SSM mitochondria for presence of activated, tyrosine phosphorylated, FGFR1. The anti-PY766- and anti-PY653/654-FGFR1 detected immunoreative bands in both control and the FGF-2-treated mitochondria. The intensity of the immunoreactive signal was clearly stronger in the FGF-2-treated SSM, indicating that direct stimulation with FGF-2 activates an FGFR1-activity at mitochondria.

Immuno-electron microscopy (EM) of cardiac ventricular sections was used to probe for presence of FGFR1 in cardiac mitochondria in situ. Immuno-EM and image acquisition was done by Dr. Pasumarthi (Dalhousie University). As shown in Figure 3-8, immuno-gold clusters, indicating of antigen-antibody interaction *in situ*, was detected in sections incubated with anti-FGFR1-antibodies. Anti-FGFR1 immuno-gold staining was observed at plasma membrane (sarcolemmal) sites, as expected, as well as at mitochondrial sites, consistent with presence of an FGFR1-protein at mitochondria. Mitochondrial reactivity with anti-Y653/654-FGFR1 antibodies indicated that mitochondrial FGFR1 is tyrosine phosphorylated (activated) *in situ*.

To examine the role of a mitochondrial FGFR1-like protein in FGF-2 mediated protection of cardiac SSM from calcium overload ('mitoprotection'), SSM were pre-treated with or without a pharmacological FGFR1 inhibitor (SU5402, 20 μM, for 15 minutes), followed by FGF-2 stimulation and exposure to 625 μM calcium. In a parallel experiment, a specific anti-FGFR1 neutralizing antibody (Neu-Ab; 20 μg/ml; Millipore MAB 125) was used to pre-treat cardiac SSM, followed by FGF-2

stimulation and exposure to calcium. Non-treated SSM were included in all experiments. At the end of each experiment, samples were centrifuged to obtain the pellet and supernatant fractions. Mitochondrial pellets and supernatants were then analyzed for cytochrome C by Western blotting. Results are shown in Figure 3-9 (± SU5402, ± FGF-2, ± Calcium), and Figure 3-10 (± Neu-ab, ± FGF-2, ± Calcium). Both sets of experiments produced similar results. As expected, calcium overload caused a significant decrease in cytochrome C present in mitochondrial pellets, and a corresponding increase in cytochrome C in supernatants showing release of cytochrome C by mitochondria in the non-treated control group. As expected, FGF-2 stimulation significantly decreased the calcium-induced cytochrome C release to the supernatant. The protective effect of FGF-2 was diminished in the presence of either SU5402, or FGFR1 Neu-Ab: these pretreatments resulted in loss of cytochrome C from the pellet fraction and robust signal for cytochrome C in the supernatant fraction, even in the presence of FGF-2. Taken together, our data point to an essential role of mitoFGFR1-like protein in mediating direct FGF-2-induced mitoprotection, and preventing calcium overload-induced cytochrome C release.

In a pilot experiment (n=2) we examine the effect of mitochondrial FGFR inhibition with SU5402 on the ability of FGF-2 to stimulate mitoCx43 phosphorylation at S262. As shown in Figure 3-9 (panel C), the FGF-2-induced upregulation of mito-P-S262-Cx43 was abolished in the presence of the inhibitor. Thus the ability of FGF-2 to stimulate mitoCx43 phosphorylation requires mito-FGFR1 activity.

Figure 3-6 Validation of anti- FGFR1 antibodies
(These experiments were done by Barbara Nickel.)

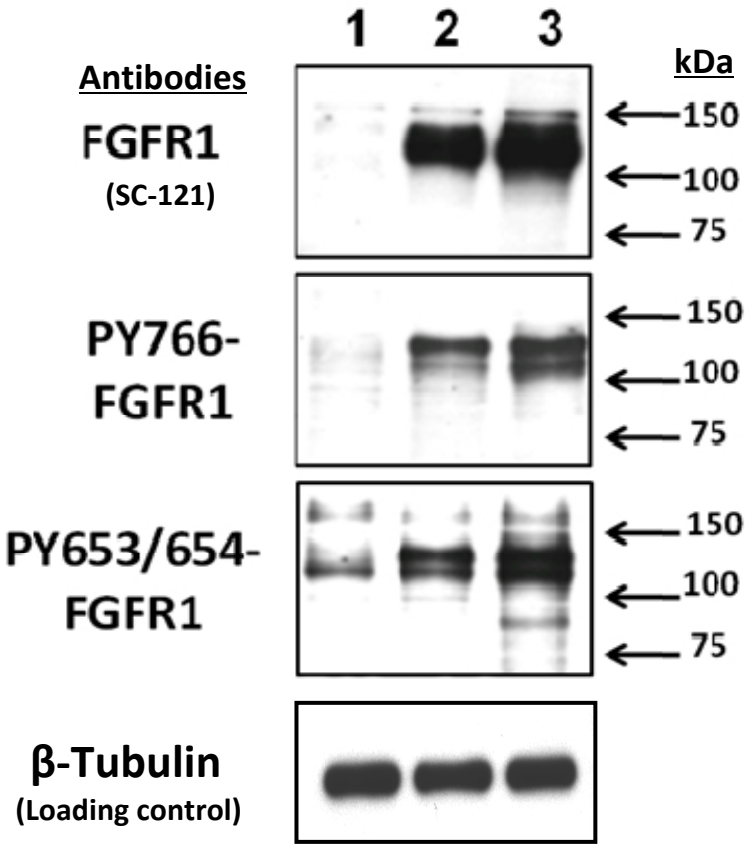

Western blots of HEK293 cell lysates (10 μg protein/ml), overexpressing/or not FGFR1 (after transient gene transfer), probed with various anti-FGFR1 antibodies, as indicated. Lanes 1, 2, 3 contain lysates from, respectively, untransfected HEK293 cells, cells transfected with a cDNA for FGFR1, cells transfected with a cDNA for FGFR1 and stimulated with FGF-2 for 5 minutes. β-tubulin is used as a loading control. Immunoreactivity against all tested antibodies increased after FGFR1 expression.

Figure 3-7 Detection of immunoreactive anti-FGFR1 proteins in cardiac SSM

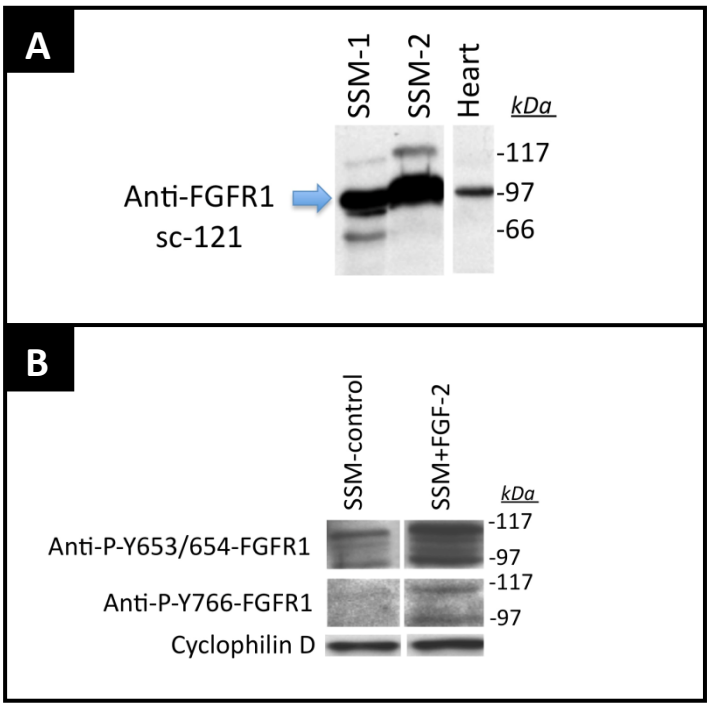

Panel (A). Western blot of two different preparations of SSM mitochondria, and a total heart lysate, all loaded at 30 μg protein/ml, probed with anti-FGFR1 (sc-121), as indicated. Both SSM preparations elicited strong immunoreactivity around 100 kDa, consistent with the size range for FGFR1. The antibodies detected a similar size band in total heart lysates. **Panel (B).** Representative Western blot (n=2) of SSM lysates before (SSM-control) and after (SSM-FGF-2) direct stimulation with FGF-2, probed with anti-P-Y653/654-FGFR1 and anti-P-Y766-FGFR1. Both phospho-FGFR1 antibodies detected immunoreactive bands in control and FGF-2-treated SSM, but the signal was more robust after FGF-2 stimulation, indicating FGFR1 activation. The blot was also probed for Cyclophilin D, to control for protein loading variations.

Figure 3-8 Detection of mitochondrial FGFR1 by immuno-electron microscopy

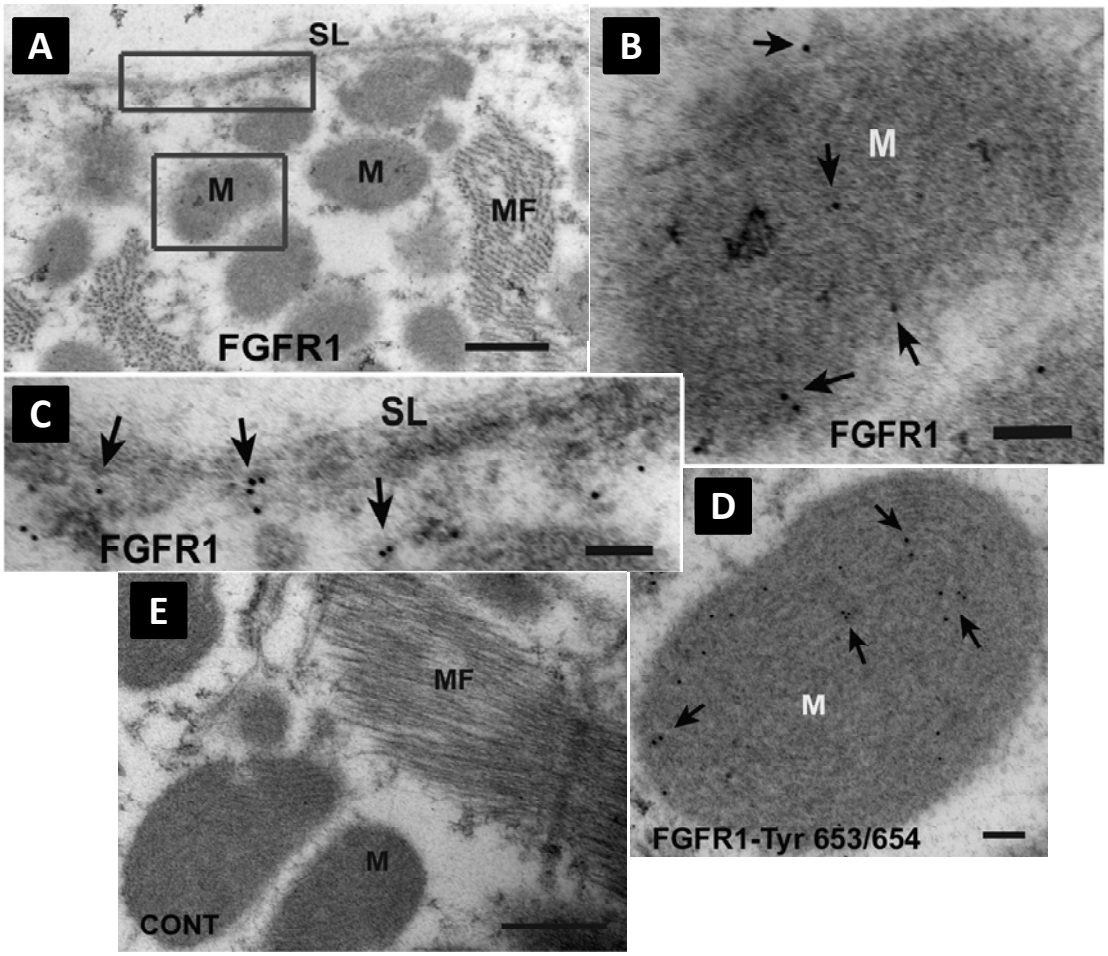

Panels A-D Immunogold labeling with anti-FGFR1, and anti phospho-FGFR1 (PY653/654) in sections from adult rat heart ventricles show clusters of immunogold particles directed against FGFR1-like molecules. Panel A represents a lower magnification of an ultrathin section processed for anti-FGFR1 staining. Boxed areas corresponding to mitochondria (M) and sarcolemma (SL) are shown as higher magnifications in panels B and C, respectively. Panel E shows a negative control (CONT) section, which lacks primary antibody and is negative for immunogold staining. MF = myofilaments. Scale bars: A, F=500 nm, B-E=100 nm. . ***PLEASE NOTE: The panel E included here is the same as panel F shown in Figure 2-1 (immuno-electron microscopy staining for anti-Cx43, or anti-FGFR1, was done using the same set/series of heart sections, and at the same time).***

Figure 3-9 Pharmacological inhibition of mitoFGFR1 prevents the direct effects of FGF2 on cardiac SSM.

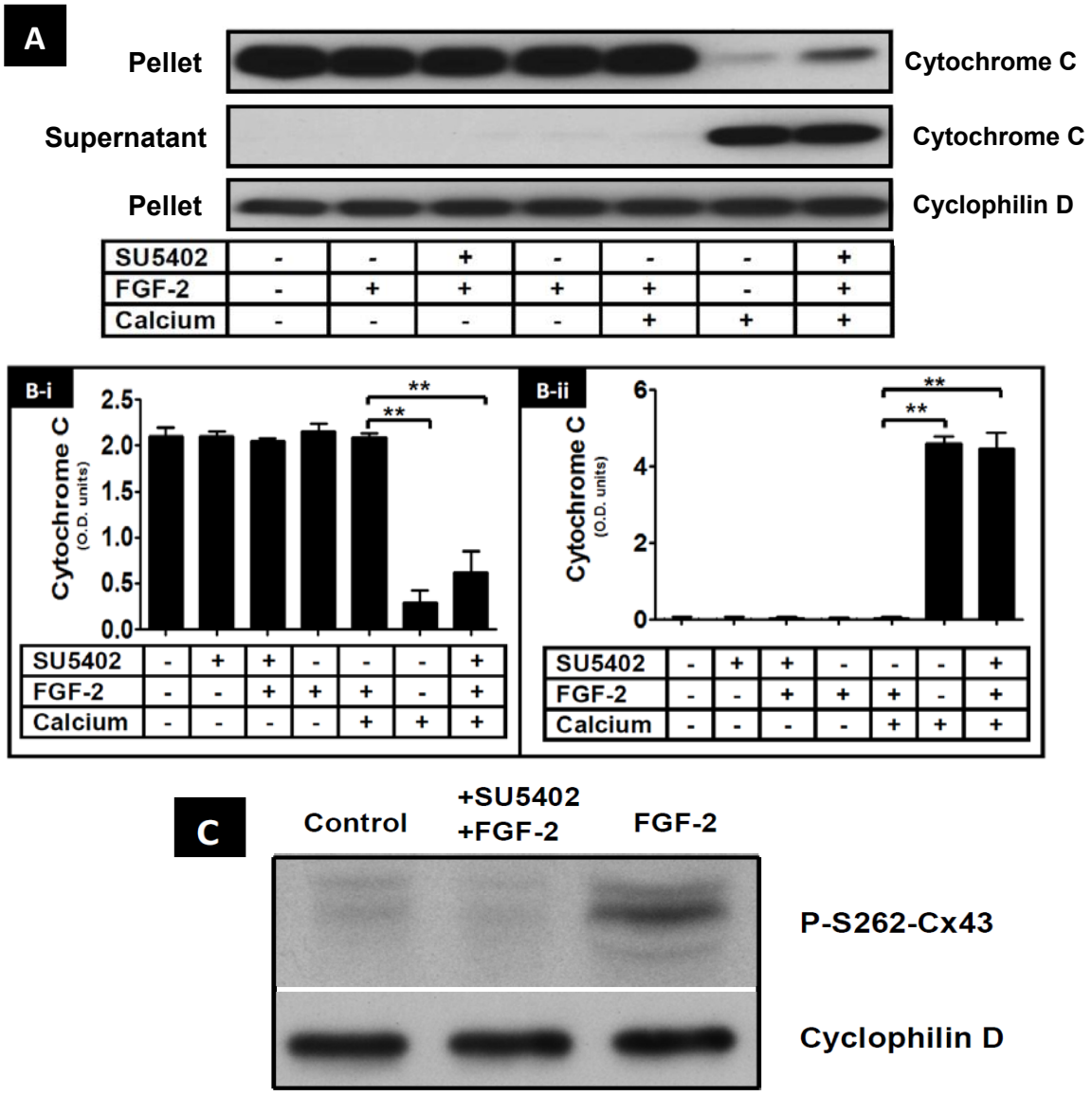

Panel (A) Representative Western blots of SSM pellets and supernatants, probed for cytochrome C, or cyclophilin D, as indicated. SSM were subjected to various treatments (± SU5402, ± FGF-2, ± Calcium), as indicated. Cyclophilin D was used as a control for equal loading of mitochondrial pellets. **Panels (B-i and ii)** show quantitative data for relative cytochrome C levels in pellets, and supernatants, from four independent experiments (n=4). Treatment with SU5402 diminishes the ability of FGF-2 to prevent calcium-overload induced cytochrome C release to the supernatant. **P<0.01 and * P<0.05. **Panel (C)** shows a Western blot of SSM lysates (20 μg/lane), stimulated or not with FGF-2, in the presence or absence of SU5402, and probed for P-S262-Cx43, as indicated.

Figure 3-10 Neutralizing anti-FGFR1 antibodies prevent the direct effects of FGF-2 on cardiac SSM.

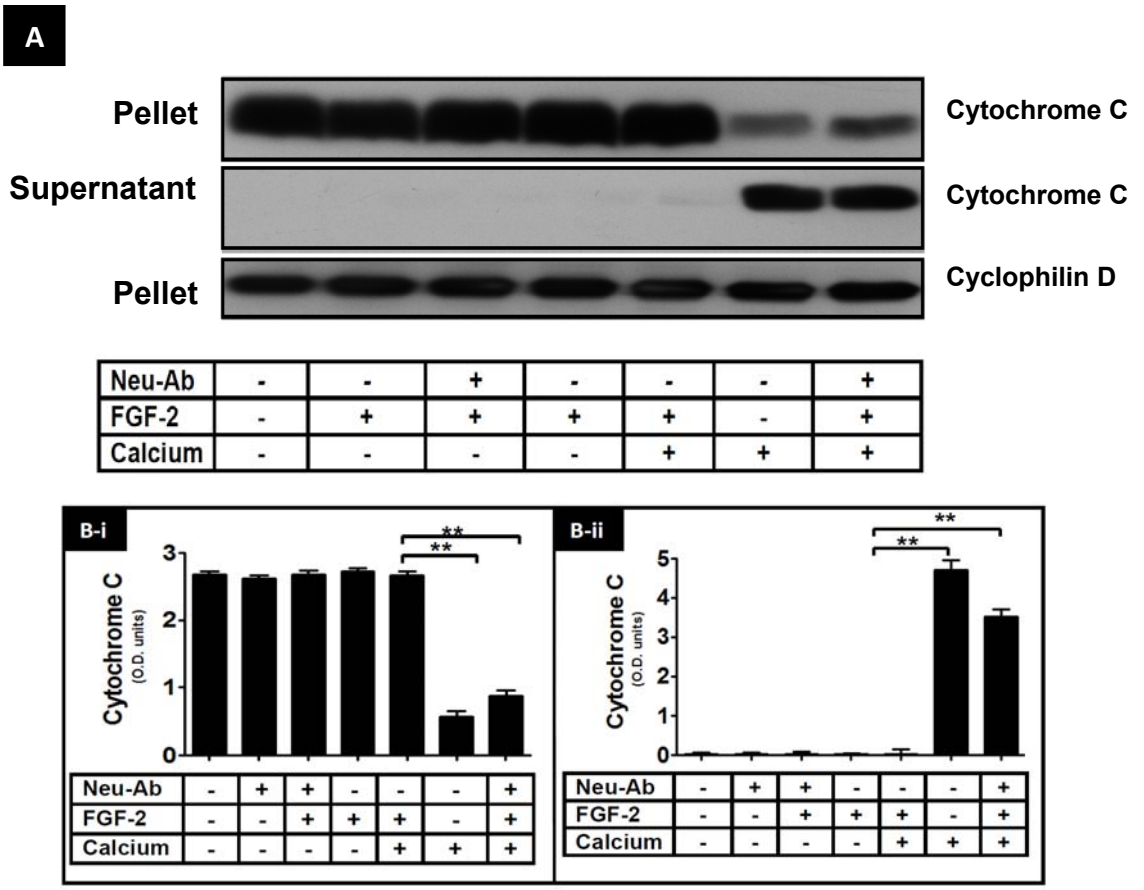

Panel (A) Representative Western blots of SSM pellets and supernatants, probed for cytochrome C, or cyclophilin D, as indicated. SSM were subjected to various treatments (± Neu-Ab, ± FGF-2, ± Calcium), as indicated. Cyclophilin D was used as a control for equal loading of mitochondrial pellets. **Panels (B-I and ii)** show quantitative data for relative cytochrome C levels in pellets, and supernatants, from four independent experiments (n=4). Treatment with Neu-Ab diminishes the ability of FGF-2 to prevent calcium-overload induced cytochrome C release to the supernatant. **P<0.01 and * P<0.05.

CHAPTER 4. DISCUSSION

1. Phosphorylation of connexin 43 at serine 262 is associated with a cardiac injury – resistant state

The purpose of the studies described in this thesis was to investigate a potential association between PKCε-dependent cardioprotection and Cx43 phosphorylation at PKCε target sites. We have now shown that several experimental treatments promoting PKCε-dependent cardioprotection also cause above normal Cx43 phosphorylation at PKCε target sites, S262 and S368 (P*Cx43). Ischemic preconditioning, FGF-2 administration before ischemia (Srisakuldee et al., 2006), as well as FGF-2 administration post-ischemia were characterized by robust increases in P-S262 and P-S368-Cx43, compared to normal hearts. A similar effect was observed when hearts were perfused with diazoxide, a compound reported to promote cardioprotection by activating the mitochondrial K_{ATP} channel (Costa and Garlid, 2008).

Phosphorylation at both the S262- and S368-sites of Cx43 is dependent on a central mediator of cardioprotection, PKCε (Budas et al., 2007; Dang et al., 2006; Doble et al., 2004; Doble et al., 2000; Miura et al., 2007) and may thus serve as "markers" for development of an injury-resistant state. Both sites regulate Cx43 properties: phosphorylation at S368 decreases coupling (Bao et al., 2007; Lampe et al., 2000) while S262 regulates Cx43-signalling functions that do not necessarily depend on GJ, such as inhibition of DNA synthesis (Dang et al., 2006; Doble et al., 2004). Both S262 and S368 sites have been previously identified as being capable of

being phosphorylated within the cell (Axelsen et al., 2006; Doble et al., 2004). Their relative levels, however, are comparatively low in the "non- protected" myocardium (Miura et al., 2007; Srisakuldee et al., 2006) indicating that the normal, in contrast to the "injury-resistant" state, does not support extensive constitutive Cx43 phosphorylation at these residues. To our knowledge, this is the first time that ischemic preconditioning or diazoxide have been shown to promote acute and significant increases in P-S262- and P-S368-Cx43 in the normal heart. It is also the first time that these phosphorylations are shown to be inducible after ischemia and during reperfusion by FGF-2. Nevertheless, our data are in broad agreement with a report that a delta-opioid receptor agonist, which promotes PKCε-mediated cardioprotection, increased cardiac P-S368-Cx43 examined only during early ischemia (Miura et al., 2007).

Loss of ATP during ischemia and subsequent activation of phosphatases result in Cx43 dephosphorylation (Jeyaraman et al., 2003). The preservation of the P*Cx43 phosphorylation state even after 30 min ischemia implies either that phosphatase activation did not occur or that P*Cx43 became resistant/ inaccessible to phosphatases. Both possibilities merit consideration. Global cytoprotective pathways activated by FGF-2 would be expected to preserve mitochondrial integrity and energy stores and prevent activation of phosphatases. It is also known that FGF-2 renders Cx43 inaccessible to antibodies recognizing epitopes within residues 260-270, a region containing the S262 sites (Doble et al., 1996). Phosphorylation of Cx43 at S368 causes conformational changes that decrease accessibility to trypsin (Bao et al., 2004). It is logical to expect that molecular changes causing "masking" of Cx43

domains from antibodies or proteolytic enzymes may also protect those domains from phosphatases.

The ability of Cx43 phosphorylation to remain elevated even after 30 min of ischemia shows that an inducible molecular signal is maintainable for some time and relays the effects of the pre-ischemic stimulus into the reperfusion stage. Such relayed effects likely include reduced metabolic coupling, proposed to mediate the protective and anti-arrhythmogenic effect of ischemic preconditioning (Miura et al., 2004). A similar suggestion was made about the role of increased phosphorylation of Cx43 at S368 in response to an opioid receptor agonist (Miura et al., 2007). In contrast to these reports implicating gap junctions in the development of cardioprotection (Miura et al., 2004; Miura et al., 2007), Li and colleagues concluded that gap junctions may not be essential for ischemic preconditioning (Li et al., 2004), since isolated cardiomyocytes which do not form gap junctions can be preconditioned. Nevertheless, as has been pointed out (Miura et al., 2007), the magnitude of protection in isolated myocytes is not as robust as in whole hearts, suggesting that isolated cells may be regulated differently. It is likely that Cx43 can contribute to ischemic preconditioning-type protection by both gap junction-dependent and independent mechanisms. There is indeed strong evidence that Cx43 hemi-channels, and mitochondrial Cx43 confer gap junction-independent cytoprotection (Schulz et al., 2007).

Gap junction uncoupling is considered beneficial during reperfusion because it prevents the spread of injurious stimuli culminating in calcium overload and cell death (Garcia-Dorado et al., 2004; Schulz and Heusch, 2006). It is reasonable to

suggest that post-conditioning cardioprotection by FGF-2 (Jiang et al., 2007; Jiang et al., 2002; Jiang et al., 2004) may be mediated, at least in part, by its ability to induce Cx43 phosphorylation during reperfusion.

In addition to promoting Cx43 phosphorylation, FGF-2 attenuated the ischemia-induced accumulation of dephosphorylated Cx43; post-ischemic FGF-2 also significantly reduced levels of dephosphorylated Cx43. Such an effect would be expected to preserve the structural integrity of intercalated disks. It would also prevent undesirable increases in permeability not only of gap junctions but also hemi-channels. While hemi-channels are normally closed, Cx43 dephosphorylation causes them to open, resulting in injury and death during cardiomyocyte ischemia-reperfusion (Shintani-Ishida et al., 2007).

The precise mechanism by which Cx43 phosphorylation at S262 contributes to cardioprotection needs to be determined. The effect may be a consequence of subtle changes in gap junction coupling, and/or Cx43 protein-protein interactions. Alternatively, or concurrently, it is possible that Cx43 hemi-channels and/or mitochondrial Cx43 are involved, as will be addressed in the following section. Certainly, PKCε is present at all subcellular sites where Cx43 is found, including intercalated disks, plasma membrane, and mitochondria, and thus it is probable that it can stimulate above normal Cx43 phosphorylation at S262 at all these locations. We suggest that because Cx43 is capable of influencing cell behavior at multiple levels it is likely to be an important effector of PKCε cardioprotection.

Finally, phosphatase inhibition exerts cardioprotection in the absence of a preconditioning stimulus (Fenton et al., 2005). Therefore, it would be pertinent to

examine whether phosphatase inhibitors increase baseline levels of P-S262-Cx43, an event which, based on our data, would be expected to promote cytoprotection.

2. The FGF-2-triggered protection of cardiac subsarcolemmal mitochondria from calcium overload is mitochondrial connexin 43-dependent

Calcium tolerance of SSM and IFM under baseline conditions: In mitochondrial populations isolated from control, unstimulated hearts we found that calcium capacity was lower in SSM compared to IFM. These findings are in agreement with previous reports (Holmuhamedov et al., 2012; Lesnefsky et al., 2001; Palmer et al., 1986). The molecular basis for the difference is not known. It is intriguing that the higher calcium capacity of IFM was associated with a relative lack of proteins generally considered to strengthen resistance of mitochondria to calcium-overload-induced mPTP, such as mitoCx43 (Boengler et al., 2006b), PKCε (Budas et al., 2010), as well as Tom-20 (Boengler et al., 2006a); conversely, the lower calcium capacity of SSM (compared to IFM) was associated with the presence of these proteins. One would be tempted to suggest that, if anything, the presence of Cx43/PKCε in mitochondria has a negative effect on calcium tolerance under baseline conditions. The situation is, however, more complex, as indicated by experiments conducted in the presence of Gap27, and by examining mitochondrial populations from FGF-2 treated hearts.

Incubation with the Gap27 peptide, which blocks Cx43 channel and hemi-channel function (Evans et al., 2012), decreased calcium tolerance of SSM even further, indicating that mitoCx43 exerts a protective effect mediated by its hemi-channel function, and that the effect is specific for SSM. Gap27 had no effect on calcium tolerance of IFM, supporting the conclusion that baseline vulnerability to

calcium is regulated by distinct, mitoCx43 channel-dependent or independent mechanisms in SSM versus IFM.

Levels of mitoP*Cx43 (mito-P-S262- or P-S368-Cx43) in control SSM were relatively low, mirroring findings for cardiac P*Cx43 (Srisakuldee et al., 2009). Thus, it can be argued that mitoCx43 phosphorylation at these specific sites (mitoP*Cx43), which occurs in addition to the constitutive phosphorylation of mitoCx43, may not be required, or may play a minor role, in mitoCx43 functionality under baseline conditions.

Calcium tolerance of SSM and IFM from FGF-2-treated hearts: FGF-2 administration to the heart increased resistance to calcium-overload-induced mPTP in both SSM and IFM. The protective effects at the mitochondrial level may be mediated by FGF-2-induced cardioprotection from ischemia and reperfusion-induced damage and dysfunction (Kardami et al., 2007b). Our studies required isolation of mitochondrial populations immediately after FGF-2 perfusion before damage would be needed to confirm the protective effect of FGF-2. Therefore, we would have needed to examine the effects of FGF-2 on damage in a separate group of hearts. This has been done in our laboratory where perfusion of the rat heart with an FGF-2- supplemented solution, results in preservation of energy stores, reduced cardiac damage and cell death, and improved recovery of contractile function after 30 minutes of global ischemia and 60 minutes of reperfusion (Jiang et al., 2002; Jiang et al., 2009; Padua et al., 1998; Padua et al., 1995).

The relative magnitude of the protective effect of FGF-2 was higher in SSM (by 70%), providing further evidence for differences between the IFM and SSM

mitochondria populations. Increased responsiveness to a protective manipulation has been noted previously for SSM. SSM are more sensitive, compared to IFM, to diazoxide–mediated protection from calcium injury (Holmuhamedov et al., 2012). Diazoxide-induced protection of the whole heart is mediated by the opening of the mitochondrial K_{ATP} channel; it remains to be determined whether the protective effects of FGF-2 perfusion on SSM versus IFM are mediated by differential effects on the mito-K_{ATP} channel and downstream signals.

The protective effect of FGF-2 on SSM required the hemi-channel function of mitoCx43, as it was eliminated in the presence of Gap27. Thus, hemi-channel functionality is mediating both baseline as well as FGF-2-induced calcium tolerance of SSM. These findings are in agreement with a previously study, reporting that inhibition of rat brain mitoCx43 with the channel blocker carboxonolone increased vulnerability to calcium-induced mPTP (Azarashvili et al., 2011). Cx43 mimetic peptides have been used by other groups to show that mitoCx43 is stimulating ADP-dependent complex I respiration by a mechanism requiring hemi-channel functionality (Boengler et al., 2012).

Several reports have pointed to a positive relationship between mitoCx43 levels and cytoprotection (Boengler et al., 2005; Boengler et al., 2007; Lu et al., 2010; Lu et al., 2012). This would suggest that the FGF-2-induced increase in mitoCx43 levels observed in our studies is required to induce increased calcium tolerance in SSM. If that were the case, it should not be possible to stimulate protection in SSM *in vitro*, where mitoCx43 levels remained constant. This is not what we found: PMA stimulation of control SSM increased calcium tolerance; thus,

an increase in mitoCx43 is not necessary for a protective effect to manifest in normal mitochondria. What may be required instead of, or in parallel to, increased mitoCx43 levels, is the increase in P-S262- and/or P-S368-Cx43 that is observed in SSM after indirect FGF-2-triggered signaling or direct PMA stimulation. Our studies using perfused hearts and discussed in the previous section have pointed to an association between cellular P-S262-Cx43 and cardioprotection, and shown that P-S262-Cx43 levels are a determinant of cell tolerance to ischemic injury (Srisakuldee et al., 2009); it is plausible that a component of P-S262-Cx43-mediateed cytoprotection is exercised by mito-P-S262-Cx43.

The PMA-induced phosphorylation of mitoCx43 at S262 and S368 is mediated by mitoPKCε, as we found that it was prevented by the PKCε inhibiting peptide $\varepsilon V_{1\text{-}2}$. MitoPKCε inhibition by $\varepsilon V_{1\text{-}2}$ has been shown by others to prevent the PMA-induced increase in mitochondrial calcium tolerance (Budas et al., 2010; Costa et al., 2006b), suggesting that this would likely be the case in our experimental system as well. Indeed, as will be discussed in the following section, peptide $\varepsilon V_{1\text{-}2}$ prevented the direct, FGF-2-induced upregulation of mitochondrial calcium tolerance. MitoPKCε is important in developing increased resistance to mPTP by targeting local effectors of protection such as the mito-K_{ATP} channel and/or mito-GSK-3β (Baines, 2009; Baines et al., 2003; Budas et al., 2010; Budas and Mochly-Rosen, 2007). Because the FGF-2-triggered increased in calcium tolerance was associated with increases in relative mitoPKCε and mito-pPKCε, it is reasonable to suggest that activated mitoPKCε contributed to the FGF-2-triggered, and plasma membrane receptor transduced, protection in both SSM and IFM. In SSM, one of the

downstream targets of mitoPKCε would be mitoCx43, and mitoCx43-affected endpoints, such as complex I respiration (Boengler et al., 2012), potassium flux (Boengler et al., 2013), reactive oxygen species production (Heinzel et al., 2005), and mPTP. This would not be the case in IFM from FGF-2-treated hearts, because they lack Cx43. In IFM, additional mitochondria-residing protective signals may be engaged downstream of PKCε, such as GSK-3β (McCarthy et al., 2011). GSK-3β is present in IFM, and increases in both levels and phosphorylation at S9 after FGF-2 stimulation, as shown here. Because several cytoprotective pathways converge on GSK-3β phosphorylation at S9, resulting in inhibition of calcium-induced mPTP (Miura and Tanno, 2012), it would be important to investigate the role of mito-GSK-3β, potentially downstream of mitoPKCε, in the FGF-2- induced increased calcium tolerance of IFM.

In SSM, the molecular mechanism(s) by which P-S262- and/or P-S368-Cx43 might contribute to mitoCx43 functionality and/or SSM-mediated cytoprotection remain to be determined. It is possible that these PKCε-mediated phosphorylations may promote subtle conformational changes that strengthen or stabilize the positive effects of mitoCx43 on mitochondrial respiration and/or potassium flux (Boengler et al., 2012; Boengler et al., 2013; Miro-Casas et al., 2009). MitoCx43 phosphorylation at S262 and/or S368 may alter protein-protein interactions in a manner that would prevent mPTP. An enhanced interaction between P-S262-Cx43 and PKCε in response to FGF-2 stimulation has been reported (Doble et al., 2004; Doble et al., 2000). The four transmembrane domains of Cx43 enable stable integration at the inner mitochondrial membrane, and thus an enhanced interaction

with mitoPKCε may strengthen retention of the latter in the intermitochondrial space, and enable phosphorylation of additional targets, such as the mitoK_{ATP} channel and/or putative members of the mPTP pore (Baines et al., 2003). The importance of phosphorylation of Cx43 at S262 for interaction with other proteins was highlighted in a recent study showing that lack of phosphorylation at S262 prevented Cx43 from interacting with Kir 6.1, a constituent of the plasma membrane K_{ATP} channel (Ahmad Waza et al., 2012).

3. FGF-2 exerts direct protective effects on cardiac SSM mitochondria, mediated by a mitochondrial FGFR1, mitoPKCε, and associated with mitoP*Cx43

The series of studies presented here demonstrate that 18 kDa FGF-2 is capable of exerting direct effects on isolated cardiac SSM mitochondria. These effects include stimulation of resistance to calcium-induced cytochrome C release, and stimulation of phosphorylation of mitoCx43 at PKCε-target sites. Both effects were found to require mitoPKCε activity, as they were attenuated by the PKCε-selective inhibitory peptide εV1-2. The direct effects of FGF-2 on isolated cardiac mitochondria required the activity of an FGFR-like protein present in isolated cardiac mitochondria, as they were prevented by a pharmacological FGFR inhibitor as well as neutralizing anti-FGFR1 antibodies. Complementary evidence for presence of FGFR1 in cardiac mitochondria was provided by using validated antibodies for FGFR1, or tyrosine phosphorylated FGFR1. These antibodies detected immunoreactive bands in cardiac SSM preparations, and localized to cardiac mitochondria *in situ* in immuno-EM studies.

Like other tyrosine kinase growth factor receptors, FGFR1 is present at the plasma membrane, transducing the effects of extracellular-acting FGF-2 (Zhang et al., 2006). Several studies have, however, indicated that FGFR1 can also be found at unspecified 'cytosolic' as well as nuclear sites in fibroblastic and neuronal cells (Coleman et al., 2014; Dunham-Ems et al., 2009; Maher, 1996). The studies presented here indicate that the reported 'cytosolic' FGFR1, or at least a fraction of cytosolic FGFR1, represents mitochondria-localized FGFR1. It is hypothesized that

FGFR1 translocates to mitochondria by a mechanism employing the TOM translocase complex and an interaction with HSP90, in a manner similar to other proteins such as Cx43 or PKCε. FGFR1 and other members of the FGFR family can interact with, and are considered 'clients' of HSP90 (Laederich et al., 2011)

It is not considered likely that detection of FGFR1 at cardiac SSM is a result of sarcolemmal contamination of our mitochondrial preparations. Several antibodies recognizing plasma membrane marker proteins demonstrated the absence of plasma membrane contamination in our preparations.

The presence of a growth factor receptor at the mitochondria has been previously reported for the nerve growth factor (NGF, neurotrophin) and epidermal growth factor receptors (Wiedemann et al., 2006). In mitochondria isolated from rat brain cortex, NGF receptors mediated direct protective effects of NGF against permeability transition (Carito et al., 2012). In addition, EGFR translocated to the mitochondria in EGF-stimulated fibroblasts, where it was found associated with the cytochrome c oxidase subunit II (Cox-II) and where it was shown to promote cell survival (Boerner et al., 2004). Currently, there is no report of FGFR1 translocating to mitochondria, however, FGF-2 binding to its FGFR1 receptor at the plasma membrane results in receptor internalization and translocation to the nucleus (Dunham-Ems et al., 2006). Therefore, it is theoretically possible that FGFR1, like EGFR, translocates to mitochondria in response to extracellular FGF-2 signaling.

In general agreement with the NGF and EGFR studies, our studies show that a mitochondrial FGFR can become activated by FGF-2, and activate protective signaling leading to prevention of calcium overload induced permeability transition.

It should be noted that although our studies used exclusively SSM mitochondria, pilot, unpublished data have indicated that anti-FGFR1 immunoreactivity is also present at the IFM mitochondrial populations. In SSM, a downstream target of mitoFGFR1 activation is mitoCx43, becoming phosphorylated at S262 and S368, providing an additional association between mitoP*Cx43 and mitochondrial protection from injury. It remains to be determined whether the anti-FGFR1 signal in IFM represents a functional FGFR, and determine its downstream targets.

The presence of a functional FGFR at mitochondria implies that cytosolic levels of the 18 kDa FGF-2, or other members of the FGF family of growth factors capable of activating FGFR1, can regulate baseline mitochondrial, and therefore cellular, resistance to injury. Cytosolic FGF-2 levels can be increased by stimulation of endogenous gene expression (Jimenez et al., 2004), as well as by internalization/endocytosis of extracellular FGF-2 (Wesche et al., 2006; Zhang et al., 2006). The effects of cytosolic FGF-2 would be expected to occur in parallel to, and reinforce, those of extracellular-acting, sarcolemmal FGFR-mediated, effects. Future studies should address the effect of cytosolic FGF-2 on mitochondria in the whole cell context.

Finally, it should be noted that FGF-2 is produced by cells as high molecular weight (>20 kDa) and low molecular weight (18 kDa) isoforms, that display distinct and often opposing activities (Kardami et al., 2004). The present studies have addressed the effects of the 18 kDa FGF-2. Although high molecular weight FGF-2 is considered to have mostly nuclear activities, recent studies have demonstrated that is can be secreted to the extracellular matrix by connective tissue cells, and can

affect myocytes in a paracrine fashion (Santiago et al., 2011); it can also become internalized by cells. Future studies therefore need to also address the effects of high molecular weight FGF-2 on mitochondria.

4. Conclusions and future directions

Novel findings from the present studies have shown a link between Cx43, and mitoCx43 phosphorylation at PKCε sites, P*Cx43, and mitoP*Cx43 and an "injury-resistant" state. As shown in the summarized Figure 4, FGF-2-induced cytoprotection by binding to FGF receptor (FGFR) at the plasma membrane leads to the activation of several downstream cellular targets, including Cx43 phosphorylation at S262 and/or S368. At the mitochondria, FGF-2 was shown to exert indirect (plasma-membrane mediated) protective effects on cardiac mitochondrial populations, by mitoCx43 hemi-channel dependent (SSM) and independent (IFM) pathways. Furthermore, FGF-2 was found to be capable of exerting direct protective effects on cardiac SSM, by activating a mitochondria-based FGFR, likely FGFR1, These studies have expanded understanding of signals involved in cellular and mitochondrial response to injury in the heart and cardiomyocyte.

To obtain a better understanding of the role of P*Cx43, and mitoP*Cx43 on mPTP, it will be necessary to conduct studies in the whole cell and experimental animal context. Adenoviral gene transfer of mitochondrial targeted Cx43, and its corresponding phosphorylation mutants (for example, S262A: unable to become phosphorylated at S262, and S262D: simulating constitutive phosphorylation at site 262), may be used to address the function of P-S262-Cx43 specifically at mitochondria. Transgenic mouse models with conditional, cardiomyocyte-specific expression of Cx43, or of mitochondrial Cx43 phosphorylation mutants, will allow understanding of these phosphorylations in mediating resistance to injury *in vivo*, in

normal physiology and pathophysiology conditions. In a similar manner, transgenic mouse models with conditional, cardiomyocyte-specific expression of mitochondrial targeted FGFR1, either as a 'kinase dead' version, acting in a dominant negative fashion, or in a constitutively active state, will allow us to determine its role in cardiac cell survival.

Figure 4. The relationship between FGF-2 mediated cytoprotection/ mitochondrial protection, and mitochondrial Cx43 phosphorylation at the PKCε sites.

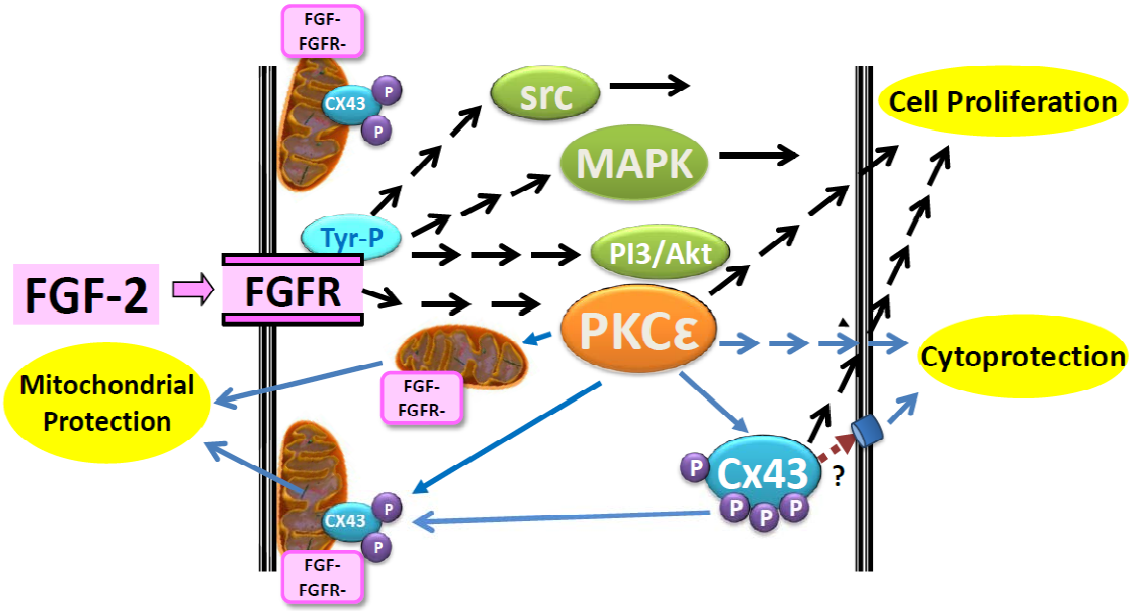

Extracellular FGF-2 initiates cytoprotection by binding to a plasma membrane FGF receptor (FGFR). Several signal transduction cascades are activated downstream of plasma membrane FGFR, including the MAPK, PI3/AKT, and PKCε activating pathways. Activated PKCε translocates to various subcellular compartments, including mitochondria, phosphorylates Cx43 at S262 and S368, and plays a central role in cardioprotection, and also mitochondrial protection. Endogenous cytosolic FGF-2, or internalized FGF-2, can be expected to exert direct effects on mitochondria, including mitochondrial Cx43 phosphorylation and mitoprotection. Dashed arrows indicate multiple steps in a pathway, while solid arrows indicate a direct interaction and/ or effect.

Chapter 5: References

Afanas'ev, I. (2011). ROS and RNS signaling in heart disorders: could antioxidant treatment be successful? Oxid Med Cell Longev *2011*, 293769.

Ahmad Waza, A., Andrabi, K., and Ul Hussain, M. (2012). Adenosine-triphosphate-sensitive K+ channel (Kir6.1): a novel phosphospecific interaction partner of connexin 43 (Cx43). Exp Cell Res *318*, 2559-2566.

Ajioka, R.S., Phillips, J.D., and Kushner, J.P. (2006). Biosynthesis of heme in mammals. Biochim Biophys Acta *1763*, 723-736.

Alcolea, S., Theveniau-Ruissy, M., Jarry-Guichard, T., Marics, I., Tzouanacou, E., Chauvin, J.P., Briand, J.P., Moorman, A.F., Lamers, W.H., and Gros, D.B. (1999). Downregulation of connexin 45 gene products during mouse heart development. Circ Res *84*, 1365-1379.

Ardehali, H., Sabbah, H.N., Burke, M.A., Sarma, S., Liu, P.P., Cleland, J.G., Maggioni, A., Fonarow, G.C., Abel, E.D., Campia, U.*, et al.* (2012). Targeting myocardial substrate metabolism in heart failure: potential for new therapies. Eur J Heart Fail *14*, 120-129.

Argaud, L., Gateau-Roesch, O., Chalabreysse, L., Gomez, L., Loufouat, J., Thivolet-Bejui, F., Robert, D., and Ovize, M. (2004). Preconditioning delays Ca2+-induced mitochondrial permeability transition. Cardiovasc Res *61*, 115-122.

Asemu, G., O'Connell, K.A., Cox, J.W., Dabkowski, E.R., Xu, W., Ribeiro, R.F., Jr., Shekar, K.C., Hecker, P.A., Rastogi, S., Sabbah, H.N.*, et al.* (2013). Enhanced resistance to permeability transition in interfibrillar cardiac mitochondria in dogs: effects of aging and long-term aldosterone infusion. Am J Physiol Heart Circ Physiol *304*, H514-528.

Ashrafian, H., and Frenneaux, M.P. (2007). Metabolic modulation in heart failure: the coming of age. Cardiovasc Drugs Ther *21*, 5-7.

Ashrafian, H., Frenneaux, M.P., and Opie, L.H. (2007). Metabolic mechanisms in heart failure. Circulation *116*, 434-448.

Axelsen, L.N., Stahlhut, M., Mohammed, S., Larsen, B.D., Nielsen, M.S., Holstein-Rathlou, N.H., Andersen, S., Jensen, O.N., Hennan, J.K., and Kjolbye, A.L. (2006). Identification of ischemia-regulated phosphorylation sites in connexin43: A possible

target for the antiarrhythmic peptide analogue rotigaptide (ZP123). J Mol Cell Cardiol *40*, 790-798.

Azarashvili, T., Baburina, Y., Grachev, D., Krestinina, O., Evtodienko, Y., Stricker, R., and Reiser, G. (2011). Calcium-induced permeability transition in rat brain mitochondria is promoted by carbenoxolone through targeting connexin43. Am J Physiol Cell Physiol *300*, C707-720.

Baines, C.P. (2009). The molecular composition of the mitochondrial permeability transition pore. J Mol Cell Cardiol *46*, 850-857.

Baines, C.P. (2010). The cardiac mitochondrion: nexus of stress. Annu Rev Physiol *72*, 61-80.

Baines, C.P., Kaiser, R.A., Purcell, N.H., Blair, N.S., Osinska, H., Hambleton, M.A., Brunskill, E.W., Sayen, M.R., Gottlieb, R.A., Dorn, G.W.*, et al.* (2005). Loss of cyclophilin D reveals a critical role for mitochondrial permeability transition in cell death. Nature *434*, 658-662.

Baines, C.P., Kaiser, R.A., Sheiko, T., Craigen, W.J., and Molkentin, J.D. (2007). Voltage-dependent anion channels are dispensable for mitochondrial-dependent cell death. Nat Cell Biol *9*, 550-555.

Baines, C.P., Song, C.X., Zheng, Y.T., Wang, G.W., Zhang, J., Wang, O.L., Guo, Y., Bolli, R., Cardwell, E.M., and Ping, P. (2003). Protein kinase Cepsilon interacts with and inhibits the permeability transition pore in cardiac mitochondria. Circ Res *92*, 873-880.

Baines, C.P., Zhang, J., Wang, G.W., Zheng, Y.T., Xiu, J.X., Cardwell, E.M., Bolli, R., and Ping, P. (2002). Mitochondrial PKCepsilon and MAPK form signaling modules in the murine heart: enhanced mitochondrial PKCepsilon-MAPK interactions and differential MAPK activation in PKCepsilon-induced cardioprotection. Circ Res *90*, 390-397.

Balaban, R.S. (1990). Regulation of oxidative phosphorylation in the mammalian cell. Am J Physiol *258*, C377-389.

Balaban, R.S., Kantor, H.L., Katz, L.A., and Briggs, R.W. (1986). Relation between work and phosphate metabolite in the in vivo paced mammalian heart. Science *232*, 1121-1123.

Bao, X., Lee, S.C., Reuss, L., and Altenberg, G.A. (2007). Change in permeant size selectivity by phosphorylation of connexin 43 gap-junctional hemichannels by PKC. Proc Natl Acad Sci U S A *104*, 4919-4924.

Bao, X., Reuss, L., and Altenberg, G.A. (2004). Regulation of purified and reconstituted connexin 43 hemichannels by protein kinase C-mediated phosphorylation of Serine 368. J Biol Chem *279*, 20058-20066.

Barja, G. (1998). Mitochondrial free radical production and aging in mammals and birds. Ann N Y Acad Sci *854*, 224-238.

Baseler, W.A., Dabkowski, E.R., Williamson, C.L., Croston, T.L., Thapa, D., Powell, M.J., Razunguzwa, T.T., and Hollander, J.M. (2011). Proteomic alterations of distinct mitochondrial subpopulations in the type 1 diabetic heart: contribution of protein import dysfunction. Am J Physiol Regul Integr Comp Physiol *300*, R186-200.

Basso, E., Fante, L., Fowlkes, J., Petronilli, V., Forte, M.A., and Bernardi, P. (2005). Properties of the permeability transition pore in mitochondria devoid of Cyclophilin D. J Biol Chem *280*, 18558-18561.

Battaglia, V., Brunati, A.M., Fiore, C., Rossi, C.A., Salvi, M., Tibaldi, E., Palermo, M., Armanini, D., and Toninello, A. (2008). Glycyrrhetinic acid as inhibitor or amplifier of permeability transition in rat heart mitochondria. Biochim Biophys Acta *1778*, 313-323.

Beardslee, M.A., Lerner, D.L., Tadros, P.N., Laing, J.G., Beyer, E.C., Yamada, K.A., Kleber, A.G., Schuessler, R.B., and Saffitz, J.E. (2000). Dephosphorylation and intracellular redistribution of ventricular connexin43 during electrical uncoupling induced by ischemia. Circ Res *87*, 656-662.

Bedner, P., Niessen, H., Odermatt, B., Willecke, K., and Harz, H. (2003). A method to determine the relative cAMP permeability of connexin channels. Exp Cell Res *291*, 25-35.

Bell, G.J., Martin, T.P., Ilyina-Kakueva, E.I., Oganov, V.S., and Edgerton, V.R. (1992). Altered distribution of mitochondria in rat soleus muscle fibers after spaceflight. J Appl Physiol (1985) *73*, 493-497.

Belzacq-Casagrande, A.S., Martel, C., Pertuiset, C., Borgne-Sanchez, A., Jacotot, E., and Brenner, C. (2009). Pharmacological screening and enzymatic assays for apoptosis. Front Biosci *14*, 3550-3562.

Beyer, E.C., Paul, D.L., and Goodenough, D.A. (1987). Connexin43: a protein from rat heart homologous to a gap junction protein from liver. J Cell Biol *105*, 2621-2629.

Beyer, E.C., Paul, D.L., and Goodenough, D.A. (1990). Connexin family of gap junction proteins. J Membr Biol *116*, 187-194.

Boengler, K., Dodoni, G., Rodriguez-Sinovas, A., Cabestrero, A., Ruiz-Meana, M., Gres, P., Konietzka, I., Lopez-Iglesias, C., Garcia-Dorado, D., Di Lisa, F.*, et al.* (2005). Connexin 43 in cardiomyocyte mitochondria and its increase by ischemic preconditioning. Cardiovasc Res *67*, 234-244.

Boengler, K., Gres, P., Cabestrero, A., Ruiz-Meana, M., Garcia-Dorado, D., Heusch, G., and Schulz, R. (2006a). Prevention of the ischemia-induced decrease in mitochondrial Tom20 content by ischemic preconditioning. J Mol Cell Cardiol *41*, 426-430.

Boengler, K., Konietzka, I., Buechert, A., Heinen, Y., Garcia-Dorado, D., Heusch, G., and Schulz, R. (2007). Loss of ischemic preconditioning's cardioprotection in aged mouse hearts is associated with reduced gap junctional and mitochondrial levels of connexin 43. Am J Physiol Heart Circ Physiol *292*, H1764-1769.

Boengler, K., Ruiz-Meana, M., Gent, S., Ungefug, E., Soetkamp, D., Miro-Casas, E., Cabestrero, A., Fernandez-Sanz, C., Semenzato, M., Di Lisa, F.*, et al.* (2012). Mitochondrial connexin 43 impacts on respiratory complex I activity and mitochondrial oxygen consumption. J Cell Mol Med *16*, 1649-1655.

Boengler, K., Schulz, R., and Heusch, G. (2006b). Connexin 43 signalling and cardioprotection. Heart *92*, 1724-1727.

Boengler, K., Stahlhofen, S., van de Sand, A., Gres, P., Ruiz-Meana, M., Garcia-Dorado, D., Heusch, G., and Schulz, R. (2009). Presence of connexin 43 in subsarcolemmal, but not in interfibrillar cardiomyocyte mitochondria. Basic Res Cardiol *104*, 141-147.

Boengler, K., Ungefug, E., Heusch, G., Leybaert, L., and Schulz, R. (2013). Connexin 43 impacts on mitochondrial potassium uptake. Front Pharmacol *4*, 73.

Boerner, J.L., Demory, M.L., Silva, C., and Parsons, S.J. (2004). Phosphorylation of Y845 on the epidermal growth factor receptor mediates binding to the mitochondrial protein cytochrome c oxidase subunit II. Mol Cell Biol *24*, 7059-7071.

Braet, K., Vandamme, W., Martin, P.E., Evans, W.H., and Leybaert, L. (2003). Photoliberating inositol-1,4,5-trisphosphate triggers ATP release that is blocked by the connexin mimetic peptide gap 26. Cell Calcium *33*, 37-48.

Britz-Cunningham, S.H., Shah, M.M., Zuppan, C.W., and Fletcher, W.H. (1995). Mutations of the Connexin43 gap-junction gene in patients with heart malformations and defects of laterality. N Engl J Med *332*, 1323-1329.

Broughton, B.R., Reutens, D.C., and Sobey, C.G. (2009). Apoptotic mechanisms after cerebral ischemia. Stroke *40*, e331-339.

Budas, G.R., Churchill, E.N., Disatnik, M.H., Sun, L., and Mochly-Rosen, D. (2010). Mitochondrial import of PKCepsilon is mediated by HSP90: a role in cardioprotection from ischaemia and reperfusion injury. Cardiovasc Res *88*, 83-92.

Budas, G.R., Churchill, E.N., and Mochly-Rosen, D. (2007). Cardioprotective mechanisms of PKC isozyme-selective activators and inhibitors in the treatment of ischemia-reperfusion injury. Pharmacol Res *55*, 523-536.

Budas, G.R., and Mochly-Rosen, D. (2007). Mitochondrial protein kinase Cepsilon (PKCepsilon): emerging role in cardiac protection from ischaemic damage. Biochem Soc Trans *35*, 1052-1054.

Bukauskas, F.F., and Verselis, V.K. (2004). Gap junction channel gating. Biochim Biophys Acta *1662*, 42-60.

Campanella, M., Pinton, P., and Rizzuto, R. (2004). Mitochondrial Ca2+ homeostasis in health and disease. Biol Res *37*, 653-660.

Carito, V., Pingitore, A., Cione, E., Perrotta, I., Mancuso, D., Russo, A., Genchi, G., and Caroleo, M.C. (2012). Localization of nerve growth factor (NGF) receptors in the mitochondrial compartment: characterization and putative role. Biochim Biophys Acta *1820*, 96-103.

Chen, H., and Chan, D.C. (2010). Physiological functions of mitochondrial fusion. Ann N Y Acad Sci *1201*, 21-25.

Chen, Q., Moghaddas, S., Hoppel, C.L., and Lesnefsky, E.J. (2006). Reversible blockade of electron transport during ischemia protects mitochondria and decreases myocardial injury following reperfusion. J Pharmacol Exp Ther *319*, 1405-1412.

Cheng, E.H., Sheiko, T.V., Fisher, J.K., Craigen, W.J., and Korsmeyer, S.J. (2003). VDAC2 inhibits BAK activation and mitochondrial apoptosis. Science *301*, 513-517.

Chipuk, J.E., Moldoveanu, T., Llambi, F., Parsons, M.J., and Green, D.R. (2010). The BCL-2 family reunion. Mol Cell *37*, 299-310.

Clarke, S.J., McStay, G.P., and Halestrap, A.P. (2002). Sanglifehrin A acts as a potent inhibitor of the mitochondrial permeability transition and reperfusion injury of the heart by binding to cyclophilin-D at a different site from cyclosporin A. J Biol Chem *277*, 34793-34799.

Coleman, S.J., Chioni, A.M., Ghallab, M., Anderson, R.K., Lemoine, N.R., Kocher, H.M., and Grose, R.P. (2014). Nuclear translocation of FGFR1 and FGF2 in pancreatic stellate cells facilitates pancreatic cancer cell invasion. EMBO Mol Med *6*, 467-481.

Cooklin, M., Wallis, W.R., Sheridan, D.J., and Fry, C.H. (1997). Changes in cell-to-cell electrical coupling associated with left ventricular hypertrophy. Circ Res *80*, 765-771.

Cooper, C.D., and Lampe, P.D. (2002). Casein kinase 1 regulates connexin-43 gap junction assembly. J Biol Chem *277*, 44962-44968.

Coppen, S.R., Dupont, E., Rothery, S., and Severs, N.J. (1998). Connexin45 expression is preferentially associated with the ventricular conduction system in mouse and rat heart. Circ Res *82*, 232-243.

Costa, A.D., and Garlid, K.D. (2008). Intramitochondrial signaling: interactions among mitoKATP, PKCepsilon, ROS, and MPT. Am J Physiol Heart Circ Physiol *295*, H874-882.

Costa, A.D., Jakob, R., Costa, C.L., Andrukhiv, K., West, I.C., and Garlid, K.D. (2006a). The mechanism by which the mitochondrial ATP-sensitive K+ channel opening and H2O2 inhibit the mitochondrial permeability transition. J Biol Chem *281*, 20801-20808.

Costa, A.D., Pierre, S.V., Cohen, M.V., Downey, J.M., and Garlid, K.D. (2008). cGMP signalling in pre- and post-conditioning: the role of mitochondria. Cardiovasc Res *77*, 344-352.

Costa, A.D., Quinlan, C.L., Andrukhiv, A., West, I.C., Jaburek, M., and Garlid, K.D. (2006b). The direct physiological effects of mitoK(ATP) opening on heart mitochondria. Am J Physiol Heart Circ Physiol *290*, H406-415.

Cross, H.R., Murphy, E., Bolli, R., Ping, P., and Steenbergen, C. (2002). Expression of activated PKC epsilon (PKC epsilon) protects the ischemic heart, without attenuating ischemic H(+) production. J Mol Cell Cardiol *34*, 361-367.

Dabkowski, E.R., Williamson, C.L., Bukowski, V.C., Chapman, R.S., Leonard, S.S., Peer, C.J., Callery, P.S., and Hollander, J.M. (2009). Diabetic cardiomyopathy-associated dysfunction in spatially distinct mitochondrial subpopulations. Am J Physiol Heart Circ Physiol *296*, H359-369.

Dang, X., Doble, B.W., and Kardami, E. (2003). The carboxy-tail of connexin-43 localizes to the nucleus and inhibits cell growth. Mol Cell Biochem *242*, 35-38.

Dang, X., Jeyaraman, M., and Kardami, E. (2006). Regulation of connexin-43-mediated growth inhibition by a phosphorylatable amino-acid is independent of gap junction-forming ability. Mol Cell Biochem *289*, 201-207.

Darrow, B.J., Fast, V.G., Kleber, A.G., Beyer, E.C., and Saffitz, J.E. (1996). Functional and structural assessment of intercellular communication. Increased conduction velocity and enhanced connexin expression in dibutyryl cAMP-treated cultured cardiac myocytes. Circ Res *79*, 174-183.

Davidson, A.M., and Halestrap, A.P. (1990). Partial inhibition by cyclosporin A of the swelling of liver mitochondria in vivo and in vitro induced by sub-micromolar [Ca2+], but not by butyrate. Evidence for two distinct swelling mechanisms. Biochem J *268*, 147-152.

de Diego, C., Pai, R.K., Chen, F., Xie, L.H., De Leeuw, J., Weiss, J.N., and Valderrabano, M. (2008). Electrophysiological consequences of acute regional ischemia/reperfusion in neonatal rat ventricular myocyte monolayers. Circulation *118*, 2330-2337.

De Marchi, U., Basso, E., Szabo, I., and Zoratti, M. (2006). Electrophysiological characterization of the Cyclophilin D-deleted mitochondrial permeability transition pore. Mol Membr Biol *23*, 521-530.

De Marchi, U., Campello, S., Szabo, I., Tombola, F., Martinou, J.C., and Zoratti, M. (2004). Bax does not directly participate in the Ca(2+)-induced permeability transition of isolated mitochondria. J Biol Chem *279*, 37415-37422.

De Vuyst, E., Boengler, K., Antoons, G., Sipido, K.R., Schulz, R., and Leybaert, L. (2011). Pharmacological modulation of connexin-formed channels in cardiac pathophysiology. Br J Pharmacol *163*, 469-483.

Di Lisa, F., Kaludercic, N., Carpi, A., Menabo, R., and Giorgio, M. (2009). Mitochondrial pathways for ROS formation and myocardial injury: the relevance of p66(Shc) and monoamine oxidase. Basic Res Cardiol *104*, 131-139.

Doble, B.W., Chen, Y., Bosc, D.G., Litchfield, D.W., and Kardami, E. (1996). Fibroblast growth factor-2 decreases metabolic coupling and stimulates phosphorylation as well as masking of connexin43 epitopes in cardiac myocytes. Circ Res *79*, 647-658.

Doble, B.W., Dang, X., Ping, P., Fandrich, R.R., Nickel, B.E., Jin, Y., Cattini, P.A., and Kardami, E. (2004). Phosphorylation of serine 262 in the gap junction protein connexin-43 regulates DNA synthesis in cell-cell contact forming cardiomyocytes. J Cell Sci *117*, 507-514.

Doble, B.W., Ping, P., Fandrich, R.R., Cattini, P.A., and Kardami, E. (2001). Protein kinase C-epsilon mediates phorbol ester-induced phosphorylation of connexin-43. Cell Commun Adhes *8*, 253-256.

Doble, B.W., Ping, P., and Kardami, E. (2000). The epsilon subtype of protein kinase C is required for cardiomyocyte connexin-43 phosphorylation. Circ Res *86*, 293-301.

Dobrowolski, R., and Willecke, K. (2009). Connexin-caused genetic diseases and corresponding mouse models. Antioxid Redox Signal *11*, 283-295.

Dorn, G.W., 2nd (2013). Mitochondrial dynamics in heart disease. Biochim Biophys Acta *1833*, 233-241.

Downey, J.M., Davis, A.M., and Cohen, M.V. (2007). Signaling pathways in ischemic preconditioning. Heart Fail Rev *12*, 181-188.

Dunham-Ems, S.M., Lee, Y.W., Stachowiak, E.K., Pudavar, H., Claus, P., Prasad, P.N., and Stachowiak, M.K. (2009). Fibroblast growth factor receptor-1 (FGFR1) nuclear dynamics reveal a novel mechanism in transcription control. Mol Biol Cell *20*, 2401-2412.

Dunham-Ems, S.M., Pudavar, H.E., Myers, J.M., Maher, P.A., Prasad, P.N., and Stachowiak, M.K. (2006). Factors controlling fibroblast growth factor receptor-1's cytoplasmic trafficking and its regulation as revealed by FRAP analysis. Mol Biol Cell *17*, 2223-2235.

Dupont, E., Matsushita, T., Kaba, R.A., Vozzi, C., Coppen, S.R., Khan, N., Kaprielian, R., Yacoub, M.H., and Severs, N.J. (2001). Altered connexin expression in human congestive heart failure. J Mol Cell Cardiol *33*, 359-371.

Ek-Vitorin, J.F., Calero, G., Morley, G.E., Coombs, W., Taffet, S.M., and Delmar, M. (1996). PH regulation of connexin43: molecular analysis of the gating particle. Biophys J *71*, 1273-1284.

Ek-Vitorin, J.F., King, T.J., Heyman, N.S., Lampe, P.D., and Burt, J.M. (2006). Selectivity of connexin 43 channels is regulated through protein kinase C-dependent phosphorylation. Circ Res *98*, 1498-1505.

Evans, W.H., Bultynck, G., and Leybaert, L. (2012). Manipulating connexin communication channels: use of peptidomimetics and the translational outputs. J Membr Biol *245*, 437-449.

Fannin, S.W., Lesnefsky, E.J., Slabe, T.J., Hassan, M.O., and Hoppel, C.L. (1999). Aging selectively decreases oxidative capacity in rat heart interfibrillar mitochondria. Arch Biochem Biophys *372*, 399-407.

Fenton, R.A., Dickson, E.W., and Dobson, J.G., Jr. (2005). Inhibition of phosphatase activity enhances preconditioning and limits cell death in the ischemic/reperfused aged rat heart. Life Sci *77*, 3375-3388.

Floyd, R.A., West, M., and Hensley, K. (2001). Oxidative biochemical markers; clues to understanding aging in long-lived species. Exp Gerontol *36*, 619-640.

Fontes, M.S., van Veen, T.A., de Bakker, J.M., and van Rijen, H.V. (2012). Functional consequences of abnormal Cx43 expression in the heart. Biochim Biophys Acta *1818*, 2020-2029.

Forbes, R.A., Steenbergen, C., and Murphy, E. (2001). Diazoxide-induced cardioprotection requires signaling through a redox-sensitive mechanism. Circ Res *88*, 802-809.

Formigli, L., Ibba-Manneschi, L., Perna, A.M., Pacini, A., Polidori, L., Nediani, C., Modesti, P.A., Nosi, D., Tani, A., Celli, A.*, et al.* (2003). Altered Cx43 expression during myocardial adaptation to acute and chronic volume overloading. Histol Histopathol *18*, 359-369.

Fournier, N., Ducet, G., and Crevat, A. (1987). Action of cyclosporine on mitochondrial calcium fluxes. J Bioenerg Biomembr *19*, 297-303.

Fry, M., Blondin, G.A., and Green, D.E. (1980). The localization of tightly bound cardiolipin in cytochrome oxidase. J Biol Chem *255*, 9967-9970.

Fry, M., and Green, D.E. (1981). Cardiolipin requirement for electron transfer in complex I and III of the mitochondrial respiratory chain. J Biol Chem *256*, 1874-1880.

Fryer, R.M., Eells, J.T., Hsu, A.K., Henry, M.M., and Gross, G.J. (2000). Ischemic preconditioning in rats: role of mitochondrial K(ATP) channel in preservation of mitochondrial function. Am J Physiol Heart Circ Physiol *278*, H305-312.

Fuchs, Y., and Steller, H. (2011). Programmed cell death in animal development and disease. Cell *147*, 742-758.

Garcia-Dorado, D., Inserte, J., Ruiz-Meana, M., Gonzalez, M.A., Solares, J., Julia, M., Barrabes, J.A., and Soler-Soler, J. (1997). Gap junction uncoupler heptanol prevents cell-to-cell progression of hypercontracture and limits necrosis during myocardial reperfusion. Circulation *96*, 3579-3586.

Garcia-Dorado, D., Rodriguez-Sinovas, A., and Ruiz-Meana, M. (2004). Gap junction-mediated spread of cell injury and death during myocardial ischemia-reperfusion. Cardiovasc Res *61*, 386-401.

Garlid, K.D., Costa, A.D., Quinlan, C.L., Pierre, S.V., and Dos Santos, P. (2009). Cardioprotective signaling to mitochondria. J Mol Cell Cardiol *46*, 858-866.

Garlid, K.D., Paucek, P., Yarov-Yarovoy, V., Murray, H.N., Darbenzio, R.B., D'Alonzo, A.J., Lodge, N.J., Smith, M.A., and Grover, G.J. (1997). Cardioprotective effect of diazoxide and its interaction with mitochondrial ATP-sensitive K+ channels. Possible mechanism of cardioprotection. Circ Res *81*, 1072-1082.

Garlid, K.D., Puddu, P.E., Pasdois, P., Costa, A.D., Beauvoit, B., Criniti, A., Tariosse, L., Diolez, P., and Dos Santos, P. (2006). Inhibition of cardiac contractility by 5-hydroxydecanoate and tetraphenylphosphonium ion: a possible role of mitoKATP in response to inotropic stress. Am J Physiol Heart Circ Physiol *291*, H152-160.

Giordano, F.J. (2005). Oxygen, oxidative stress, hypoxia, and heart failure. J Clin Invest *115*, 500-508.

Gomez, B., Jr., and Robinson, N.C. (1999). Phospholipase digestion of bound cardiolipin reversibly inactivates bovine cytochrome bc1. Biochemistry *38*, 9031-9038.

Goodenough, D.A., Goliger, J.A., and Paul, D.L. (1996). Connexins, connexons, and intercellular communication. Annu Rev Biochem *65*, 475-502.

Griffiths, E.J., and Halestrap, A.P. (1991). Further evidence that cyclosporin A protects mitochondria from calcium overload by inhibiting a matrix peptidyl-prolyl cis-trans isomerase. Implications for the immunosuppressive and toxic effects of cyclosporin. Biochem J *274 (Pt 2)*, 611-614.

Griffiths, E.J., and Halestrap, A.P. (1993). Protection by Cyclosporin A of ischemia/reperfusion-induced damage in isolated rat hearts. J Mol Cell Cardiol *25*, 1461-1469.

Griffiths, E.J., Ocampo, C.J., Savage, J.S., Stern, M.D., and Silverman, H.S. (2000). Protective effects of low and high doses of cyclosporin A against reoxygenation injury in isolated rat cardiomyocytes are associated with differential effects on mitochondrial calcium levels. Cell Calcium *27*, 87-95.

Grover, G.J., Parham, C.S., Sleph, P.G., and Moreland, S. (1989). Anti-ischemic and vasorelaxant effects of the new benzazepine calcium channel blocker SQ 31,765. J Pharmacol Exp Ther *251*, 1020-1025.

Halestrap, A.P., Clarke, S.J., and Javadov, S.A. (2004). Mitochondrial permeability transition pore opening during myocardial reperfusion--a target for cardioprotection. Cardiovasc Res *61*, 372-385.

Halestrap, A.P., and Davidson, A.M. (1990). Inhibition of Ca2(+)-induced large-amplitude swelling of liver and heart mitochondria by cyclosporin is probably caused by the inhibitor binding to mitochondrial-matrix peptidyl-prolyl cis-trans isomerase and preventing it interacting with the adenine nucleotide translocase. Biochem J *268*, 153-160.

Harris, D.A., and Das, A.M. (1991). Control of mitochondrial ATP synthesis in the heart. Biochem J *280 (Pt 3)*, 561-573.

Haugan, K., Marcussen, N., Kjolbye, A.L., Nielsen, M.S., Hennan, J.K., and Petersen, J.S. (2006). Treatment with the gap junction modifier rotigaptide (ZP123) reduces infarct size in rats with chronic myocardial infarction. J Cardiovasc Pharmacol *47*, 236-242.

Hausenloy, D.J., Maddock, H.L., Baxter, G.F., and Yellon, D.M. (2002). Inhibiting mitochondrial permeability transition pore opening: a new paradigm for myocardial preconditioning? Cardiovasc Res *55*, 534-543.

Hawat, G., Benderdour, M., Rousseau, G., and Baroudi, G. (2010). Connexin 43 mimetic peptide Gap26 confers protection to intact heart against myocardial ischemia injury. Pflugers Arch *460*, 583-592.

Heather, L.C., Cole, M.A., Tan, J.J., Ambrose, L.J., Pope, S., Abd-Jamil, A.H., Carter, E.E., Dodd, M.S., Yeoh, K.K., Schofield, C.J.*, et al.* (2012). Metabolic adaptation to chronic hypoxia in cardiac mitochondria. Basic Res Cardiol *107*, 268.

Heinzel, F.R., Luo, Y., Li, X., Boengler, K., Buechert, A., Garcia-Dorado, D., Di Lisa, F., Schulz, R., and Heusch, G. (2005). Impairment of diazoxide-induced formation of reactive oxygen species and loss of cardioprotection in connexin 43 deficient mice. Circ Res *97*, 583-586.

Hennan, J.K., Swillo, R.E., Morgan, G.A., Keith, J.C., Jr., Schaub, R.G., Smith, R.P., Feldman, H.S., Haugan, K., Kantrowitz, J., Wang, P.J.*, et al.* (2006). Rotigaptide (ZP123) prevents spontaneous ventricular arrhythmias and reduces infarct size during myocardial ischemia/reperfusion injury in open-chest dogs. J Pharmacol Exp Ther *317*, 236-243.

Hennan, J.K., Swillo, R.E., Morgan, G.A., Rossman, E.I., Kantrowitz, J., Butera, J., Petersen, J.S., Gardell, S.J., and Vlasuk, G.P. (2009). GAP-134 ([2S,4R]-1-[2-aminoacetyl]4-benzamidopyrrolidine-2-carboxylic acid) prevents spontaneous ventricular arrhythmias and reduces infarct size during myocardial ischemia/reperfusion injury in open-chest dogs. J Cardiovasc Pharmacol Ther *14*, 207-214.

Hoch, F.L. (1998). Cardiolipins and mitochondrial proton-selective leakage. J Bioenerg Biomembr *30*, 511-532.

Hofer, T., Servais, S., Seo, A.Y., Marzetti, E., Hiona, A., Upadhyay, S.J., Wohlgemuth, S.E., and Leeuwenburgh, C. (2009). Bioenergetics and permeability transition pore opening in heart subsarcolemmal and interfibrillar mitochondria: effects of aging and lifelong calorie restriction. Mech Ageing Dev *130*, 297-307.

Hoh, J.H., John, S.A., and Revel, J.P. (1991). Molecular cloning and characterization of a new member of the gap junction gene family, connexin-31. J Biol Chem *266*, 6524-6531.

Holmuhamedov, E.L., Oberlin, A., Short, K., Terzic, A., and Jahangir, A. (2012). Cardiac subsarcolemmal and interfibrillar mitochondria display distinct responsiveness to protection by diazoxide. PLoS One *7*, e44667.

Hoppel, C.L., Tandler, B., Parland, W., Turkaly, J.S., and Albers, L.D. (1982). Hamster cardiomyopathy. A defect in oxidative phosphorylation in the cardiac interfibrillar mitochondria. J Biol Chem *257*, 1540-1548.

Houten, S.M., and Wanders, R.J. (2010). A general introduction to the biochemistry of mitochondrial fatty acid beta-oxidation. J Inherit Metab Dis *33*, 469-477.

Hovius, R., Lambrechts, H., Nicolay, K., and de Kruijff, B. (1990). Improved methods to isolate and subfractionate rat liver mitochondria. Lipid composition of the inner and outer membrane. Biochim Biophys Acta *1021*, 217-226.

Huang, X.D., Sandusky, G.E., and Zipes, D.P. (1999). Heterogeneous loss of connexin43 protein in ischemic dog hearts. J Cardiovasc Electrophysiol *10*, 79-91.

Hunter, D.R., Haworth, R.A., and Southard, J.H. (1976). Relationship between configuration, function, and permeability in calcium-treated mitochondria. J Biol Chem *251*, 5069-5077.

Ingwall, J.S. (2009). Energy metabolism in heart failure and remodelling. Cardiovasc Res *81*, 412-419.

Jain, S.K., Schuessler, R.B., and Saffitz, J.E. (2003). Mechanisms of delayed electrical uncoupling induced by ischemic preconditioning. Circ Res *92*, 1138-1144.

Jansen, J.A., van Veen, T.A., de Bakker, J.M., and van Rijen, H.V. (2010). Cardiac connexins and impulse propagation. J Mol Cell Cardiol *48*, 76-82.

Jennings, R.B., Murry, C.E., Steenbergen, C., Jr., and Reimer, K.A. (1990). Development of cell injury in sustained acute ischemia. Circulation *82*, II2-12.

Jeyaraman, M., Tanguy, S., Fandrich, R.R., Lukas, A., and Kardami, E. (2003). Ischemia-induced dephosphorylation of cardiomyocyte connexin-43 is reduced by okadaic acid and calyculin A but not fostriecin. Mol Cell Biochem *242*, 129-134.

Jeyaraman, M.M., Srisakuldee, W., Nickel, B.E., and Kardami, E. (2012). Connexin43 phosphorylation and cytoprotection in the heart. Biochim Biophys Acta *1818*, 2009-2013.

Jiang, Z.S., Jeyaraman, M., Wen, G.B., Fandrich, R.R., Dixon, I.M., Cattini, P.A., and Kardami, E. (2007). High- but not low-molecular weight FGF-2 causes cardiac hypertrophy in vivo; possible involvement of cardiotrophin-1. J Mol Cell Cardiol *42*, 222-233.

Jiang, Z.S., Padua, R.R., Ju, H., Doble, B.W., Jin, Y., Hao, J., Cattini, P.A., Dixon, I.M., and Kardami, E. (2002). Acute protection of ischemic heart by FGF-2: involvement of

FGF-2 receptors and protein kinase C. Am J Physiol Heart Circ Physiol *282*, H1071-1080.

Jiang, Z.S., Srisakuldee, W., Soulet, F., Bouche, G., and Kardami, E. (2004). Non-angiogenic FGF-2 protects the ischemic heart from injury, in the presence or absence of reperfusion. Cardiovasc Res *62*, 154-166.

Jiang, Z.S., Wen, G.B., Tang, Z.H., Srisakuldee, W., Fandrich, R.R., and Kardami, E. (2009). High molecular weight FGF-2 promotes postconditioning-like cardioprotection linked to activation of protein kinase C isoforms, as well as Akt and p70 S6 kinases. [corrected]. Can J Physiol Pharmacol *87*, 798-804.

Jimenez, S.K., Sheikh, F., Jin, Y., Detillieux, K.A., Dhaliwal, J., Kardami, E., and Cattini, P.A. (2004). Transcriptional regulation of FGF-2 gene expression in cardiac myocytes. Cardiovasc Res *62*, 548-557.

Jin, H., Chemaly, E.R., Lee, A., Kho, C., Hadri, L., Hajjar, R.J., and Akar, F.G. (2010). Mechanoelectrical remodeling and arrhythmias during progression of hypertrophy. FASEB J *24*, 451-463.

Jozwiak, J., and Dhein, S. (2008). Local effects and mechanisms of antiarrhythmic peptide AAP10 in acute regional myocardial ischemia: electrophysiological and molecular findings. Naunyn Schmiedebergs Arch Pharmacol *378*, 459-470.

Kaba, R.A., Coppen, S.R., Dupont, E., Skepper, J.N., Elneil, S., Haw, M.P., Pepper, J.R., Yacoub, M.H., Rothery, S., and Severs, N.J. (2001). Comparison of connexin 43, 40 and 45 expression patterns in the developing human and mouse hearts. Cell Commun Adhes *8*, 339-343.

Kajiyama, K., Pauly, D.F., Hughes, H., Yoon, S.B., Entman, M.L., and McMillin-Wood, J.B. (1987). Protection by verapamil of mitochondrial glutathione equilibrium and phospholipid changes during reperfusion of ischemic canine myocardium. Circ Res *61*, 301-310.

Kalcheva, N., Qu, J., Sandeep, N., Garcia, L., Zhang, J., Wang, Z., Lampe, P.D., Suadicani, S.O., Spray, D.C., and Fishman, G.I. (2007). Gap junction remodeling and cardiac arrhythmogenesis in a murine model of oculodentodigital dysplasia. Proc Natl Acad Sci U S A *104*, 20512-20516.

Kanemitsu, M.Y., Loo, L.W., Simon, S., Lau, A.F., and Eckhart, W. (1997). Tyrosine phosphorylation of connexin 43 by v-Src is mediated by SH2 and SH3 domain interactions. J Biol Chem *272*, 22824-22831.

Kang, J., Kang, N., Lovatt, D., Torres, A., Zhao, Z., Lin, J., and Nedergaard, M. (2008). Connexin 43 hemichannels are permeable to ATP. J Neurosci *28*, 4702-4711.

Kardami, E., Dang, X., Iacobas, D.A., Nickel, B.E., Jeyaraman, M., Srisakuldee, W., Makazan, J., Tanguy, S., and Spray, D.C. (2007a). The role of connexins in controlling cell growth and gene expression. Prog Biophys Mol Biol *94*, 245-264.

Kardami, E., Detillieux, K., Ma, X., Jiang, Z., Santiago, J.J., Jimenez, S.K., and Cattini, P.A. (2007b). Fibroblast growth factor-2 and cardioprotection. Heart Fail Rev *12*, 267-277.

Kardami, E., Jiang, Z.S., Jimenez, S.K., Hirst, C.J., Sheikh, F., Zahradka, P., and Cattini, P.A. (2004). Fibroblast growth factor 2 isoforms and cardiac hypertrophy. Cardiovasc Res *63*, 458-466.

Khairallah, R.J., O'Shea, K.M., Brown, B.H., Khanna, N., Des Rosiers, C., and Stanley, W.C. (2010). Treatment with docosahexaenoic acid, but not eicosapentaenoic acid, delays Ca2+-induced mitochondria permeability transition in normal and hypertrophied myocardium. J Pharmacol Exp Ther *335*, 155-162.

Kida, M., Fujiwara, H., Ishida, M., Kawai, C., Ohura, M., Miura, I., and Yabuuchi, Y. (1991). Ischemic preconditioning preserves creatine phosphate and intracellular pH. Circulation *84*, 2495-2503.

Klionsky, D.J., and Emr, S.D. (2000). Autophagy as a regulated pathway of cellular degradation. Science *290*, 1717-1721.

Kobara, M., Tatsumi, T., Matoba, S., Yamahara, Y., Nakagawa, C., Ohta, B., Matsumoto, T., Inoue, D., Asayama, J., and Nakagawa, M. (1996). Effect of ischemic preconditioning on mitochondrial oxidative phosphorylation and high energy phosphates in rat hearts. J Mol Cell Cardiol *28*, 417-428.

Kodde, I.F., van der Stok, J., Smolenski, R.T., and de Jong, J.W. (2007). Metabolic and genetic regulation of cardiac energy substrate preference. Comp Biochem Physiol A Mol Integr Physiol *146*, 26-39.

Kokoszka, J.E., Waymire, K.G., Levy, S.E., Sligh, J.E., Cai, J., Jones, D.P., MacGregor, G.R., and Wallace, D.C. (2004). The ADP/ATP translocator is not essential for the mitochondrial permeability transition pore. Nature *427*, 461-465.

Korge, P., Yang, L., Yang, J.H., Wang, Y., Qu, Z., and Weiss, J.N. (2011). Protective role of transient pore openings in calcium handling by cardiac mitochondria. J Biol Chem *286*, 34851-34857.

Kostin, S., Dammer, S., Hein, S., Klovekorn, W.P., Bauer, E.P., and Schaper, J. (2004). Connexin 43 expression and distribution in compensated and decompensated cardiac hypertrophy in patients with aortic stenosis. Cardiovasc Res *62*, 426-436.

Kostin, S., Rieger, M., Dammer, S., Hein, S., Richter, M., Klovekorn, W.P., Bauer, E.P., and Schaper, J. (2003). Gap junction remodeling and altered connexin43 expression in the failing human heart. Mol Cell Biochem *242*, 135-144.

Kowaltowski, A.J., Seetharaman, S., Paucek, P., and Garlid, K.D. (2001). Bioenergetic consequences of opening the ATP-sensitive K(+) channel of heart mitochondria. Am J Physiol Heart Circ Physiol *280*, H649-657.

Kroemer, G., Galluzzi, L., and Brenner, C. (2007). Mitochondrial membrane permeabilization in cell death. Physiol Rev *87*, 99-163.

Kroemer, G., Galluzzi, L., Vandenabeele, P., Abrams, J., Alnemri, E.S., Baehrecke, E.H., Blagosklonny, M.V., El-Deiry, W.S., Golstein, P., Green, D.R.*, et al.* (2009). Classification of cell death: recommendations of the Nomenclature Committee on Cell Death 2009. Cell Death Differ *16*, 3-11.

Kroemer, G., Marino, G., and Levine, B. (2010). Autophagy and the integrated stress response. Mol Cell *40*, 280-293.

Krysko, D.V., Vanden Berghe, T., D'Herde, K., and Vandenabeele, P. (2008). Apoptosis and necrosis: detection, discrimination and phagocytosis. Methods *44*, 205-221.

Kung, G., Konstantinidis, K., and Kitsis, R.N. (2011). Programmed necrosis, not apoptosis, in the heart. Circ Res *108*, 1017-1036.

Kuznetsov, A.V., Hermann, M., Saks, V., Hengster, P., and Margreiter, R. (2009). The cell-type specificity of mitochondrial dynamics. Int J Biochem Cell Biol *41*, 1928-1939.

Kwong, L.K., and Sohal, R.S. (1998). Substrate and site specificity of hydrogen peroxide generation in mouse mitochondria. Arch Biochem Biophys *350*, 118-126.

Laclau, M.N., Boudina, S., Thambo, J.B., Tariosse, L., Gouverneur, G., Bonoron-Adele, S., Saks, V.A., Garlid, K.D., and Dos Santos, P. (2001). Cardioprotection by ischemic preconditioning preserves mitochondrial function and functional coupling between adenine nucleotide translocase and creatine kinase. J Mol Cell Cardiol *33*, 947-956.

Laederich, M.B., Degnin, C.R., Lunstrum, G.P., Holden, P., and Horton, W.A. (2011). Fibroblast growth factor receptor 3 (FGFR3) is a strong heat shock protein 90 (Hsp90) client: implications for therapeutic manipulation. J Biol Chem *286*, 19597-19604.

Laird, D.W. (2006). Life cycle of connexins in health and disease. Biochem J *394*, 527-543.

Laird, D.W. (2010). The gap junction proteome and its relationship to disease. Trends Cell Biol *20*, 92-101.

Lakatta, E.G., Mitchell, J.H., Pomerance, A., and Rowe, G.G. (1987). Human aging: changes in structure and function. J Am Coll Cardiol *10*, 42A-47A.

Lampe, P.D., Cooper, C.D., King, T.J., and Burt, J.M. (2006). Analysis of Connexin43 phosphorylated at S325, S328 and S330 in normoxic and ischemic heart. J Cell Sci *119*, 3435-3442.

Lampe, P.D., and Lau, A.F. (2000). Regulation of gap junctions by phosphorylation of connexins. Arch Biochem Biophys *384*, 205-215.

Lampe, P.D., and Lau, A.F. (2004). The effects of connexin phosphorylation on gap junctional communication. Int J Biochem Cell Biol *36*, 1171-1186.

Lampe, P.D., TenBroek, E.M., Burt, J.M., Kurata, W.E., Johnson, R.G., and Lau, A.F. (2000). Phosphorylation of connexin43 on serine368 by protein kinase C regulates gap junctional communication. J Cell Biol *149*, 1503-1512.

Lapidus, R.G., and Sokolove, P.M. (1994). The mitochondrial permeability transition. Interactions of spermine, ADP, and inorganic phosphate. J Biol Chem *269*, 18931-18936.

Lee, D., Oka, T., Hunter, B., Robinson, A., Papp, S., Nakamura, K., Srisakuldee, W., Nickel, B.E., Light, P.E., Dyck, J.R.*, et al.* (2013). Calreticulin induces dilated cardiomyopathy. PLoS One *8*, e56387.

Lemasters, J.J., Qian, T., Bradham, C.A., Brenner, D.A., Cascio, W.E., Trost, L.C., Nishimura, Y., Nieminen, A.L., and Herman, B. (1999). Mitochondrial dysfunction in the pathogenesis of necrotic and apoptotic cell death. J Bioenerg Biomembr *31*, 305-319.

Lerner, D.L., Beardslee, M.A., and Saffitz, J.E. (2001). The role of altered intercellular coupling in arrhythmias induced by acute myocardial ischemia. Cardiovasc Res *50*, 263-269.

Lesnefsky, E.J., Chen, Q., Moghaddas, S., Hassan, M.O., Tandler, B., and Hoppel, C.L. (2004). Blockade of electron transport during ischemia protects cardiac mitochondria. J Biol Chem *279*, 47961-47967.

Lesnefsky, E.J., Gallo, D.S., Ye, J., Whittingham, T.S., and Lust, W.D. (1994). Aging increases ischemia-reperfusion injury in the isolated, buffer-perfused heart. J Lab Clin Med *124*, 843-851.

Lesnefsky, E.J., and Hoppel, C.L. (2008). Cardiolipin as an oxidative target in cardiac mitochondria in the aged rat. Biochim Biophys Acta *1777*, 1020-1027.

Lesnefsky, E.J., Lundergan, C.F., Hodgson, J.M., Nair, R., Reiner, J.S., Greenhouse, S.W., Califf, R.M., and Ross, A.M. (1996). Increased left ventricular dysfunction in elderly patients despite successful thrombolysis: the GUSTO-I angiographic experience. J Am Coll Cardiol *28*, 331-337.

Lesnefsky, E.J., Minkler, P., and Hoppel, C.L. (2009). Enhanced modification of cardiolipin during ischemia in the aged heart. J Mol Cell Cardiol *46*, 1008-1015.

Lesnefsky, E.J., Slabe, T.J., Stoll, M.S., Minkler, P.E., and Hoppel, C.L. (2001). Myocardial ischemia selectively depletes cardiolipin in rabbit heart subsarcolemmal mitochondria. Am J Physiol Heart Circ Physiol *280*, H2770-2778.

Lesnefsky, E.J., Tandler, B., Ye, J., Slabe, T.J., Turkaly, J., and Hoppel, C.L. (1997). Myocardial ischemia decreases oxidative phosphorylation through cytochrome oxidase in subsarcolemmal mitochondria. Am J Physiol *273*, H1544-1554.

Leung, A.W., Varanyuwatana, P., and Halestrap, A.P. (2008). The mitochondrial phosphate carrier interacts with cyclophilin D and may play a key role in the permeability transition. J Biol Chem *283*, 26312-26323.

Li, G., Whittaker, P., Yao, M., Kloner, R.A., and Przyklenk, K. (2002a). The gap junction uncoupler heptanol abrogates infarct size reduction with preconditioning in mouse hearts. Cardiovasc Pathol *11*, 158-165.

Li, H., Brodsky, S., Kumari, S., Valiunas, V., Brink, P., Kaide, J., Nasjletti, A., and Goligorsky, M.S. (2002b). Paradoxical overexpression and translocation of connexin43 in homocysteine-treated endothelial cells. Am J Physiol Heart Circ Physiol *282*, H2124-2133.

Li, X., Heinzel, F.R., Boengler, K., Schulz, R., and Heusch, G. (2004). Role of connexin 43 in ischemic preconditioning does not involve intercellular communication through gap junctions. J Mol Cell Cardiol *36*, 161-163.

Li, Y., Huang, T.T., Carlson, E.J., Melov, S., Ursell, P.C., Olson, J.L., Noble, L.J., Yoshimura, M.P., Berger, C., Chan, P.H.*, et al.* (1995). Dilated cardiomyopathy and neonatal lethality in mutant mice lacking manganese superoxide dismutase. Nat Genet *11*, 376-381.

Liesa, M., Palacin, M., and Zorzano, A. (2009). Mitochondrial dynamics in mammalian health and disease. Physiol Rev *89*, 799-845.

Lill, R., and Muhlenhoff, U. (2005). Iron-sulfur-protein biogenesis in eukaryotes. Trends Biochem Sci *30*, 133-141.

Lips, D.J., deWindt, L.J., van Kraaij, D.J., and Doevendans, P.A. (2003). Molecular determinants of myocardial hypertrophy and failure: alternative pathways for beneficial and maladaptive hypertrophy. Eur Heart J *24*, 883-896.

Lu, G., Haider, H., Porollo, A., and Ashraf, M. (2010). Mitochondria-specific transgenic overexpression of connexin-43 simulates preconditioning-induced cytoprotection of stem cells. Cardiovasc Res *88*, 277-286.

Lu, G., Jiang, S., Ashraf, M., and Haider, K.H. (2012). Subcellular preconditioning of stem cells: mito-Cx43 gene targeting is cytoprotective via shift of mitochondrial Bak and Bcl-xL balance. Regen Med *7*, 323-334.

Lucas, D.T., and Szweda, L.I. (1998). Cardiac reperfusion injury: aging, lipid peroxidation, and mitochondrial dysfunction. Proc Natl Acad Sci U S A *95*, 510-514.

Maher, P.A. (1996). Identification and characterization of a novel, intracellular isoform of fibroblast growth factor receptor-1(FGFR-1). J Cell Physiol *169*, 380-390.

Makazan, Z., Saini, H.K., and Dhalla, N.S. (2007). Role of oxidative stress in alterations of mitochondrial function in ischemic-reperfused hearts. Am J Physiol Heart Circ Physiol *292*, H1986-1994.

Manning, J.R., Perkins, S.O., Sinclair, E.A., Gao, X., Zhang, Y., Newman, G., Pyle, W.G., and Schultz Jel, J. (2013). Low molecular weight fibroblast growth factor-2 signals via protein kinase C and myofibrillar proteins to protect against postischemic cardiac dysfunction. Am J Physiol Heart Circ Physiol *304*, H1382-1396.

Marcil, M., Bourduas, K., Ascah, A., and Burelle, Y. (2006). Exercise training induces respiratory substrate-specific decrease in Ca^{2+}-induced permeability transition pore opening in heart mitochondria. Am J Physiol Heart Circ Physiol *290*, H1549-1557.

Martel, C., Huynh le, H., Garnier, A., Ventura-Clapier, R., and Brenner, C. (2012). Inhibition of the Mitochondrial Permeability Transition for Cytoprotection: Direct versus Indirect Mechanisms. Biochem Res Int *2012*, 213403.

Marzo, I., Brenner, C., Zamzami, N., Susin, S.A., Beutner, G., Brdiczka, D., Remy, R., Xie, Z.H., Reed, J.C., and Kroemer, G. (1998). The permeability transition pore complex: a target for apoptosis regulation by caspases and bcl-2-related proteins. J Exp Med *187*, 1261-1271.

Matsunaga, S., Okigaki, M., Takeda, M., Matsui, A., Honsho, S., Katsume, A., Kishita, E., Che, J., Kurihara, T., Adachi, Y.*, et al.* (2009). Endothelium-targeted overexpression of constitutively active FGF receptor induces cardioprotection in mice myocardial infarction. J Mol Cell Cardiol *46*, 663-673.

McCarthy, J., Lochner, A., Opie, L.H., Sack, M.N., and Essop, M.F. (2011). PKCepsilon promotes cardiac mitochondrial and metabolic adaptation to chronic hypobaric hypoxia by GSK3beta inhibition. J Cell Physiol *226*, 2457-2468.

Miller, W.L. (2011). Role of mitochondria in steroidogenesis. Endocr Dev *20*, 1-19.

Miro-Casas, E., Ruiz-Meana, M., Agullo, E., Stahlhofen, S., Rodriguez-Sinovas, A., Cabestrero, A., Jorge, I., Torre, I., Vazquez, J., Boengler, K.*, et al.* (2009). Connexin43 in cardiomyocyte mitochondria contributes to mitochondrial potassium uptake. Cardiovasc Res *83*, 747-756.

Miura, T., Ohnuma, Y., Kuno, A., Tanno, M., Ichikawa, Y., Nakamura, Y., Yano, T., Miki, T., Sakamoto, J., and Shimamoto, K. (2004). Protective role of gap junctions in preconditioning against myocardial infarction. Am J Physiol Heart Circ Physiol *286*, H214-221.

Miura, T., and Tanno, M. (2012). The mPTP and its regulatory proteins: final common targets of signalling pathways for protection against necrosis. Cardiovasc Res *94*, 181-189.

Miura, T., Yano, T., Naitoh, K., Nishihara, M., Miki, T., Tanno, M., and Shimamoto, K. (2007). Delta-opioid receptor activation before ischemia reduces gap junction permeability in ischemic myocardium by PKC-epsilon-mediated phosphorylation of connexin 43. Am J Physiol Heart Circ Physiol *293*, H1425-1431.

Moghaddas, S., Hoppel, C.L., and Lesnefsky, E.J. (2003). Aging defect at the QO site of complex III augments oxyradical production in rat heart interfibrillar mitochondria. Arch Biochem Biophys *414*, 59-66.

Monette, J.S., Gomez, L.A., Moreau, R.F., Bemer, B.A., Taylor, A.W., and Hagen, T.M. (2010). Characteristics of the rat cardiac sphingolipid pool in two mitochondrial subpopulations. Biochem Biophys Res Commun *398*, 272-277.

Morgan, M.J., Kim, Y.S., and Liu, Z.G. (2008). TNFalpha and reactive oxygen species in necrotic cell death. Cell Res *18*, 343-349.

Mughal, W., Dhingra, R., and Kirshenbaum, L.A. (2012). Striking a balance: autophagy, apoptosis, and necrosis in a normal and failing heart. Current hypertension reports *14*, 540-547.

Muller, W. (1976). Subsarcolemmal mitochondria and capillarization of soleus muscle fibers in young rats subjected to an endurance training. A morphometric study of semithin sections. Cell Tissue Res *174*, 367-389.

Muramatsu, Y., Furuichi, Y., Tojo, N., Moriguchi, A., Maemoto, T., Nakada, H., Hino, M., and Matsuoka, N. (2007). Neuroprotective efficacy of FR901459, a novel derivative of cyclosporin A, in in vitro mitochondrial damage and in vivo transient cerebral ischemia models. Brain Res *1149*, 181-190.

Murry, C.E., Jennings, R.B., and Reimer, K.A. (1986). Preconditioning with ischemia: a delay of lethal cell injury in ischemic myocardium. Circulation *74*, 1124-1136.

Muzio, M., Chinnaiyan, A.M., Kischkel, F.C., O'Rourke, K., Shevchenko, A., Ni, J., Scaffidi, C., Bretz, J.D., Zhang, M., Gentz, R.*, et al.* (1996). FLICE, a novel FADD-homologous ICE/CED-3-like protease, is recruited to the CD95 (Fas/APO-1) death--inducing signaling complex. Cell *85*, 817-827.

Nagy, J.I., Li, W.E., Roy, C., Doble, B.W., Gilchrist, J.S., Kardami, E., and Hertzberg, E.L. (1997). Selective monoclonal antibody recognition and cellular localization of an unphosphorylated form of connexin43. Exp Cell Res *236*, 127-136.

Nakagawa, T., Shimizu, S., Watanabe, T., Yamaguchi, O., Otsu, K., Yamagata, H., Inohara, H., Kubo, T., and Tsujimoto, Y. (2005). Cyclophilin D-dependent mitochondrial permeability transition regulates some necrotic but not apoptotic cell death. Nature *434*, 652-658.

Naus, C.C., and Laird, D.W. (2010). Implications and challenges of connexin connections to cancer. Nat Rev Cancer *10*, 435-441.

Nordberg, J., and Arner, E.S. (2001). Reactive oxygen species, antioxidants, and the mammalian thioredoxin system. Free Radic Biol Med *31*, 1287-1312.

Ong, S.B., Hall, A.R., and Hausenloy, D.J. (2013). Mitochondrial dynamics in cardiovascular health and disease. Antioxid Redox Signal *19*, 400-414.

Opie, L.H. (1968). Metabolism of the heart in health and disease. I. Am Heart J *76*, 685-698.

Ott, M., Robertson, J.D., Gogvadze, V., Zhivotovsky, B., and Orrenius, S. (2002). Cytochrome c release from mitochondria proceeds by a two-step process. Proc Natl Acad Sci U S A *99*, 1259-1263.

Padua, R.R., Merle, P.L., Doble, B.W., Yu, C.H., Zahradka, P., Pierce, G.N., Panagia, V., and Kardami, E. (1998). FGF-2-induced negative inotropism and cardioprotection are inhibited by chelerythrine: involvement of sarcolemmal calcium-independent protein kinase C. J Mol Cell Cardiol *30*, 2695-2709.

Padua, R.R., Sethi, R., Dhalla, N.S., and Kardami, E. (1995). Basic fibroblast growth factor is cardioprotective in ischemia-reperfusion injury. Mol Cell Biochem *143*, 129-135.

Pain, T., Yang, X.M., Critz, S.D., Yue, Y., Nakano, A., Liu, G.S., Heusch, G., Cohen, M.V., and Downey, J.M. (2000). Opening of mitochondrial K(ATP) channels triggers the preconditioned state by generating free radicals. Circ Res *87*, 460-466.

Palmer, J.W., Tandler, B., and Hoppel, C.L. (1977). Biochemical properties of subsarcolemmal and interfibrillar mitochondria isolated from rat cardiac muscle. J Biol Chem *252*, 8731-8739.

Palmer, J.W., Tandler, B., and Hoppel, C.L. (1985). Biochemical differences between subsarcolemmal and interfibrillar mitochondria from rat cardiac muscle: effects of procedural manipulations. Arch Biochem Biophys *236*, 691-702.

Palmer, J.W., Tandler, B., and Hoppel, C.L. (1986). Heterogeneous response of subsarcolemmal heart mitochondria to calcium. Am J Physiol *250*, H741-748.

Papp, R., Gonczi, M., Kovacs, M., Seprenyi, G., and Vegh, A. (2007). Gap junctional uncoupling plays a trigger role in the antiarrhythmic effect of ischaemic preconditioning. Cardiovasc Res *74*, 396-405.

Paznekas, W.A., Boyadjiev, S.A., Shapiro, R.E., Daniels, O., Wollnik, B., Keegan, C.E., Innis, J.W., Dinulos, M.B., Christian, C., Hannibal, M.C.*, et al.* (2003). Connexin 43 (GJA1) mutations cause the pleiotropic phenotype of oculodentodigital dysplasia. Am J Hum Genet *72*, 408-418.

Peters, N.S., Green, C.R., Poole-Wilson, P.A., and Severs, N.J. (1993). Reduced content of connexin43 gap junctions in ventricular myocardium from hypertrophied and ischemic human hearts. Circulation *88*, 864-875.

Petronilli, V., Miotto, G., Canton, M., Brini, M., Colonna, R., Bernardi, P., and Di Lisa, F. (1999). Transient and long-lasting openings of the mitochondrial permeability transition pore can be monitored directly in intact cells by changes in mitochondrial calcein fluorescence. Biophys J *76*, 725-734.

Petronilli, V., Szabo, I., and Zoratti, M. (1989). The inner mitochondrial membrane contains ion-conducting channels similar to those found in bacteria. FEBS Lett *259*, 137-143.

Ping, P., Zhang, J., Pierce, W.M., Jr., and Bolli, R. (2001). Functional proteomic analysis of protein kinase C epsilon signaling complexes in the normal heart and during cardioprotection. Circ Res *88*, 59-62.

Piot, C., Croisille, P., Staat, P., Thibault, H., Rioufol, G., Mewton, N., Elbelghiti, R., Cung, T.T., Bonnefoy, E., Angoulvant, D.*, et al.* (2008). Effect of cyclosporine on reperfusion injury in acute myocardial infarction. N Engl J Med *359*, 473-481.

Porter, G.A., Jr., Hom, J., Hoffman, D., Quintanilla, R., de Mesy Bentley, K., and Sheu, S.S. (2011). Bioenergetics, mitochondria, and cardiac myocyte differentiation. Prog Pediatr Cardiol *31*, 75-81.

Puglisi, R.N., Strande, L., Santos, M., Schulte, G., Hewitt, C.W., and Whalen, T.V. (1996). Beneficial effects of cyclosporine and rapamycin in small bowel ischemic injury. J Surg Res *65*, 115-118.

Quist, A.P., Rhee, S.K., Lin, H., and Lal, R. (2000). Physiological role of gap-junctional hemichannels. Extracellular calcium-dependent isosmotic volume regulation. J Cell Biol *148*, 1063-1074.

Rasola, A., Sciacovelli, M., Chiara, F., Pantic, B., Brusilow, W.S., and Bernardi, P. (2010). Activation of mitochondrial ERK protects cancer cells from death through inhibition of the permeability transition. Proc Natl Acad Sci U S A *107*, 726-731.

Remo, B.F., Giovannone, S., and Fishman, G.I. (2012). Connexin43 cardiac gap junction remodeling: lessons from genetically engineered murine models. J Membr Biol *245*, 275-281.

Ritov, V.B., Menshikova, E.V., He, J., Ferrell, R.E., Goodpaster, B.H., and Kelley, D.E. (2005). Deficiency of subsarcolemmal mitochondria in obesity and type 2 diabetes. Diabetes *54*, 8-14.

Riva, A., Tandler, B., Lesnefsky, E.J., Conti, G., Loffredo, F., Vazquez, E., and Hoppel, C.L. (2006). Structure of cristae in cardiac mitochondria of aged rat. Mech Ageing Dev *127*, 917-921.

Riva, A., Tandler, B., Loffredo, F., Vazquez, E., and Hoppel, C. (2005). Structural differences in two biochemically defined populations of cardiac mitochondria. Am J Physiol Heart Circ Physiol *289*, H868-872.

Robaye, B., Mosselmans, R., Fiers, W., Dumont, J.E., and Galand, P. (1991). Tumor necrosis factor induces apoptosis (programmed cell death) in normal endothelial cells in vitro. Am J Pathol *138*, 447-453.

Robinson, N.C., Strey, F., and Talbert, L. (1980). Investigation of the essential boundary layer phospholipids of cytochrome c oxidase using Triton X-100 delipidation. Biochemistry *19*, 3656-3661.

Rodriguez-Sinovas, A., Boengler, K., Cabestrero, A., Gres, P., Morente, M., Ruiz-Meana, M., Konietzka, I., Miro, E., Totzeck, A., Heusch, G.*, et al.* (2006). Translocation of connexin 43 to the inner mitochondrial membrane of cardiomyocytes through the heat shock protein 90-dependent TOM pathway and its importance for cardioprotection. Circ Res *99*, 93-101.

Rodriguez-Sinovas, A., Garcia-Dorado, D., Ruiz-Meana, M., and Soler-Soler, J. (2004). Enhanced effect of gap junction uncouplers on macroscopic electrical properties of reperfused myocardium. J Physiol *559*, 245-257.

Rodriguez-Sinovas, A., Sanchez, J.A., Fernandez-Sanz, C., Ruiz-Meana, M., and Garcia-Dorado, D. (2012). Connexin and pannexin as modulators of myocardial injury. Biochim Biophys Acta *1818*, 1962-1970.

Rodriguez-Sinovas, A., Sanchez, J.A., Gonzalez-Loyola, A., Barba, I., Morente, M., Aguilar, R., Agullo, E., Miro-Casas, E., Esquerda, N., Ruiz-Meana, M.*, et al.* (2010). Effects of substitution of Cx43 by Cx32 on myocardial energy metabolism, tolerance to ischaemia and preconditioning protection. J Physiol *588*, 1139-1151.

Ruiz-Meana, M., Garcia-Dorado, D., Hofstaetter, B., Piper, H.M., and Soler-Soler, J. (1999). Propagation of cardiomyocyte hypercontracture by passage of Na(+) through gap junctions. Circ Res *85*, 280-287.

Ruiz-Meana, M., Garcia-Dorado, D., Miro-Casas, E., Abellan, A., and Soler-Soler, J. (2006). Mitochondrial Ca2+ uptake during simulated ischemia does not affect permeability transition pore opening upon simulated reperfusion. Cardiovasc Res *71*, 715-724.

Ruiz-Meana, M., Nunez, E., Miro-Casas, E., Martinez-Acedo, P., Barba, I., Rodriguez-Sinovas, A., Inserte, J., Fernandez-Sanz, C., Hernando, V., Vazquez, J.*, et al.* (2014). Ischemic preconditioning protects cardiomyocyte mitochondria through mechanisms independent of cytosol. J Mol Cell Cardiol *68*, 79-88.

Sadoshima, J. (2011). Sirt3 targets mPTP and prevents aging in the heart. Aging (Albany NY) *3*, 12-13.

Saez, J.C., Retamal, M.A., Basilio, D., Bukauskas, F.F., and Bennett, M.V. (2005). Connexin-based gap junction hemichannels: gating mechanisms. Biochim Biophys Acta *1711*, 215-224.

Saez, J.C., Schalper, K.A., Retamal, M.A., Orellana, J.A., Shoji, K.F., and Bennett, M.V. (2010). Cell membrane permeabilization via connexin hemichannels in living and dying cells. Exp Cell Res *316*, 2377-2389.

Saffitz, J.E., Hoyt, R.H., Luke, R.A., Lee Kanter, H., and Beyer, E.C. (1992). Cardiac myocyte interconnections at gap junctions Role in normal and abnormal electrical conduction. Trends Cardiovasc Med *2*, 56-60.

Salameh, A., Krautblatter, S., Karl, S., Blanke, K., Gomez, D.R., Dhein, S., Pfeiffer, D., and Janousek, J. (2009). The signal transduction cascade regulating the expression of the gap junction protein connexin43 by beta-adrenoceptors. Br J Pharmacol *158*, 198-208.

Santiago, J.J., Ma, X., McNaughton, L.J., Nickel, B.E., Bestvater, B.P., Yu, L., Fandrich, R.R., Netticadan, T., and Kardami, E. (2011). Preferential accumulation and export of high molecular weight FGF-2 by rat cardiac non-myocytes. Cardiovasc Res *89*, 139-147.

Saotome, M., Katoh, H., Yaguchi, Y., Tanaka, T., Urushida, T., Satoh, H., and Hayashi, H. (2009). Transient opening of mitochondrial permeability transition pore by reactive oxygen species protects myocardium from ischemia-reperfusion injury. Am J Physiol Heart Circ Physiol *296*, H1125-1132.

Saxton, N.E., Barclay, J.L., Clouston, A.D., and Fawcett, J. (2002). Cyclosporin A pretreatment in a rat model of warm ischaemia/reperfusion injury. J Hepatol *36*, 241-247.

Schonfeld, P., Wieckowski, M.R., and Wojtczak, L. (2000). Long-chain fatty acid-promoted swelling of mitochondria: further evidence for the protonophoric effect of fatty acids in the inner mitochondrial membrane. FEBS Lett *471*, 108-112.

Schulz, R., Boengler, K., Totzeck, A., Luo, Y., Garcia-Dorado, D., and Heusch, G. (2007). Connexin 43 in ischemic pre- and postconditioning. Heart Fail Rev *12*, 261-266.

Schulz, R., Gres, P., Skyschally, A., Duschin, A., Belosjorow, S., Konietzka, I., and Heusch, G. (2003). Ischemic preconditioning preserves connexin 43 phosphorylation during sustained ischemia in pig hearts in vivo. FASEB J *17*, 1355-1357.

Schulz, R., and Heusch, G. (2006). Connexin43 and ischemic preconditioning. Adv Cardiol *42*, 213-227.

Schwanke, U., Konietzka, I., Duschin, A., Li, X., Schulz, R., and Heusch, G. (2002). No ischemic preconditioning in heterozygous connexin43-deficient mice. Am J Physiol Heart Circ Physiol *283*, H1740-1742.

Schwarzer, M., Schrepper, A., Amorim, P.A., Osterholt, M., and Doenst, T. (2013). Pressure overload differentially affects respiratory capacity in interfibrillar and subsarcolemmal mitochondria. Am J Physiol Heart Circ Physiol *304*, H529-537.

Sepp, R., Severs, N.J., and Gourdie, R.G. (1996). Altered patterns of cardiac intercellular junction distribution in hypertrophic cardiomyopathy. Heart *76*, 412-417.

Severs, N.J. (1994). Gap junction alterations in the failing heart. Eur Heart J *15 Suppl D*, 53-57.

Severs, N.J., Bruce, A.F., Dupont, E., and Rothery, S. (2008). Remodelling of gap junctions and connexin expression in diseased myocardium. Cardiovasc Res *80*, 9-19.

Shaw, J., and Kirshenbaum, L.A. (2008). Molecular regulation of autophagy and apoptosis during ischemic and non-ischemic cardiomyopathy. Autophagy *4*, 427-434.

Shaw, M., Cohen, P., and Alessi, D.R. (1998). The activation of protein kinase B by H2O2 or heat shock is mediated by phosphoinositide 3-kinase and not by mitogen-activated protein kinase-activated protein kinase-2. Biochem J *336 (Pt 1)*, 241-246.

Sheikh, F., Fandrich, R.R., Kardami, E., and Cattini, P.A. (1999). Overexpression of long or short FGFR-1 results in FGF-2-mediated proliferation in neonatal cardiac myocyte cultures. Cardiovasc Res *42*, 696-705.

Sheikh, F., Sontag, D.P., Fandrich, R.R., Kardami, E., and Cattini, P.A. (2001). Overexpression of FGF-2 increases cardiac myocyte viability after injury in isolated mouse hearts. Am J Physiol Heart Circ Physiol *280*, H1039-1050.

Shin, G., Sugiyama, M., Shoji, T., Kagiyama, A., Sato, H., and Ogura, R. (1989). Detection of mitochondrial membrane damages in myocardial ischemia with ESR spin labeling technique. J Mol Cell Cardiol *21*, 1029-1036.

Shintani-Ishida, K., Uemura, K., and Yoshida, K. (2007). Hemichannels in cardiomyocytes open transiently during ischemia and contribute to reperfusion injury following brief ischemia. Am J Physiol Heart Circ Physiol *293*, H1714-1720.

Simburger, E., Stang, A., Kremer, M., and Dermietzel, R. (1997). Expression of connexin43 mRNA in adult rodent brain. Histochem Cell Biol *107*, 127-137.

Simon, A.M., and Goodenough, D.A. (1998). Diverse functions of vertebrate gap junctions. Trends Cell Biol *8*, 477-483.

Singh, D., Chander, V., and Chopra, K. (2005). Cyclosporine protects against ischemia/reperfusion injury in rat kidneys. Toxicology *207*, 339-347.

Siwik, D.A., Tzortzis, J.D., Pimental, D.R., Chang, D.L., Pagano, P.J., Singh, K., Sawyer, D.B., and Colucci, W.S. (1999). Inhibition of copper-zinc superoxide dismutase induces cell growth, hypertrophic phenotype, and apoptosis in neonatal rat cardiac myocytes in vitro. Circ Res *85*, 147-153.

Solan, J.L., Fry, M.D., TenBroek, E.M., and Lampe, P.D. (2003). Connexin43 phosphorylation at S368 is acute during S and G2/M and in response to protein kinase C activation. J Cell Sci *116*, 2203-2211.

Solan, J.L., and Lampe, P.D. (2007). Key connexin 43 phosphorylation events regulate the gap junction life cycle. J Membr Biol *217*, 35-41.

Solan, J.L., and Lampe, P.D. (2008). Connexin 43 in LA-25 cells with active v-src is phosphorylated on Y247, Y265, S262, S279/282, and S368 via multiple signaling pathways. Cell Commun Adhes *15*, 75-84.

Solan, J.L., and Lampe, P.D. (2009). Connexin43 phosphorylation: structural changes and biological effects. Biochem J *419*, 261-272.

Solan, J.L., Marquez-Rosado, L., Sorgen, P.L., Thornton, P.J., Gafken, P.R., and Lampe, P.D. (2007). Phosphorylation at S365 is a gatekeeper event that changes the structure of Cx43 and prevents down-regulation by PKC. J Cell Biol *179*, 1301-1309.

Soldani, C., and Scovassi, A.I. (2002). Poly(ADP-ribose) polymerase-1 cleavage during apoptosis: an update. Apoptosis *7*, 321-328.

Sparagna, G.C., and Lesnefsky, E.J. (2009). Cardiolipin remodeling in the heart. J Cardiovasc Pharmacol *53*, 290-301.

Srisakuldee, W., Jeyaraman, M.M., Nickel, B.E., Tanguy, S., Jiang, Z.S., and Kardami, E. (2009). Phosphorylation of connexin-43 at serine 262 promotes a cardiac injury-resistant state. Cardiovasc Res *83*, 672-681.

Srisakuldee, W., Nickel, B.E., Fandrich, R.R., Jiang, Z.S., and Kardami, E. (2006). Administration of FGF-2 to the heart stimulates connexin-43 phosphorylation at protein kinase C target sites. Cell Commun Adhes *13*, 13-19.

Stanley, W.C. (2004). Myocardial energy metabolism during ischemia and the mechanisms of metabolic therapies. J Cardiovasc Pharmacol Ther *9 Suppl 1*, S31-45.

Suda, T., Takahashi, T., Golstein, P., and Nagata, S. (1993). Molecular cloning and expression of the Fas ligand, a novel member of the tumor necrosis factor family. Cell *75*, 1169-1178.

Sun, X.M., Butterworth, M., MacFarlane, M., Dubiel, W., Ciechanover, A., and Cohen, G.M. (2004). Caspase activation inhibits proteasome function during apoptosis. Mol Cell *14*, 81-93.

Tandler, B., and Hoppel, C.L. (1972). Possible division of cardiac mitochondria. Anat Rec *173*, 309-323.

Tanguy, S., Durand, G., Reboul, C., Polidori, A., Pucci, B., Dauzat, M., and Obert, P. (2006). Protection against reactive oxygen species injuries in rat isolated perfused

hearts: effect of LPBNAH, a new amphiphilic spin-trap derived from PBN. Cardiovasc Drugs Ther *20*, 147-149.

Totzeck, A., Boengler, K., van de Sand, A., Konietzka, I., Gres, P., Garcia-Dorado, D., Heusch, G., and Schulz, R. (2008). No impact of protein phosphatases on connexin 43 phosphorylation in ischemic preconditioning. Am J Physiol Heart Circ Physiol *295*, H2106-2112.

Ueta, H., Ogura, R., Sugiyama, M., Kagiyama, A., and Shin, G. (1990). O2-. spin trapping on cardiac submitochondrial particles isolated from ischemic and non-ischemic myocardium. J Mol Cell Cardiol *22*, 893-899.

Van Kempen, M.J., Vermeulen, J.L., Moorman, A.F., Gros, D., Paul, D.L., and Lamers, W.H. (1996). Developmental changes of connexin40 and connexin43 mRNA distribution patterns in the rat heart. Cardiovasc Res *32*, 886-900.

Van Remmen, H., and Richardson, A. (2001). Oxidative damage to mitochondria and aging. Exp Gerontol *36*, 957-968.

Vandenabeele, P., Declercq, W., Van Herreweghe, F., and Vanden Berghe, T. (2010). The role of the kinases RIP1 and RIP3 in TNF-induced necrosis. Sci Signal *3*, re4.

Varanyuwatana, P., and Halestrap, A.P. (2012). The roles of phosphate and the phosphate carrier in the mitochondrial permeability transition pore. Mitochondrion *12*, 120-125.

Vaseva, A.V., Marchenko, N.D., Ji, K., Tsirka, S.E., Holzmann, S., and Moll, U.M. (2012). p53 opens the mitochondrial permeability transition pore to trigger necrosis. Cell *149*, 1536-1548.

Vendelin, M., Beraud, N., Guerrero, K., Andrienko, T., Kuznetsov, A.V., Olivares, J., Kay, L., and Saks, V.A. (2005). Mitochondrial regular arrangement in muscle cells: a "crystal-like" pattern. Am J Physiol Cell Physiol *288*, C757-767.

Verrecchia, F., Duthe, F., Duval, S., Duchatelle, I., Sarrouilhe, D., and Herve, J.C. (1999). ATP counteracts the rundown of gap junctional channels of rat ventricular myocytes by promoting protein phosphorylation. J Physiol *516 (Pt 2)*, 447-459.

Walensky, L.D., and Gavathiotis, E. (2011). BAX unleashed: the biochemical transformation of an inactive cytosolic monomer into a toxic mitochondrial pore. Trends Biochem Sci *36*, 642-652.

Wang, J., Nachtigal, M.W., Kardami, E., and Cattini, P.A. (2013). FGF-2 protects cardiomyocytes from doxorubicin damage via protein kinase C-dependent effects on efflux transporters. Cardiovasc Res *98*, 56-63.

Wang, L., Cherednichenko, G., Hernandez, L., Halow, J., Camacho, S.A., Figueredo, V., and Schaefer, S. (2001). Preconditioning limits mitochondrial Ca(2+) during ischemia in rat hearts: role of K(ATP) channels. Am J Physiol Heart Circ Physiol *280*, H2321-2328.

Wang, N., De Bock, M., Antoons, G., Gadicherla, A.K., Bol, M., Decrock, E., Evans, W.H., Sipido, K.R., Bukauskas, F.F., and Leybaert, L. (2012). Connexin mimetic peptides inhibit Cx43 hemichannel opening triggered by voltage and intracellular Ca2+ elevation. Basic Res Cardiol *107*, 304.

Wang, X., and Gerdes, A.M. (1999). Chronic pressure overload cardiac hypertrophy and failure in guinea pigs: III. Intercalated disc remodeling. J Mol Cell Cardiol *31*, 333-343.

Wang, Y., Ebermann, L., Sterner-Kock, A., Wika, S., Schultheiss, H.P., Dorner, A., and Walther, T. (2009). Myocardial overexpression of adenine nucleotide translocase 1 ameliorates diabetic cardiomyopathy in mice. Exp Physiol *94*, 220-227.

Warn-Cramer, B.J., Lampe, P.D., Kurata, W.E., Kanemitsu, M.Y., Loo, L.W., Eckhart, W., and Lau, A.F. (1996). Characterization of the mitogen-activated protein kinase phosphorylation sites on the connexin-43 gap junction protein. J Biol Chem *271*, 3779-3786.

Watford, M. (1991). The urea cycle: a two-compartment system. Essays Biochem *26*, 49-58.

Wei, J.Y. (1992). Age and the cardiovascular system. N Engl J Med *327*, 1735-1739.

Weiss, J.N., Korge, P., Honda, H.M., and Ping, P. (2003). Role of the mitochondrial permeability transition in myocardial disease. Circ Res *93*, 292-301.

Wesche, J., Malecki, J., Wiedlocha, A., Skjerpen, C.S., Claus, P., and Olsnes, S. (2006). FGF-1 and FGF-2 require the cytosolic chaperone Hsp90 for translocation into the cytosol and the cell nucleus. J Biol Chem *281*, 11405-11412.

Whelan, R.S., Kaplinskiy, V., and Kitsis, R.N. (2010). Cell death in the pathogenesis of heart disease: mechanisms and significance. Annu Rev Physiol *72*, 19-44.

Wiedemann, F.R., Siemen, D., Mawrin, C., Horn, T.F., and Dietzmann, K. (2006). The neurotrophin receptor TrkB is colocalized to mitochondrial membranes. Int J Biochem Cell Biol *38*, 610-620.

Willecke, K., Eiberger, J., Degen, J., Eckardt, D., Romualdi, A., Guldenagel, M., Deutsch, U., and Sohl, G. (2002). Structural and functional diversity of connexin genes in the mouse and human genome. Biol Chem *383*, 725-737.

Williamson, C.L., Dabkowski, E.R., Baseler, W.A., Croston, T.L., Alway, S.E., and Hollander, J.M. (2010). Enhanced apoptotic propensity in diabetic cardiac mitochondria: influence of subcellular spatial location. Am J Physiol Heart Circ Physiol *298*, H633-642.

Winterbourn, C.C., and Hampton, M.B. (2008). Thiol chemistry and specificity in redox signaling. Free Radic Biol Med *45*, 549-561.

Yabe, K., Nasa, Y., Sato, M., Iijima, R., and Takeo, S. (1997). Preconditioning preserves mitochondrial function and glycolytic flux during an early period of reperfusion in perfused rat hearts. Cardiovasc Res *33*, 677-685.

Ye, Z.C., Wyeth, M.S., Baltan-Tekkok, S., and Ransom, B.R. (2003). Functional hemichannels in astrocytes: a novel mechanism of glutamate release. J Neurosci *23*, 3588-3596.

Zamzami, N., El Hamel, C., Maisse, C., Brenner, C., Munoz-Pinedo, C., Belzacq, A.S., Costantini, P., Vieira, H., Loeffler, M., Molle, G.*, et al.* (2000). Bid acts on the permeability transition pore complex to induce apoptosis. Oncogene *19*, 6342-6350.

Zhang, F., and Pasumarthi, K.B. (2007). Ultrastructural and immunocharacterization of undifferentiated myocardial cells in the developing mouse heart. J Cell Mol Med *11*, 552-560.

Zhang, X., Ibrahimi, O.A., Olsen, S.K., Umemori, H., Mohammadi, M., and Ornitz, D.M. (2006). Receptor specificity of the fibroblast growth factor family. The complete mammalian FGF family. J Biol Chem *281*, 15694-15700.

Zoratti, M., and Szabo, I. (1994). Electrophysiology of the inner mitochondrial membrane. J Bioenerg Biomembr *26*, 543-553.

Zorov, D.B., Kinnally, K.W., and Tedeschi, H. (1992). Voltage activation of heart inner mitochondrial membrane channels. J Bioenerg Biomembr *24*, 119-124.

APPENDIX

OXFORD UNIVERSITY PRESS LICENSE TERMS AND CONDITIONS

Apr 16, 2014

This is a License Agreement between Wattamon Srisakuldee ("You") and Oxford University Press ("Oxford University Press") provided by Copyright Clearance Center ("CCC"). The license consists of your order details, the terms and conditions provided by Oxford University Press, and the payment terms and conditions.

All payments must be made in full to CCC. For payment instructions, please see information listed at the bottom of this form.

License Number	3370871202474
License date	Apr 16, 2014
Licensed content publisher	Oxford University Press
Licensed content publication	Cardiovascular Research
Licensed content title	Phosphorylation of connexin-43 at serine 262 promotes a cardiac injury-resistant state:
Licensed content author	Wattamon Srisakuldee, Maya M. Jeyaraman, Barbara E. Nickel, Stéphane Tanguy, Zhi-Sheng Jiang, Elissavet Kardami
Licensed content date	09/01/2009
Type of Use	Thesis/Dissertation
Institution name	None
Title of your work	Studies on the role of connexin43 phosphorylation in the injury-resistant heart
Publisher of your work	n/a
Expected publication date	Apr 2014
Permissions cost	0.00 USD
Value added tax	0.00 USD
TotalTotal	**0.00 USD**
TotalTotal	**0.00 USD**
Terms and Conditions	

STANDARD TERMS AND CONDITIONS FOR REPRODUCTION OF MATERIAL FROM AN OXFORD UNIVERSITY PRESS JOURNAL

1. Use of the material is restricted to the type of use specified in your order details.
2. This permission covers the use of the material in the English language in the following territory: world. If you have requested additional permission to translate this material, the terms and conditions of this reuse will be set out in clause 12.
3. This permission is limited to the particular use authorized in (1) above and does not allow you to sanction its use elsewhere in any other format other than specified above, nor does it apply to quotations, images, artistic works etc that have been reproduced from other sources which may be part of the material to be used.
4. No alteration, omission or addition is made to the material without our written consent. Permission must be re-cleared with Oxford University Press if/when you decide to reprint.
5. The following credit line appears wherever the material is used: author, title, journal, year, volume, issue number, pagination, by permission of Oxford University Press or the sponsoring society if the journal is a society journal. Where a journal is being published on behalf of a learned society, the details of that society must be included in the credit line.
6. For the reproduction of a full article from an Oxford University Press journal for whatever purpose, the corresponding author of the material concerned should be informed of the proposed use. Contact details for the corresponding authors of all Oxford University Press journal contact can be found alongside either the abstract or full text of the article concerned,

accessible from www.oxfordjournals.org Should there be a problem clearing these rights, please contact journals.permissions@oup.com

7. If the credit line or acknowledgement in our publication indicates that any of the figures, images or photos was reproduced, drawn or modified from an earlier source it will be necessary for you to clear this permission with the original publisher as well. If this permission has not been obtained, please note that this material cannot be included in your publication/photocopies.

8. While you may exercise the rights licensed immediately upon issuance of the license at the end of the licensing process for the transaction, provided that you have disclosed complete and accurate details of your proposed use, no license is finally effective unless and until full payment is received from you (either by Oxford University Press or by Copyright Clearance Center (CCC)) as provided in CCC's Billing and Payment terms and conditions. If full payment is not received on a timely basis, then any license preliminarily granted shall be deemed automatically revoked and shall be void as if never granted. Further, in the event that you breach any of these terms and conditions or any of CCC's Billing and Payment terms and conditions, the license is automatically revoked and shall be void as if never granted. Use of materials as described in a revoked license, as well as any use of the materials beyond the scope of an unrevoked license, may constitute copyright infringement and Oxford University Press reserves the right to take any and all action to protect its copyright in the materials.

9. This license is personal to you and may not be sublicensed, assigned or transferred by you to any other person without Oxford University Press's written permission.

10. Oxford University Press reserves all rights not specifically granted in the combination of (i) the license details provided by you and accepted in the course of this licensing transaction, (ii) these terms and conditions and (iii) CCC's Billing and Payment terms and conditions.

11. You hereby indemnify and agree to hold harmless Oxford University Press and CCC, and their respective officers, directors, employs and agents, from and against any and all claims arising out of your use of the licensed material other than as specifically authorized pursuant to this license.

12. Other Terms and Conditions:

v1.4

If you would like to pay for this license now, please remit this license along with your payment made payable to "COPYRIGHT CLEARANCE CENTER" otherwise you will be invoiced within 48 hours of the license date. Payment should be in the form of a check or money order referencing your account number and this invoice number RLNK501279993.

Once you receive your invoice for this order, you may pay your invoice by credit card. Please follow instructions provided at that time.

Make Payment To:
Copyright Clearance Center
Dept 001
P.O. Box 843006
Boston, MA 02284-3006

For suggestions or comments regarding this order, contact RightsLink Customer Support:
customercare@copyright.com or +1-877-622-5543 (toll free in the US) or +1-978-646-2777.

Gratis licenses (referencing $0 in the Total field) are free. Please retain this printable license for your reference. No payment is required.

OXFORD UNIVERSITY PRESS LICENSE TERMS AND CONDITIONS

Apr 16, 2014

This is a License Agreement between Wattamon Srisakuldee ("You") and Oxford University Press ("Oxford University Press") provided by Copyright Clearance Center ("CCC"). The license consists of your order details, the terms and conditions provided by Oxford University Press, and the payment terms and conditions.

All payments must be made in full to CCC. For payment instructions, please see information listed at the bottom of this form.

License Number	3370900322856
License date	Apr 16, 2014
Licensed content publisher	Oxford University Press
Licensed content publication	Cardiovascular Research
Licensed content title	The FGF-2-triggered protection of cardiac subsarcolemmal mitochondria from calcium overload is mitochondrial connexin 43-dependent:
Licensed content author	Wattamon Srisakuldee, Zhanna Makazan, Barbara E. Nickel, Feixiong Zhang, James A. Thliveris, Kishore B.S. Pasumarthi, Elissavet Kardami
Licensed content date	03/20/2014
Type of Use	Thesis/Dissertation
Institution name	
Title of your work	Studies on the role of connexin43 phosphorylation in the injury-resistant heart
Publisher of your work	n/a
Expected publication date	Apr 2014
Permissions cost	0.00 USD
Value added tax	0.00 USD
Total	0.00 USD
Total	0.00 USD
Terms and Conditions	

STANDARD TERMS AND CONDITIONS FOR REPRODUCTION OF MATERIAL FROM AN OXFORD UNIVERSITY PRESS JOURNAL

1. Use of the material is restricted to the type of use specified in your order details.

2. This permission covers the use of the material in the English language in the following territory: world. If you have requested additional permission to translate this material, the terms and conditions of this reuse will be set out in clause 12.

3. This permission is limited to the particular use authorized in (1) above and does not allow you to sanction its use elsewhere in any other format other than specified above, nor does it apply to quotations, images, artistic works etc that have been reproduced from other sources which may be part of the material to be used.

4. No alteration, omission or addition is made to the material without our written consent. Permission must be re-cleared with Oxford University Press if/when you decide to reprint.

5. The following credit line appears wherever the material is used: author, title, journal, year, volume, issue number, pagination, by permission of Oxford University Press or the sponsoring society if the journal is a society journal. Where a journal is being published on behalf of a learned society, the details of that society must be included in the credit line.

6. For the reproduction of a full article from an Oxford University Press journal for whatever purpose, the corresponding author of the material concerned should be informed of the proposed use. Contact details for the corresponding authors of all Oxford University Press journal contact can be found alongside either the abstract or full text of the article concerned, accessible from www.oxfordjournals.org Should there be a problem clearing these rights, please contact journals.permissions@oup.com

7. If the credit line or acknowledgement in our publication indicates that any of the figures, images or photos was reproduced, drawn or modified from an earlier source it will be necessary for you to clear this permission with the original publisher as well. If this permission has not been obtained, please note that this material cannot be included in your publication/photocopies.

8. While you may exercise the rights licensed immediately upon issuance of the license at the end of the licensing process for the transaction, provided that you have disclosed complete and accurate details of your proposed use, no license is finally effective unless and until full payment is received from you (either by Oxford University Press or by Copyright Clearance Center (CCC)) as provided in CCC's Billing and Payment terms and conditions. If full payment is not received on a timely basis, then any license preliminarily granted shall be deemed automatically revoked and shall be void as if never granted. Further, in the event that you breach any of these terms and conditions or any of CCC's Billing and Payment terms and conditions, the license is automatically revoked and shall be void as if never granted. Use of materials as described in a revoked license, as well as any use of the materials beyond the scope of an unrevoked license, may constitute copyright infringement and Oxford University Press reserves the right to take any and all action to protect its copyright in the materials.

9. This license is personal to you and may not be sublicensed, assigned or transferred by you to any other person without Oxford University Press's written permission.

10. Oxford University Press reserves all rights not specifically granted in the combination of (i) the license details provided by you and accepted in the course of this licensing transaction, (ii) these terms and conditions and (iii) CCC's Billing and Payment terms and conditions.

11. You hereby indemnify and agree to hold harmless Oxford University Press and CCC, and

their respective officers, directors, employs and agents, from and against any and all claims arising out of your use of the licensed material other than as specifically authorized pursuant to this license.

12. Other Terms and Conditions:

v1.4

If you would like to pay for this license now, please remit this license along with your payment made payable to "COPYRIGHT CLEARANCE CENTER" otherwise you will be invoiced within 48 hours of the license date. Payment should be in the form of a check or money order referencing your account number and this invoice number RLNK501280058.
Once you receive your invoice for this order, you may pay your invoice by credit card. Please follow instructions provided at that time.

Make Payment To:
Copyright Clearance Center
Dept 001
P.O. Box 843006
Boston, MA 02284-3006

For suggestions or comments regarding this order, contact RightsLink Customer Support: customercare@copyright.com or +1-877-622-5543 (toll free in the US) or +1-978-646-2777.

Gratis licenses (referencing $0 in the Total field) are free. Please retain this printable license for your reference. No payment is required.